EFFECTS OF LATTICE LEGS AND SLEEVES ON SPUDCAN PENETRATION PERFORMANCE

SIM WEE KEAT

NATIONAL UNIVERSITY OF SINGAPORE

2012

EFFECTS OF LATTICE LEGS AND SLEEVES ON SPUDCAN PENETRATION PERFORMANCE

SIM WEE KEAT

(BEng., Hons)

A THESIS SUBMITTED

FOR THE DEGREE OF MASTER OF ENGINEERING

DEPARTMENT OF CIVIL ENGINEERING

NATIONAL UNIVERSITY OF SINGAPORE

2012

To my parents, slibings, wife, Ho Thi Ngoc Tran

and

beloved new-born baby daughter, Sharlet Sim.

ABSTRACT

Offshore industry professionals frequently face challenges when predicting spudcan foundation bearing capacity of jack-up rigs with deep leg penetration in both normally consolidated and over-consolidated clays.

In the present study, centrifuge modeling technique was adopted to simulate a simplified operation of an individual spudcan with and without lattice legs in both normally consolidated and over-consolidated clays. With an intensively instrumented centrifuge setup, the experiments were performed to quantify the bearing responses and penetration with special attention paid to the influence of lattice legs or truss-work.

The experimental results presented that the sleeve resistance of the lattice legs and spudcan end bearing capacity constitute to the ultimate bearing responses. The sleeve resistance component was substantially influenced by the opening ratio of the lattice legs of jack-up rigs which is also directly associated with the spudcan end bearing capacity coefficient. From the centrifuge tests, it was observed that the some similarities between bearing capacity spudcan with lattice legs and pile bearing capacity. It was also established that the spudcan with lattice legs would perform better than those without sleeve as the bearing capacity coefficients decreased with the increase in opening ratio for both normally consolidated and over-consolidated clays. Under the high g environment in the centrifuge laboratory, the proposed method was proven capable of estimating the bearing capacity of spudcan with lattice legs as well as the penetration depth.

Keywords: clays, bearing responses, jack-up rigs, lattice legs, spudcan penetration,

ACKNOWLEDGEMENTS

It has been a great pleasure and rare opportunity for me to pursue my postgraduate study in the Centre for Soft Ground Engineering and Centre for Offshore Research and Engineering at National University of Singapore (NUS). Firstly, I would like to express my most sincere gratitude to my supervisor, Professor Lee Fook Hou for his continuous guidance and support throughout the entire course of my postgraduate research. His invaluable comments, patience, encouragement and constructive criticisms are greatly appreciated and bore in mind.

I would also like to acknowledge the financial support of NUS RP 264-000-257-305 and RP 264-000-257-490. Without this fund, the whole research cannot be fully accomplished and materialized. In addition, tokens of appreciation should certainly and absolutely be given to the laboratory technicians and professional officer of Geotechnical and Geotechnical Centrifuge Laboratories: Mr John Choy Moon Nien, Madam Jamilah, Mr Loo Leong Huat, Mr Shaja Khan, Mr Tan Lye Heng, Mr Wong Chew Yuen, Mr Foo Hee Ann and Dr Shen Ruifu. Without their utmost assistance, efforts and time, the centrifuge model tests cannot be completely accomplished.

I am also very fortunate and grateful to have Dr Goh Siang Huat as friend instead of assistant professor to share his past experience and provide some critical advices.

I would like to thank my friends and classmates at National University of Singapore: Dr Zhang Yaodong, Ye Feijian, Sun Jie, Liu Yong, Wu Jun, Karma, Korakod and etc. I would never forget those seniors who have left the campus and yet willing to share their valuable experiences with me.

My fullest appreciation is also given to Dr Ng Tiong Guan of GeoEng Consultant Private Limited and Dr Kevin Wong of University of Utah who led me to the geotechnical engineering research. Their invaluable encouragement during these few years will be remembered forever.

Last but not least, I specially intend to thank my parents, siblings, wife, Ho Thi Ngoc Tran and beloved new-born baby girl, Sharlet Sim for their eternal love, moral support and blessing throughout the whole postgraduate course.

Table of Contents

List of Tables

List of Figures

List of Symbols

Related to geotechnical engineering

A	plan area of spudcan
Ar	opening area ratio, defined as the ratio between opening and surface area of the sleeve
c_v	coefficient of consolidation
D	diameter of spudcan
d	penetration depth
g	gravity constant
H_{cr}	critical depth at which the spudcan cavity remains stable
H_f	backfilled soil height
k	rate of shear strength increasing with depth
N_c	bearing capacity coefficient
N_{cd}	bearing capacity coefficient for deep spudcan embedment
N_{co}	bearing capacity coefficient by Houlsby and Martin (2003) and Hossain *et al.* (2006)
Q_s	shaft friction
Q_p	vertical bearing force
q_u	ultimate bearing capacity
s_u	undrained shear strength
s_{uavg}	average undrained shear strength
s_{um}	undrained shear strength at ground surface

s_{uo}	undrained shear strength at depth corresponding to the maximum cross-sectional area of spudcan
V	volume of embedded spudcan inclusive of shaft
V_b	volume of embedded spudcan
V_o	vertical penetration resistance
v	velocity of penetration or extraction
w	moisture content
z	penetration depth from mud-line or relative to widest spudcan cross sectional area
α	dimensionless roughness factor for soil spudcan interface
β	angle of spudcan tip
ρ	rate of shear strength increasing with depth
γ	bulk unit weight
γ'	effective or submerged unit weight

CHAPTER 1 INTRODUCTION

1.1 SPUDCANS: FOUNDATION OF MOBILE JACK-UP RIGS

1.1.1 BRIEF HISTORY

The earliest jack-up platform is firstly introduced in 1869 by Samuel Lewis under the description of a United States patent application (Veldman and Lagers, 1997). It was not realized until 1954, when Delong McDermott Number 1 became the first ever unit to utilize the jack-up fundamentals for offshore drilling fully. Delong McDermott Number 1 was converted and modified from one of the Delong Docks: a pontoon with a substantial number of tubular legs which could be mobilized in up and down directions through cut-outs in the pontoon. The Delong Docks, which were frequently used as mobile wharves for industrial purposes during the 1940s, could be towed to the desired location with their legs withdrawn up from the water. Once in stationary position, their legs could be lowered with the pontoon elevated off the water using the similar principle as the modern jack-ups.

Like many of early jack-ups, Delong McDermott Number 1 resembled a conventional drilling barge with attached legs and jacks, which were also frequented in number. In 1956, R.G. LeTourneau, a former entrepreneur in earth-moving equipment (Ackland, 1949), revolutionized the design of jack-ups by reducing the number of independent legs to three instead of four (Stiff *et al*., 1997). Another innovative and latest improvement in the jack-up rig design was the electrically driven rack and

pinion jacking system, which permitted the continuous motions of truss-work legs during both preloading and extraction phases. This new system can effectively and efficiently replace the 'gripper' jacks where slippage frequently occurred on the smooth leg surface (Veldman and Lagers, 1997). In view of the usefulness and effectiveness on both revolutionary features, they are highly recognizable and therefore incorporated in today's jack-up rigs. Zepata's jack-up rig, Scorpian, which was deployed in 25m deep waters in the Gulf of Mexico, was the first of many offshore platforms operated by the company Marathon LeTourneau. Because of these contributing factors, that was why they could dominate early jack-up design during the 1960s and 1970s with increasing size rigs.

Ever since their first deployment, jack-ups have continuously been improved, evolved and enhanced to be adopted in deeper waters (Carlsen *et al*., 1986). Some of the largest units can now function over 150m of water in the relatively harsh North Sea environment (Hambly *et al*., 1990; Veldman and Lagers, 1997). Furthermore, one jack-up rig can currently operate for an extended period at single location in the role of production unit (Bennett and Sharples, 1987). A good example of long period use of jack-ups is in the economically marginal field development in the Danish dominance of North Sea. A specifically built jack-up is being used in 60m water depths as a production platform with an expected life span of ten years (Baerheim *et al*., 1997). A further example is the Shearwater development, where jack-up drilling operation is planned to continue for two and a half years in90m water depth in Northern part of North Sea (Offshore Technology, 1999).

1.1.2 FUNCTION OF JACK-UP UNITS IN OIL AND GAS INDUSTRIES

Over many decades in practice, the majority of the world's offshore drilling platforms have been evolved to enable oil and gas drilling activities in deeper and harsher environments (Carlsen *et al*., 1986; Bennett and Sharples, 1987; Hambly *et al*., 1990; Veldman and Lagers, 1997). Hence, the offshore drilling platforms are classified into several categories from shallow water platform to deep water semi-submersibles with respect to water depths, refer to Figure 1.1. Among all types of rigs, the mobile jack-up rig is the most commonly deployed in Southeast Asia.

Jack-ups rigs have been extensively deployed for maintenance, construction, oil and gas exploration and temporary production of oil and gas fields in shallow waters up to 150m deep. As illustrated in Figure 1.2 and Figure 1.3, a modern jack-up rig typically comprises of a buoyant triangular hull supported by three or four independent truss-work legs (Young *et al*., 1984; Dier *et al*., 2004; Vazquez *et al*., 2005) with individual footings, which are termed as "spudcans" (Young *et al*., 1984; Poulos, 1988). This particular type of footing is effectively circular or polygonal in plan with a shallow conical underside profile (in the order of 15 to 30° to the horizontal)and a sharp protruding spigot (see Figure 1.4) to facilitate initial seabed location and provide additional horizontal stability (Martin, 1994; SNAME, 1994, 1997, 2002, 2008) as depicted schematically in Figure 1.5. Dependent on the overall capacity and its purpose of a jack-up rig, the spudcan diameter varies up to 20m for post 1980 designs. Since the jack-up rig is highly mobile in nature, its spudcan foundation is not designed to cater for a site-specific soil condition. Hence, site assessment is an important part of spudcan operation.

1.2 JACK-UP RIGS INSTALLATION PROCEDURES

The typical steps in mobile jack-up rig installation are presented in Figure 1.6. Nowadays, rack and pinion systems are usually used for each lattice leg to permit

smooth continuous jacking of the hull (Bennet and KeppelFELS, 2005).

As shown in Figure 1.7, the jack-up rig is towed to the desired location with the lattice legs elevated out of the water. After arriving at the desired location, their legs are lowered down until the individual spudcan rests on the seabed as reflected in Figure 1.8. Once the jack-up unit has been positioned stationary, the spudcans are jacked into the seabed until the resulting soil bearing resistance is closely equivalent to the submerged weight of the jack-up unit and its truss-work legs (see Point A'). When an adequate bearing capacity exists for the hull to be lifted clear of the water, the deeper legs' penetration will be induced concurrently with the decrease in buoyant force supporting the platform. Typically, the hull is then raised approximately 1.5m above sea level at this phase and corresponding spudcan load displacement response will shift from Point A' to Point A as illustrated in Figure 1.7.

Before commencing its operation, the jack-up rig requires to be preloaded sufficiently through lattice leg to withstand the maximum anticipated combination of environmental and live loads without causing additional leg penetration or soil bearing capacity failure. From other perspectives, the preloading process is targeted to assist the resulting bearing capacity of the spudcan to exceed that needed during extreme storm loading by an acceptable safety margin.

After the platform has been lifted clear out of sea surface by about 1.5m, the spudcan foundations are preloaded by pumping sea water into the ballast tanks within the hull. Usually, it is a universal practice to preload the foundation to 1.3 to 2 times the working vertical load (operational light ship weight) or a 50 years design storm in terms of wind load, wave load and current load or whichever greater. The full preload is held for a minimum duration of 2 to 4 hours after the spudcan foundation penetration has ceased (Young *et al*., 1984). However, in some cases, this process

may require around 24 to 36 hours. In soft seabed conditions, the spudcan could penetrate up to 2 to 3 diameters before stabilizing (Endley *et al*., 1981; Craig and Higham, 1985; Craig and Chua, 1990): this corresponds to point B in Figure 1.7. After preloading, the water within the ballast tanks is discharged and the hull is then raised further to provide an adequate air gap of 12 m to 15 m for subsequent operation.

During operation, the spudcans may be subjected to overturning moments, horizontal loads such as waves, winds and currents and variations in vertical load arising from environmental action on the structures. In a design storm of 50 years return frequency, wave and wind induced overturning moments may impose an additional or extra load as much as 20% to 50% of the gravity load whereas horizontal loads may range from one-tenth to one-third of the vertical load (McClelland *et al*., 1981; Baglioni *et al*., 1982; Kee and Ims, 1984). Young *et al*. (1981) reported that the maximum spudcan loads are generally ranged from 18 MN to 49 MN and this corresponds to maximum bearing capacity of approximate 192 kPa to 235 kPa for spudcan diameter of 10 m to 15 m. For an example, the Marathon Gorilla rig with 20.1 m diameter spudcans was designed with a maximum penetration load of 102 MN or equivalent to a bearing capacity of 335 kPa in 1983.

McClelland *et al*. (1981) pointed out that there are totally six types of potential failure of spudcan foundations associated with soil foundation interaction problems: inadequate leg length during maximum preload, punch through during installation, excessive storm penetration, footing instability due to scouring, seafloor instability and inability to extract spudcan.

1.3 SPUDCAN DESIGN PRINCIPLES AND METHODLOGIES

1.3.1 CONVENTIONAL VERTICAL BEARING CAPACITY

The short term or undrained bearing capacity of shallow foundation at a specific depth, d, under the action of purely vertical loading for onshore foundations can be determined as:

$$q_u = s_u N_c + \gamma d \quad (1.1)$$

Where s_u is the soil undrained shear strength, γ is the soil bulk unit weight, N_c is the dimensionless bearing capacity coefficient and d is the depth of penetration of spudcanas presented in Figure 1.9. If the spudcan rests on the surface of the seabed (d is equal to zero), the equation 1.1 can be adjusted to as illustrated below (refer to Figure 1.9a):

$$q_u = s_u N_c \quad (1.2)$$

When the spudcan penetrates into the seabed where the cavity above the footing remains open (H is equal to d) which could be the case in very firm clay (Gemeinhardt and Focht, 1970; Endley *et al*., 1981), the equation 1.1 can be adopted (refer to Figure 1.9b). On the other hand, if the cavity above the footing is completely backfilled (H is equal to zero), which is usually the case in normally consolidated clay (Endley *et al*., 1981; Kee and Ims, 1984; Le Tirant and Pérol, 1993),

the contribution of overburden pressure, γd, will be fully negated (refer to Figure 1.9c). However, if soil is intermediate between soft and stiff, the cavity above the footing may remain open partially. Thus, the contribution of overburden pressure, γd, shall be decreased by the amount,γ(d-H) and the equation 1.1 will be generalized in this form of equation 1.3.

$$q_u = s_u N_c + \gamma d - \gamma(d - H) \quad (1.3)$$

If the spudcan is considered to be footing in a fully developed cavity, submerged in water, the bulk unit weight, γ should be replaced by γ'. This gives:

$$q_u = s_u N_c + \gamma' d \quad (1.4)$$

$$q_u = s_u N_c + \gamma' d - \gamma'(d - H) \quad (1.5)$$

Since the impact of the overburden stress,$\gamma' d - \gamma'(d - H)$, on the bearing capacity, q_u is insignificant or negligible, the overburden stress terms,$\gamma' d - \gamma'(d - H)$, in equation 1.5 can be simply replaced with $\gamma' \frac{V}{A}$ whereas V is the combined volume of embedded spudcan and A is the largest cross sectional area of spudcan as expressed in equation 1.6.

$$q_u = s_u N_c + \gamma' \frac{V}{A} \quad (1.6)$$

Moreover, the spudcan can be assumed to be equivalently circular in plan and the dimensionless bearing capacity coefficient for the circular footing (Skempton, 1951) shall be listed as:

$$N_c = 6\left(1 + 0.2\frac{d}{D}\right) \leq 9 \quad (1.7)$$

When the value of the dimensionless bearing capacity coefficient, N_c, must not exceed 9, the value of $\frac{d}{D}$ shall be restricted to less than or equal to 2.5. In addition, in order to ensure this method is applicable, the undrained shear strengths, s_u, between 0.5 to 1diameters below the spudcan cannot vary more than 50% from the average value (Skempton, 1951; Gemeinhardt and Focht, 1970; Kee and Ims, 1984; Young *et al*., 1984).

Endley *et al.* (1981) proposed that better prediction of bearing response and spudcan penetration could be obtained by assuming that the cavity above the spudcan is completely backfilled. In this case, this will lead to more conservative design. Spudcan foundations undergo progressive penetration during preloading, unlike onshore pre-embedded foundations or offshore skirted foundations. Unfortunately, the spudcan penetration is still generally assessed by the bearing capacity profile obtained from a series of "wished in place" spudcans at successively increasing depths (Endley *et al*., 1981). More importantly, the influences of lattice legs or truss-work on spudcan bearing response and penetration are not yet addressed.

1.3.2 VERTICAL BEARING CAPACITY (AFTER SNAME, 1994, 1997, 2002, 2008)

The short term or undrained bearing capacity of a shallow foundation at a specific depth, d under purely vertical loading is similar with the proposed equation 1.4 under Section 1.3.1. The two definitions for ultimate bearing capacity, q_u, under this section and Section 1.3.1 are identical in the case where an open cavity exists above

the spudcan but for the more general case where back-flow occurs, a more precise form of the bearing capacity equation (SNAME 1994, 1997, 2002, 2008) is as:

$$q_u = N_c s_u + \gamma' d - p'_o + \frac{\gamma' V}{A} \quad (1.8)$$

Where s_u is the soil undrained shear strength, γ' is the soil effective unit weight, N_c is the dimensionless bearing capacity coefficient, d is the depth of penetration of spudcan, p'_o is the effective overburden pressure, V is the combined volume of embedded spudcan and leg and A is the largest cross sectional area of the spudcan.

Deep penetration at a soft clay site is usually associated with partial or full back-flow above spudcan as reported from field experience (Endley *et al*., 1981; Kee and Ims, 1984) and centrifuge model tests (Craig and Chua, 1990, 1991; Hossain *et al*., 2003, 2004a, 2004b, 2005b, 2006). Any soil back-flow flowing into the cavity induced by spudcan penetration affects the bearing response in two specific ways: (1) by negating the overburden stress contribution, $\gamma' d$, through an increase in applied preload pressure, p'_o and (2) by increasing the shear resistance and bearing capacity coefficient, N_c, as the failure mechanism currently must penetrate through the backfilled soil. Skempton (1951) method is intended to reduce the bearing resistance and increase the penetration depth. For very deep penetration, any surface cavity above the spudcan may become insignificant. Therefore, the bearing capacity equation can be simplified as follows from equation 1.8:

$$q_u = N_{cd} s_u + \frac{\gamma' V}{A} \quad (1.9)$$

Where N_{cd} is a value corresponding to a deep flow mechanism around fully embedded spudcan. A limiting deep bearing capacity factor, N_{cdu}, is reached when the failure mechanism does not extend to a free soil surface (Hossain *et al*., 2006, 2009b).

Although the spudcans are closer being circular in plan, SNAME (1994, 1997, 2002, 2008), bearing capacity coefficients are still largely based on the factors developed for surface strip footings (Prandtl, 1921; Davis and Booker, 1973) and then adjusted for shape and embedment depth following the semi empirical approach of Skempton (1951) and Brinch Hansen (1970).

SNAME (1994, 1997, 2002, 2008) estimated the maximum depth of cavity from solutions for the stability of an open hole above the spudcan by recommending conservative solutions by Meyerhof (1972) in accordance to Rankine pressures for uniform undrained shear strength and an upper bound plasticity solutions of Britto and Kusakabe (1982, 1983) for normally consolidated or lightly over-consolidated soil where the undrained shear strength increases markedly with depth as presented in Figure 1.10. The degree of backflow above a penetrating spudcan is currently expressed in terms of a stability number, N_s, as:

$$N_s = \frac{\gamma' H_w}{s_u} \tag{1.10}$$

Where γ' is the soil effective unit weight, H_w is the maximum cavity depth at which wall failure is initiated and s_u is the homogeneous undrained shear strength. SNAME (1994, 1997, 2002, 2008) also suggested that for non-homogeneous clay the average undrained shear strength over the depth of the cavity should be adopted. With the maximum cavity depth, H_w, as presented in equation 1.11, the effective overburden stress in terms of p'_o can be determined.

$$H_w = \frac{N_s s_u}{\gamma'} \tag{1.11}$$

Unfortunately, the spudcan penetration is still generally assessed by the bearing

capacity profile obtained from a series of "wished in place'' spudcans at successively increasing depths (Endley *et al*., 1981). Similarly, the effects of lattice leg or truss-work on spudcan bearing response and penetration are also not addressed and examined.

1.4 OBJECTIVES AND SCOPES OF THIS STUDY

Nowadays, most of the world's offshore drilling operations are performed using jack-up platforms. Jack-up rigs are getting larger and expanding their geographical areas of operations and situating in a location throughout the year in harsher environments, being functioned frequently in tandem with fixed structures and installing new flexible platforms and evolving into semi-permanent production platforms (Hambly *et al*., 1990; Hampson and Power, 1992; Henriques and Petrobras, 1995; Veldman and Lagers, 1997). Even though these units were initially designed for shallow waters, there is still an increasing demand for their functions in deeper waters (Carlsen *et al*., 1986; Bennett and Sharples, 1987; Veldman and Lagers, 1997). In order to fulfill with all these increasing and extending roles as well as to avoid excessive pessimistic design, it is currently imperative to envisage seabed behavior prior to installation during deep penetration especially in the bearing capacity problem. In view of this addressed issue, research study has been implemented or conducted at National University of Singapore to investigate or examine the spudcan lattice leg interaction mechanism. This study is also parted of an industrial collaboration with America Bureau of Shipping (ABS). The objectives of this research are:

1. To assess the influence of lattice legs on spudcan bearing response and penetration for both normally consolidated and over-consolidated clays.

2. To identify an effective method of estimating the bearing response due to the interaction between spudcan and lattice legs.

In view of the complexity of simulating the spudcan bearing capacity problem numerically associated with large soil deformation, centrifuge modeling technique has been adopted in this study. This modeling technique permits a proper simulation of the whole process of spudcan operation using small scaled models in the laboratory with significant reduction in soil consolidation period.

In the present study, a single spudcan was investigated on the centrifuge models of normally consolidated and over-consolidated remoulded Malaysian kaolin clay. The role of kaolin clay allows relatively fast consolidation of large specimen from a slurry state. The simulation mainly comprises of spudcan penetration with and without lattice legs or truss-work. The spudcan with and without lattice legs and truss-work was installed in-flight to a depth of approximately 1.5 times spudcan diameter under undrained condition for both normally consolidated and over-consolidated clays. Finally, based on the outcomes or results obtained from centrifuge testing, a more effective method of evaluating spudcan bearing capacity and penetration was presented.

1.5 STRUCTURE OF DISSERTATION

Chapter 2 includes a literature review relevant to the behavior of jack-up footing subjected to purely vertical loading on cohesive soils. The fundamentals of quantifying vertical bearing capacity during preloading and installation are discussed in details. This thesis is mainly based on revealing bearing responses and bearing capacity coefficients during footing penetration. Recent worldwide experimental works in this specific area will be presented. Publications, which are devoted to

depict soil characteristics and bearing capacity from numerical analysis, have also been discussed.

Chapter 3 elaborates the techniques used in this research. The discussion can be summarized as follows: (1) centrifuge modeling techniques, (2) development of scaling laws and (3) probable effects of centrifuge scaling. Firstly, it outlines the design, construction and operation of the centrifuge testing apparatus. The arrangements for displacement instrumentation, data acquisition and computerized control of the apparatus are summarized. Secondly, the clay specimen preparation techniques in terms of normally consolidated and over-consolidated clays used for the physical modeling program will be reported accordingly. Finally, test strategies and procedures will be closely followed and described.

Chapter 4 contains a detailed explanation of the results of the centrifuge tests performed using the apparatus, strategies and procedures mentioned in Chapter 3. This chapter is completely dedicated to an in-depth analysis of experimental results. The results from successful centrifuge tests and finite element analyses by other researchers can be coupled together to form a comparative story so that some significant conclusions can be drawn in the coming chapter.

Chapter 5 summarizes the important conclusions from this works and provides some suggestions for future research.

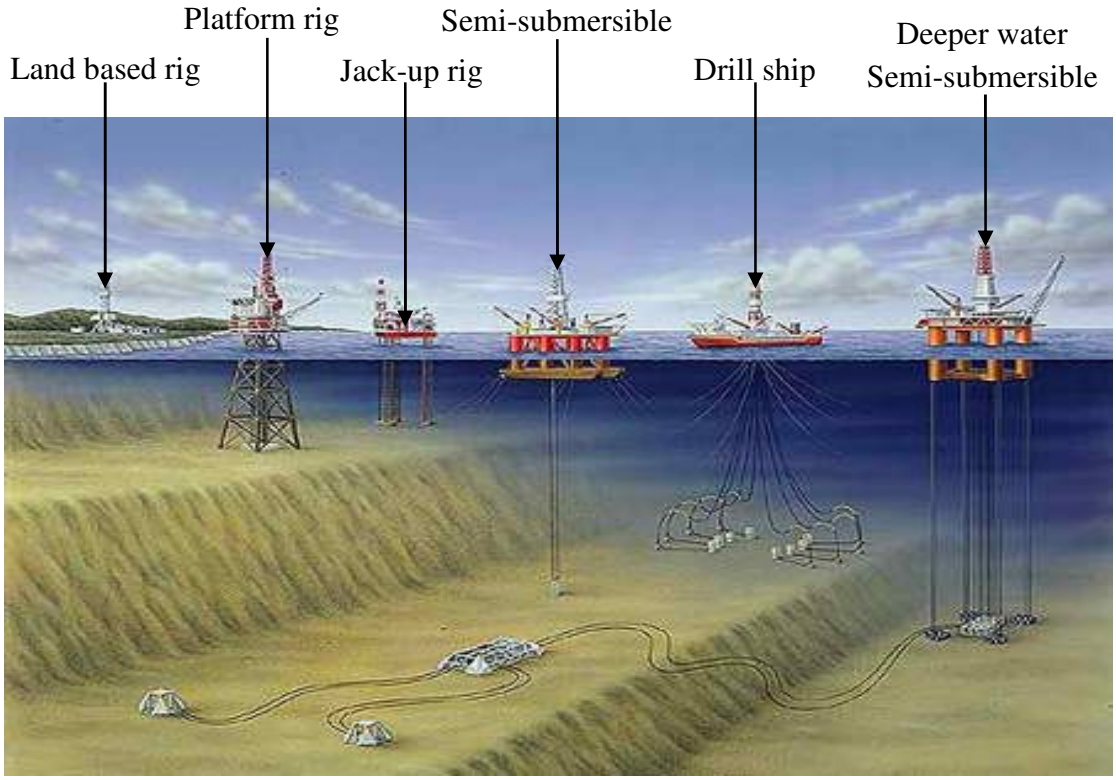

Figure 1.1 Types of drilling rigs

Figure 1.2 Mobile jack-up rig in operation

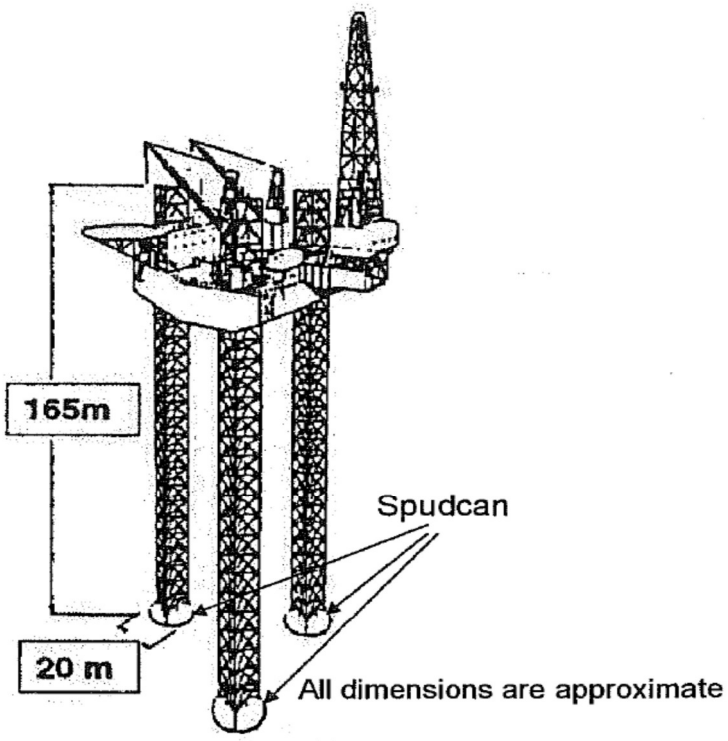

Figure 1.3 Mobile jack-up rig in an elevated position (after Kee and Ims, 1984)

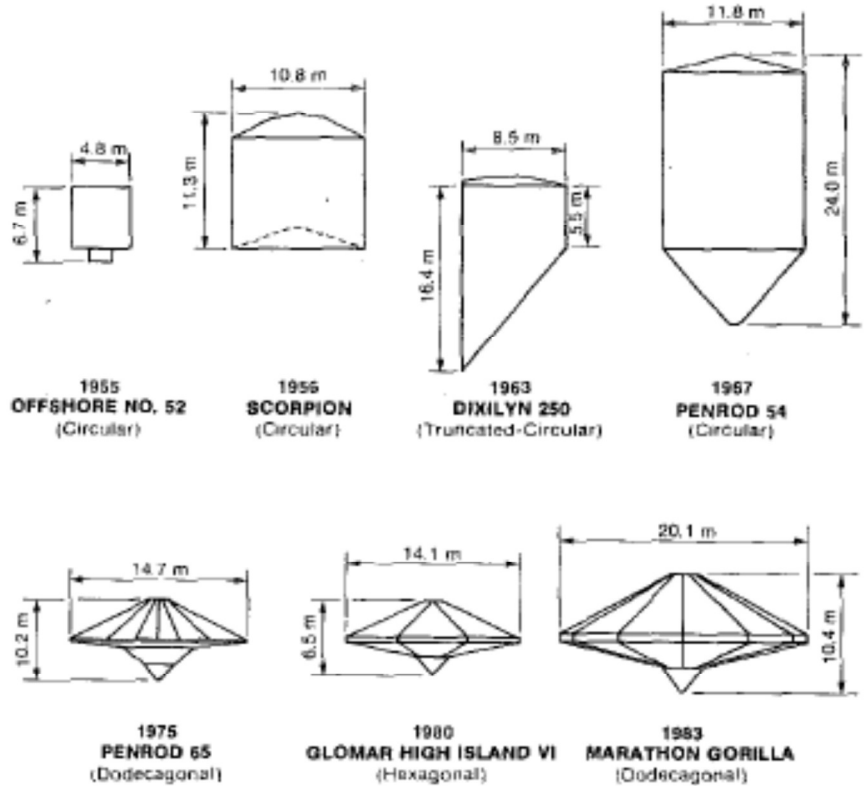

Figure 1.4 Examples of typical spudcan footings (after McClelland *et al.*, 1981)

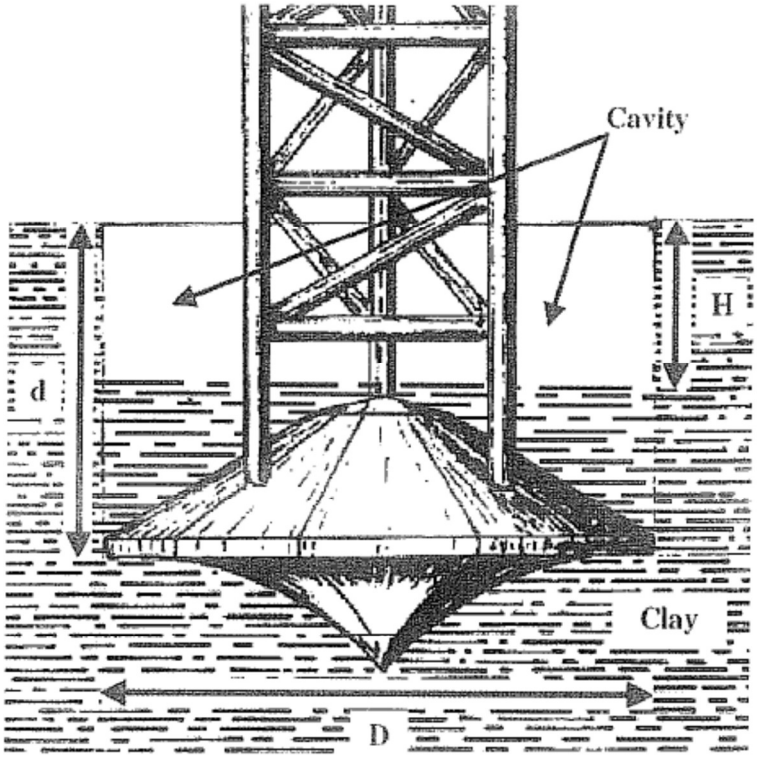

Figure 1.5 Spudcan supported jack-up rig on clayey seabed (after Le Tirant, 1979)

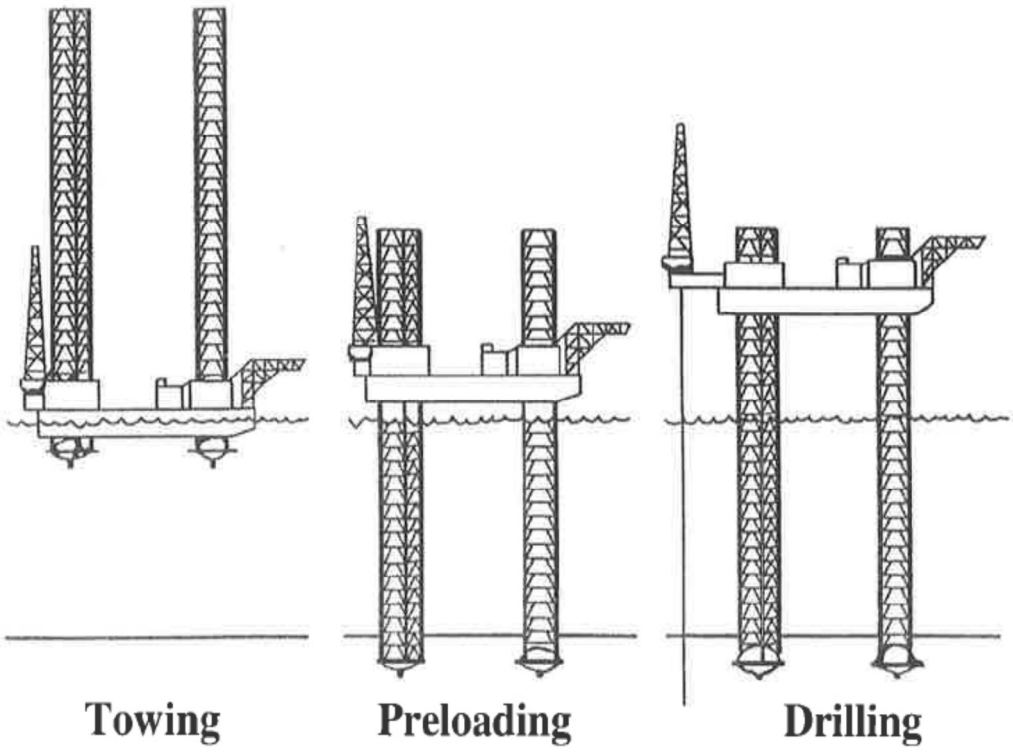

Figure 1.6 Jack-up installation procedures(after Young *et al.*, 1984)

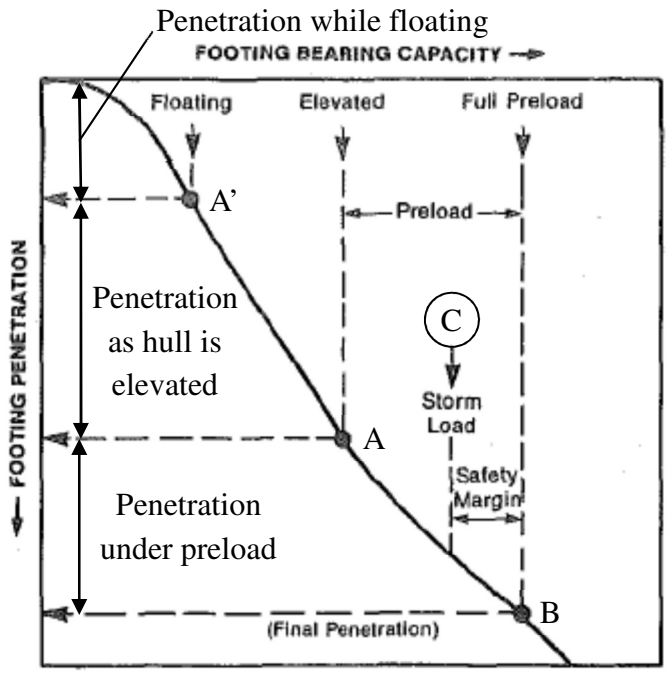

Figure 1.7 Installation and preloading of footings in normally consolidated clays (after Young *et al.*, 1984)

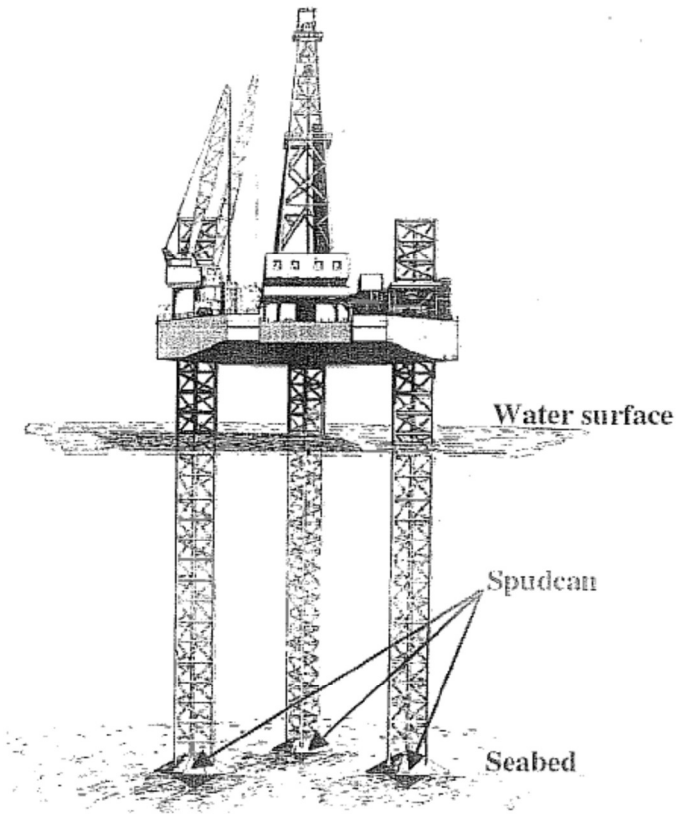

Figure 1.8 Typical tripod jack-up rig rests on the seabed (after Le Tirant, 1979)

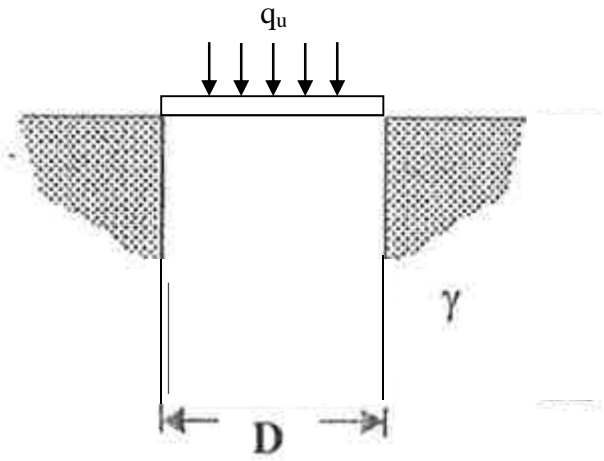

$$q_u = s_u N_c$$

Figure 1.9a Bearing response of footing on the clay surface

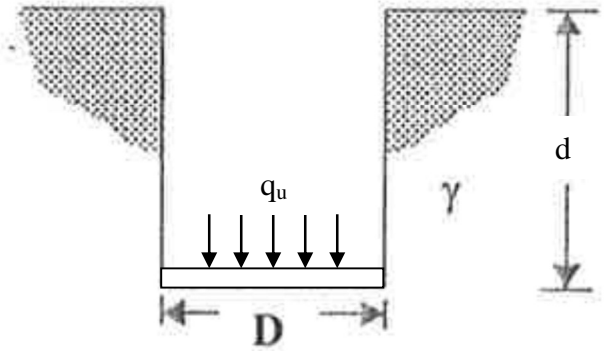

$$q_u = s_u N_c + \gamma d$$

Figure 1.9b Bearing response of footing in clay

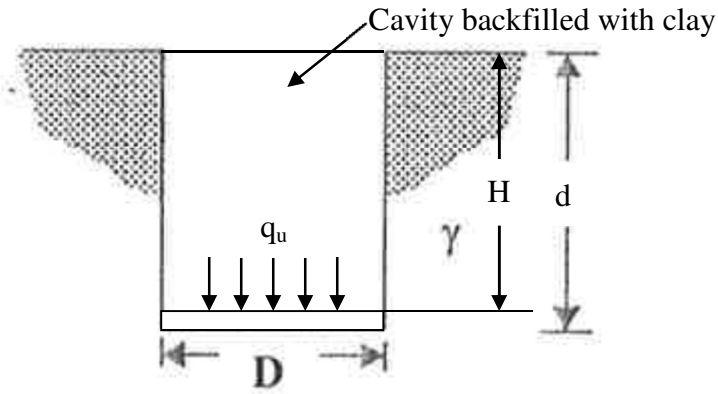

$$q_u = s_u N_c + \gamma' d - \gamma'(d - H)$$

Figure 1.9c Bearing response of footing in clay with backfilled soil

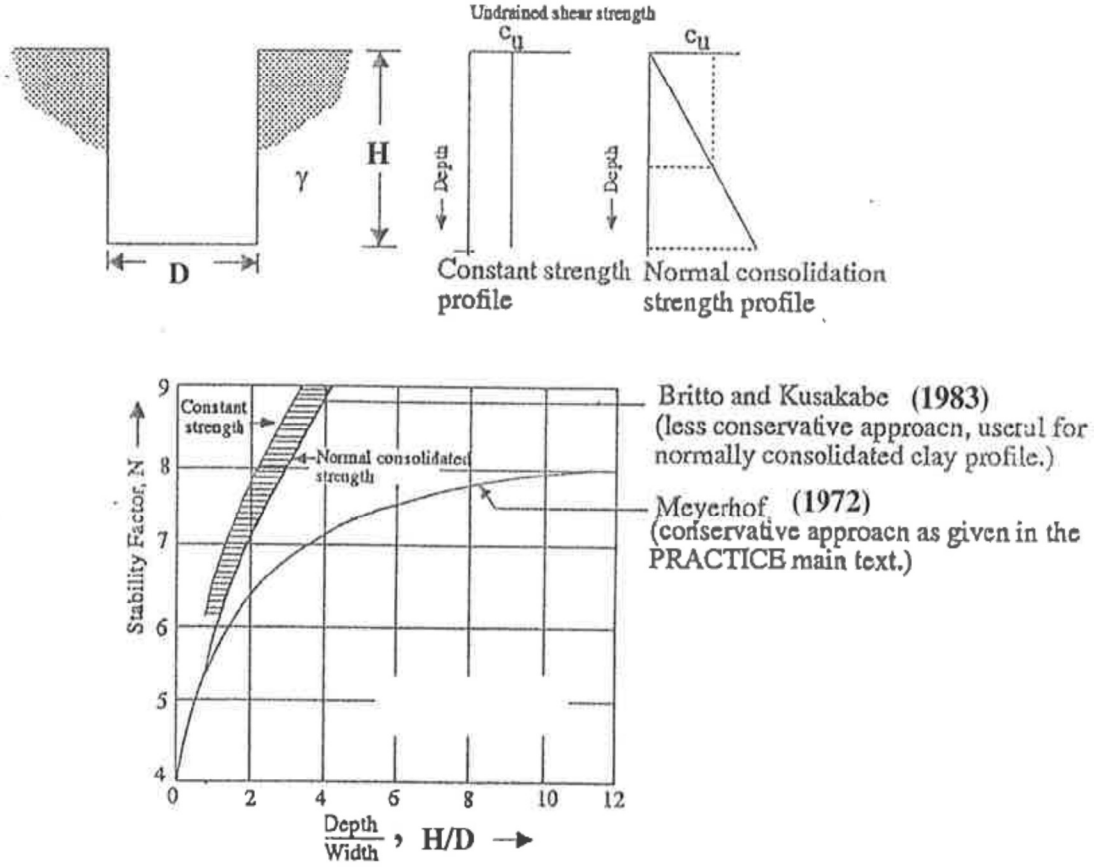

Figure 1.10 Stability numbers for cylindrical excavations in clay (after SNAME, 1994, 1997, 2002, 2008)

CHAPTER 2 LITERATURE REVIEW

2.1 OVERVIEW

This chapter surveys previous works which have been done on the performance of jack-up footing in clay. Issues relating to bearing capacity during preloading and installation will be reviewed in detail.

More specifically, previous works on the effects of spudcan penetration, operations and extraction will be elaborated. This includes centrifuge modeling, numerical modeling and field measurements.

As shown in Table 2.1, many studies investigating spudcan behavior have been conducted over the past two to three decades and a substantial number relied upon centrifuge modeling. During the late 1980s and early 1990s, the studies concentrated on the behavior of a single spudcan under cyclic loading in sand (James and Tanaka, 1984; Tan, 1990; Santa Maria, 1988; Ng, 1999; Ng *et al.*, 1994, 1996, 1998, 2002). Subsequently, Dean *et al.* (1995, 1997b, 1998) extended the research to a three legged jack-up model using drum centrifuge and numerical modeling. Spudcan fixity under combined loading was also studied (e.g. Martin, 1994; Martin and Houlsby, 2000, 2001) using plasticity solutions and verified by 1g laboratory tests. Later, the research was extended to two-dimensional jack-up rig model and simplified wave loading (Martin and Houlsby, 1999; Cassidy, 1999). Recently, three-dimensional numerical model incorporating dynamic analysis and environmental loading is conducted at the Centre for Offshore Foundation System (COFS) of University of Western Australia (e.g. Vlahos *et al.*, 2005; Bienen and Cassidy, 2005, 2009a, 2009b; Bienen, 2009).

Much of the studies to date relate only to spudcans without lattice. Spudcans with lattice legs have not been extensively studied. Some initial studies were conducted by Springman and Schofield (1998). In addition, Menzies and Roper (2008) also used some jack-up rig cases in the Gulf of Mexico to examine the significance of lattice legs in spudcan behavior.

2.2 DESIGN METHODOLOGY – CURRENTLY USED BEARING CAPACITY RELATIONS FOR SPUDCAN FOOTING

2.2.1 SKEMPTON (1951)

Skempton's (1951) relation has been widely used to predict the jack-up footing penetrations (e.g. SNAME, 1994, 1997, 2002, 2008; ISO, 2003). The basic form of Skempton's (1951) bearing capacity equation for an equivalent circular spudcan shape without soil backflow is listed as follows:

$$q_u = 6\left(1 + 0.2\frac{d}{D}\right)s_{uavg} + \gamma'_{avgH}H + \frac{\gamma'_{avg}V}{A} \qquad (2.1)$$

Where D is the spudcan diameter, d is the penetration depth of the maximum cross sectional area of spudcan from surface, q_u is the undrained bearing capacity, s_{uavg} is the average undrained shear strength at 0.5D beneath the maximum cross section of the spudcan (Young *et al.*, 1984), H is the limiting cavity depth, V is the embedded volume of spudcan, A is the largest cross sectional area of the spudcan, γ'_{avgH} is the average submerged unit weight from the surface to the depth of the spudcan cavity and γ'_{avg} is the average submerged unit weight of soil displaced by the spudcan. If the soil above the spudcan backflows and fills the spudcan cavity completely, the term

$\gamma'_{avgH}H$ vanishes and equation 2.1 simplifies to:

$$q_u = 6\left(1 + 0.2\frac{d}{D}\right)s_{uavg} + \frac{\gamma'_{avg}V}{A} \quad (2.2)$$

The depth factor $\left(1 + 0.2\frac{d}{D}\right)$ is limited to values less than or equal to 1.5 for both equations 2.1 and 2.2 for normally consolidated clays whose undrained shear strength profiles increase gradually with depth (Gemeinhardt and Focht, 1970; Young *et al.*, 1984).

2.2.2 HANSEN (1970)

The bearing capacity method proposed by Hansen (1970) was initially used by Fugro-McClelland Marine Geoscience to compute penetration resistance for jack-up rig spudcan foundations. Hansen's (1970) relation is identical to that of Skempton (1951) with only two significant differences:

(1) Hansen proposed a bearing capacity coefficient of 5.14 instead of 6and;

(2) Average shear strength value corresponding to a smaller depth.

The general expression of Hansen's (1970) bearing capacity equation for computing spudcan penetration with no soil backflow is listed as follows:

$$q_u = 5.14\left(1.2 + 0.4\tan^{-1}\frac{d}{D}\right)s_{uavg} + \gamma'_{avgH}H + \frac{\gamma'_{avg}V}{A} \quad (2.3)$$

where s_{uavg} is the average undrained shear strength to 0.25D beneath the maximum cross section of the spudcan. If spudcan cavity is completely backfilled, the equation 2.3 reduces to:

$$q_u = 5.14\left(1.2 + 0.4\tan^{-1}\frac{d}{D}\right)s_{uavg} + \frac{\gamma'_{avg}V}{A} \quad (2.4)$$

2.2.3 HOULSBY AND MARTIN (2003)

Based on bearing capacity analysis incorporating spudcan tip features such as cone angle, cone roughness, embedment depth and rate of undrained shear strength increasing with depth, Houlsby and Martin (2003) proposed a bearing capacity equation for spudcan penetration resistance with no soil backflow:

$$q_u = N_{co}s_{uo} + \gamma'_{avgH}H + \frac{\gamma'_{avg}V}{A} \quad (2.5)$$

where N_{co} is the bearing capacity coefficient and s_{uo} is the shear strength at depth corresponding to the maximum cross-sectional area of spudcan. If there is complete soil backflow, equation 2.5 becomes:

$$q_u = N_{co}s_{uo} + \frac{\gamma'_{avg}V}{A} \quad (2.6)$$

The bearing capacity factor, N_{co}, for linearly increasing undrained shear strength profiles with depth and smooth and rough footings can be derived using the relations:

$$N_1 = 5.69\left[1 - 0.21\cos\left(\frac{\beta}{2}\right)\right]\left(1 + \frac{d}{D}\right)^{0.34} \quad (2.7)$$

$$N_2 = 0.5 + 0.36\left[\frac{1}{\tan\left(\frac{\beta}{2}\right)}\right] - 0.4\left(\frac{d}{D}\right)^2 \quad (2.8)$$

$$N_{co\alpha} = \left(N_1 + N_2\frac{D\rho}{s_{uo}}\right)\left[1 + (0.212\alpha - 0.097\alpha^2)\left(1 - 0.53\frac{d}{d+D}\right)\right] \quad (2.9)$$

$$N_{co} = N_{co\alpha} + \frac{\alpha}{\tan\left(\frac{\beta}{2}\right)}\left[1 + \frac{1}{6\tan\left(\frac{\beta}{2}\right)}\frac{D\rho}{s_{uo}}\right] \quad (2.10)$$

Where α is a dimensionless roughness factor for soil spudcan interface, β is the angle of spudcan tip and ρ is the rate of shear strength increasing with depth. However, if there is more than one cone angle for a spudcan such as β_1 and β_2, the largest cone angle, β_2, coincident with the majority of the spudcan volume shall be adopted (see Figure 2.1).

2.2.4 HOSSAIN *et al.* (2006)

Using results from centrifuge models and numerical analyses, Hossain *et al.* (2006) proposed a bearing capacity equation for spudcan at shallow depth with an open cavity:

$$q_u = N_{co}s_{uo} + \gamma'_{avgH}H_{cr} + \frac{\gamma'_{avg}V}{A} \quad (2.11)$$

where N_{co} is given by

$$N_{co} = \left[1 + \frac{d}{1.3D}\left(1 - \frac{d}{4D}\right)\right]N_{cm} \quad (2.12)$$

N_{cm} is the bearing capacity factor at the surface, s_{uo} is the shear strength at the depth corresponding to the maximum cross-sectional area of spudcan and H_{cr} is the critical depth at which the spudcan cavity remains stable. In cases of complete soil backfill, Hossain *et al.* (2006) proposed the following:

$$q_u = N_{cd}s_{uo} + \frac{\gamma'_{avg}V}{A} \quad (2.13)$$

where N_{cd} is the bearing capacity coefficient for deep spudcan embedment and is given by:

$$N_{cd} = 10\left(1 + 0.075\frac{d}{D}\right) \qquad \text{For } \frac{H_{cr}}{D} < \frac{d}{D} \leq 2 \tag{2.14}$$

$$N_{cd} = 11.5 \qquad \text{For } \frac{d}{D} > 2 \tag{2.15}$$

2.3 PREVIOUS SPUDCAN WORKS

Previous works in this area can be broadly classified into four categories:

(i) High g model studies,

(ii) 1g model studies,

(iii) Fully theoretical and numerical studies, and

(iv) Field data study.

2.3.1 HIGH g MODEL STUDIES (WITH AND WITHOUT THEORETICAL AND NUMERICAL SUPPORTING STUDIES)

2.3.1.1 James and Tanaka (1984) and James and Shi (1988)

James and Tanaka (1984) and James and Shi (1988) studied spudcanon dry sand beds using centrifuge models. The spudcan model represented a maximum prototype diameter of 7.2m with limited penetration. Their findings led to dimensionless

bearing capacity coefficients that were about three times than those obtained using 1g tests. These were also equivalent to a variation in mobilized angle of friction between 0° and 6°, reflecting a decrease in the amount of dilation in sand at field stress levels when compared with traditional 1g models.

2.3.1.2 Craig and Chua (1990a)

Craig and Chua (1990a) studied the penetration of the spudcan footings into uniform and stratified deposits using centrifuge models. In the experiments, a 140mm-diameter model spudcan was penetrated into uniform consolidated clay beds with different undrained shear strengths. The characteristic undrained shear strengths were deduced from the water content of the soil. Craig and Chua (1990a) observed that the cavity above the spudcan remained vertical up to0.9D.

2.3.1.3 Craig and Chua (1990b, 1991)

Craig and Chua (1990b, 1991) also examined soil flow around a penetrating spudcan using dry spaghetti markers inserted vertically into the clay bed across the strongbox centerline as non-reinforcing flexible indicators of gross deformation. The sample was bisected post-test to reveal the deformation of the spaghetti markers. Figure 2.2(a) and (b) present the photographs of soil deformation below and around the spudcan footing in clay with undrained shear strength of 29 kPa at penetrations around 0.75D and 1.6D respectively. At a shallow penetration of 0.75D (Craig and Chua, 1990b), the cavity formed in the clay bed remained open and lateral distortion due to soil flow was visible but confined within three radial distances of the spudcan centerline. At a deeper penetration of 1.6D (Craig and Chua, 1991), the clay wedge was forced down with the footing and this resulted in the clay flowingaround the footing from base to the footing top. In case of layered soils especially where sand overlies clay, soil plug was observed in 1g models whereas a completely different

mechanism of vertical punching was observed in high-g centrifuge models.

2.3.1.4 Tani and Craig (1995)

Tani and Craig (1995) reported a study comprising of centrifuge model tests under 100g condition and theoretical analysis using stress characteristics. The objective of the study was the bearing capacity of smooth and rough circular foundations on soft clay with strength increasing with depth. Model clay beds, each 410mm thick, were prepared by hydraulic gradient method (Zelikson, 1969) to produce a final effective consolidation stress of 20 kPa and 420 kPa at top and bottom respectively. Undrained shear strength was measured using an in-flight cone penetrometer. The measured bearing capacity coefficients matched well with those of Houlsby and Wroth (1983) for smooth footing. However, the shape and depth factors were strongly influenced by the degree of strength non-homogeneity of clay, $\frac{kD}{s_{uo}}$ (Davis and Booker, 1973; Dyvik *et al.*, 1989). In other words, the bearing capacity coefficient was directly affected by the degree of strength non-homogeneity as well.

2.3.1.5 Dean *et al.* (1998)

Dean *et al.* (1998) reported drum centrifuge tests of model three-leg jack-ups on kaolin clay. The tests modeled one prototype jack-up with 6.5m diameter 13° conical spudcans, one with 6.5m diameter flat based spudcans and one with 13m diameter flat based spudcans. Speswhite kaolin clay bed was pre-consolidated to an overburden effective stress of 600 kPa so that the final depth was approximately twice the footing diameter. Water was introduced at lower gravity through the sand layer surrounding the clay. Undrained shear strength was measured by a hand driven miniature vane after completion of footing tests in 1g environment and the results are shown in Figure 2.3. Slightly different strengths were measured at identical gravity

of 128g. The bearing responses during both preloading and reloading at both 128g and 256g was in good agreements, see in Figure 2.4. This indicates an absence of footing size effect. Although prototype times required in preloading were longer than typical model preloading periods at field scales, little or no drainage of the clay was anticipated during the model preloading.

2.3.1.6 Springman and Schofield (1998)

Springman and Schofield (1998) reported a series of centrifuge tests on a single latticed jack-up platform with soft kaolin clay in 100g environment. The single jack-up platform forms 80% of the area of the spudcan horizontal projected area while the open lattice leg comprises of 42% of the equivalent square solid leg. The single latticed jack-up platform was installed by self-weight penetration with means of a drive chain and a series of pulley wheels. The remoulded kaolin clay was prepared by a three-stages consolidation process: firstly uniform stress of 110 kPa, secondly downward hydraulic gradient (Philips, 1988) to create steady water pressure of 50 kPa at the surface to 0 kPa at the base and finally both uniform stress of 225 kPa and downward hydraulic gradient to produce steady pore pressure of 165 kPa at the surface to 0 kPa at the base. From the centrifuge experiments, the shear forces, which were obtained by differentiation of measured bending moments, at the bottom of the lattice leg did not agree with the theoretical values even though the shear forces at the top of lattice leg coincided with the theoretical ones. Owing to these differences, the lattice leg may be viewed as a pile embedded in the soil and appeared to rotate at a certain location along the pile when subjected to lateral loading instead of vertical loading. All of the lateral loads had been distributed onto clay when the lattice legs were embedded in soil and the bottom moment connection is equivalent to zero (Dean *et al.*, 1993). Springman and Schofield (1998) also confirmed that the portion of lattice leg with clay infill was also observed after the test and the lattice leg was forcibly acting on the vertical soil surface to squeeze soil through the lattice leg

instead of flowing into the lattice to close the gap. This also agreed well with the suggestion that the lattice legs provided some temporary resistance to soil backflow. However, only lateral loading was applied to the jack-up. Since the square lattice leg tended to yield a higher net ultimate lateral pressure with no reduction at shallower depths, the values of less than $9s_u$ should be used as benchmark values against the centrifuge values. More importantly, the data measured in the centrifuge were roughly two-thirds of those predicted theoretically using limiting lateral pressure of $9s_u$. In other words, the value of $9s_u$ should not be adopted when there was only small fraction of mobilized lateral thrust at greater depths.

2.3.1.7 Hossain *et al.* (2003, 2004a, 2005b, 2006) and Hossain and Randolph (2008, 2009a, 2009b, 2010a)

Hossain *et al.* (2003, 2004a, 2005b, 2006) and Hossain and Randolph (2008, 2009a, 2009b, 2010a) reported the centrifuge model tests incorporating with particle image velocimetry and close range photogrammetry (White *et al.*, 2001a, 2001b, 2003), together with large deformation finite element analysis (Carter and Balaam, 1990; Hu and Randolph, 1998a, 1998b) on homogeneous and non-homogeneous clays to investigate the limiting depth of spudcan cavity. Hossain *et al.* (2003, 2004a, 2005b, 2006) and Hossain and Randolph (2008, 2009a, 2009b, 2010a) had showed that the maximum cavity depth is controlled by the bearing capacity and flow failure instead of wall failure of cavity. They also proposed the relations to estimate the limiting cavity depth of the spudcan, H_{cr}:

$$\frac{H_{cr}}{D} = \left[\left(\frac{s_{um}}{\gamma' D}\right)^{\left(1-\frac{k}{\gamma'}\right)}\right]^{0.55} - \frac{1}{4}\left(\frac{s_{um}}{\gamma' D}\right)^{\left(1-\frac{k}{\gamma'}\right)} \qquad (2.17)$$

For shallow penetration prior to any backflow ($d \leq H_{cr}$), the bearing capacity coefficients, N_c, is related to the penetration resistance by:

$$q_u = N_c s_{uo} + \gamma' d + \gamma' \frac{V}{A} \quad (2.18)$$

For penetration depths larger than the limiting cavity, the bearing capacity coefficients are given by:

$$q_u = N_{cd} s_{uo} + \gamma' \frac{V}{A} \quad (2.19)$$

$$N_{cd} = 10\left(1 + 0.065\frac{d}{D}\right) \leq 11.3 \quad (2.20)$$

Lattice legs were not modeled in Hossain *et al.*'s (2003, 2004a, 2005b, 2006) and Hossain and Randolph's (2008, 2009a, 2009b, 2010a) studies.

2.3.2 1g MODEL STUDIES (WITH AND WITHOUT THEORETICAL AND NUMERICAL SUPPORTING STUDIES)

2.3.2.1 Santa Maria (1988) and Santa Maria and Houlsby (1988)

Santa Maria (1988) and Santa Maria and Houlsby (1988) reported a 1g model testing program involving monotonic and cyclic loadings. Four types of footings, namely flat plate, a 120° cone, a 60° cone and a 50mm-diameter spudcan were studied. Kaolin clay samples were consolidated under a maximum pressure of 200 kPa. Miniature vane shear tests were conducted on the clay sample after the completion of each test. These showed that the undrained shear strength of the soil was uniform at about 10 kPa throughout the sample thickness.

2.3.2.2 Houlsby and Martin (1992)

Houlsby and Martin (1992) conducted 1g model studies into spudcan foundations under vertical and combined loadings. A model spudcan of 100mm diameter with a basic cone angle of 154° and sharper 76° conical tip was studied. Speswhite kaolin slurry was consolidated at pre-consolidation pressure of 200 kPa and finally followed by a 15mm high water level, which was maintained to prepare heavily over-consolidated clay deposit. The observed vertical bearing capacity was found to compare well with theoretical prediction from Wroth and Houlsby (1985). As the experiments were conducted in 1g environment, the effects of overburden pressure and soil backflow were not correctly modeled.

2.3.2.3 Martin (1994) and Martin and Houlsby (2000)

Martin (1994) and Martin and Houlsby (2000) also reported a series of laboratory tests carried out in 1g condition. The 125mm diameter Dural footing was fabricated in accordance with the representative spudcan profile adopted for the joint industry study of jack-up foundation fixity (Noble Denton Associate, 1987). The tests were performed on a heavily over-consolidated kaolin clay sample (Houlsby and Martin 1992). A 15mm high water level covered the entire clay samples after consolidation and during testing. The clay beds were prepared so that their undrained shear strengths, measured by miniature vane shear test, profile followed that given by Ladd *et al.*'s (1977) and Wood's (1990) relations:

$$\frac{s_u}{\sigma'_v} = 0.25\mathrm{OCR}^{0.75} \qquad (2.16)$$

Footing loading and reloading tests were performed with a consistent velocity of

0.33mm/sec and penetration depths up to 1.6 times diameters. However, although soil backflow occurred after 1D, backfilled soil above the spudcan did not have a significant influence on the measured vertical load during the test because of the 1g nature of the laboratory tests.

2.3.2.4 Vlahos *et al.* (2005)

Vlahos *et al.* (2005) reported the results from a series of 1g model tests conducted using a 1:250 scaled three legged jack-up unit model, equipped with three 72mm diameter spudcan footings on normally consolidated soft clays. Heavily over-consolidated clay was prepared by consolidation up to a final overburden pressure of 110 kPa. The jack-up unit was installed at a consistent rate of 1.5mm/sec. Soil characterization tests were undertaken using a T-bar penetrometer, both before and after completion of footing penetration tests. The strength profiles indicated a 5 to 10% change between pre-test and post-test undrained shear strength as in Figure 2.5.

2.3.3 FULLY THEORETICAL AND NUMERICAL STUDIES

2.3.3.1 Hu and Randolph (1999), Hu *et al.* (2001) and Mehryar *et al.* (2002)

Soil flow mechanism during foundation continuous penetration was studied by Hu and Randolph (1999) and Hu *et al.* (2001). In their numerical studies, a smooth flat circular plate was penetrated into normally consolidated clay with the strength increasing linearly with depth. Soil flow mechanisms illustrated that the soil initially

flowed towards the top until $\frac{d}{D}$ exceeded 2. The zone of lateral deformation around the plate edge was approximate 0.6R to 0.7R for smooth and rough interfaces respectively. From continuous penetration and pre-embedded analyses, Mehryar *et al.* (2002) also studied soil flow mechanisms during penetration of a smooth spudcan using upper bound plasticity analysis. Localized soil flow was found to initiate at $\frac{d}{D} > 1.27$. The analyses indicated that smooth and rough interfaces led to very different soil flow. The lateral extent of the disturbed zone around the plate edge was about 1R, which was longer than that from finite element analysis.

2.3.3.2 Martin and Randolph (2001)

Martin and Randolph (2001) conducted the upper and lower bound analyses for surface and buried flat plate circular foundation with the predicted soil collapse mechanisms. Even though this investigation had accounted for the effects of degree of strength non-homogeneity, shape and relative roughness of the footing, it still did not cater for steady state continuous penetration and the cavity effect.

2.3.3.3 Wang and Carter (2002)

Wang and Carter (2002) used the finite element program AFENA to perform large deformation analyses for deep penetration of circular footings into layered clays in order to study the bearing responses, plastic zone development, effects of soil weight and relative thickness of the top layer. The two layers of clays are assumed to have different strengths but the strength is also assumed to remain constant within each layer.

2.3.3.4 Houlsby and Martin (2003)

Houlsby and Martin (2003) used lower bound analysis to determine alternative bearing capacity factors of conical circular foundations. The bearing capacity factors, N_c, were related to the cone angle, cone roughness, embedment depth and the rate of increase of undrained shear strength with depth of the clay. The soil was assumed to be weightless and rigid plastic response while the space above the footing was occupied by a rigid, smooth sided shaft. Consequently, the vertical capacity of the spudcan may be significantly higher than of a real spudcan wherein the soil was free to backflow. Therefore, these results may not be applicable to real spudcan foundations.

2.3.3.5 Salgado *et al.* (2004)

Salgado *et al.* (2004) reported bearing capacity coefficients for deeply embedded flat circular foundations with a rough base using upper and lower bounds finite element analyses. The soil was assumed to be weightless and rigid plastic while the cavity above the spudcan was filled with soil which can either impose an overburden stress on the top of spudcan or else detach from the spudcan. Bearing capacity factors ranging from 11 to 13.7 were obtained. However, the assumption of weightless soil may limit its applicability to real scenarios.

2.3.3.6 Edwards *et al.* (2005)

Edwards *et al.* (2005) reported small strain finite element analyses of embedded rough circular foundation using Imperial College Finite Element Program (ICFEP) (Potts and Zdravkovic, 1999). The soil was modeled using the Tresca model and constant undrained shear strength of 50 kPa with depth. The results of the finite element analyses were in agreement withthose of Martin (2001), Martin and Randolph (2001), Houlsby and Martin (2003) and Salgado *et al.* (2004) for embedded circular foundation. However, these results may not accurately reflect the vertical capacity

of a fully embedded spudcan since the modeling of a smooth sided shaft above the spudcan prevented the soil backfill (Salgado *et al.*, 2004). Furthermore, the assumption of uniform strength may render it inapplicable to real scenarios.

2.3.4 FIELD DATA STUDY

2.3.4.1 Menzies and Roper (2008)

Menzies and Roper (2008) reported a series of back analyses which compared field measurements of spudcan penetration resistance from thirteen locations at Gulf of Mexico with relations of Skempton (1951), Brinch Hansen (1970), Martin and Houlsby (2003) and Hossain *et al.* (2006). They noted that the SNAME (1994, 1997, 2002, 2008) recommended methods, that is Skempton's (1951) and Hansen's (1970) gave reasonable predictions of the average penetration under a given penetration load. On the other hand, Martin and Houlsby's (2003) method tends to predict for a deeper penetration than the measured value whereas Hossain *et al.*'s (2006) method tends to predict a shallower penetration. Two factors affecting the load penetration prediction, i.e. spudcan geometry and spudcan cavity, are also discussed. In conclusion, Menzies and Roper (2008) suggested that delayed soil backflow arising from obstruction by structural trusses and cords of jack-up legs might have affected the penetration resistance. This phenomenon will certainly affect the load penetration response of spudcan foundation varying with depth.

2.4 EXISTING KNOWLEDGE GAP – EFFECT OF LATTICE LEG

From the literature review mentioned earlier, Springman and Schofield (1998) had mentioned the potential effect of lattice leg on bearing response of spudcan such as

load response behavior and bearing capacity coefficient during preloading and penetration stages. Moreover, the latticed spudcan may potentially enhance its bearing capacity since it may be viewed as circular pile (Randolph and Houlsby, 1984). Menzies and Roper (2008) also suggested that the soil backflow could be delayed due to the obstruction of lattice legs after performing the series of back analyses compared with field data from Gulf of Mexico even though after Hossain *et al.* (2006) had confirmed the bearing capacity of spudcan could decrease due to the soil backflow.

With all aforementioned hypothesis, there is currently no centrifuge model or numerical model tests conducted to investigate the effect of the lattice leg on spudcan penetration behavior and bearing capacity coefficient.

Above all, the majority of the studies except Wang and Carter (2002) and Hossain *et al.* (2009) were limited to pre-embedded analysis with no account taken of changes of soil flow regime and complex evolving pattern of soil strengths in the vicinity of the spudcan with and without lattice legs during progressive penetration.

Therefore, in the present study, a single spudcan with or without lattice legs was penetrated to a depth of about 1.5 times spudcan diameter on the centrifuge models of normally consolidated and over-consolidated remoulded Malaysian kaolin clay under undrained condition so that the contribution of lattice legs in terms of spudcan bearing capacity and resistance to soil backflow mechanism can be identified.

Research area	Researcher	Soil type	Modeling technique
Spudcan penetration	Craig and Chua (1990a, 1991)	Sand and clay	Centrifuge
	Finnie (1993)	Calcareous	Centrifuge
	Lu *et al.* (2001)	NC clay	Large deformation FE
	Mehryar *et al*. (2002)	NC clay	Large deformation FE
	Hossain *et al.* (2003, 2004a)	Uniform clay	Centrifuge and PIV
	Hossain *et al.* (2004b)	NC Clay	Large deformation FE
	Barboza-Cruz (2005)	NC Clay	Large deformation FE
	Hossain and Hu (2004, 2005)	Uniform and NC clays	Centrifuge and PIV
	Hossain *et al*. (2005b, 2006)	NC clay	Centrifuge and PIV
	Hossain and Randolph (2008, 2009a, 2009b)	NC clay	Centrifuge, PIV and large deformation FE
	Qiu*et al*. (2010)	Uniform clay	Large deformation FE
Spudcan sliding	Allersma *et al.* (1997)	Sand	Centrifuge
Spudcan versus caisson	Cassidy *et al.* (2004)	Clay	Centrifuge
	Vlahos (2004); Vlahos *et al.* (2005)	Clay	1g model and FE
Spudcan extraction	Craig and Chua (1990b)	Uniform clay	Centrifuge
	Purwana (2006); Purwana *et al.* (2005, 2006, 2008, 2009, 2010)	NC Clay	Centrifuge and PIV
	Zhou (2006); Zhou *et al*. (2009)	NC Clay	FE
	Bienen *et al.* (2009)	NC Clay	Centrifuge
	Gaudin *et al.* (2010a)	NC Clay	Centrifuge

Research area	Researcher	Soil type	Modeling technique
Spudcan punch-through	Finnie and Randolph (1994)	Calcareous	Centrifuge
	Hossain *et al.* (2005a, 2008)	Stiff and soft clays	Centrifuge and PIV
	Teh (2008); Teh *et al.* (2005, 2008, 2009, 2010)	Sand and clay	Centrifuge and PIV
	Tjhayono *et al.* (2008)	Stiff and soft clays	Centrifuge and PIV
	Lee (2009); Lee *et al.* (2009)	Sand and clay	Centrifuge and PIV
	Hossain and Randolph (2007, 2009c, 2010a, 2010b)	Layered clays	Centrifuge, PIV and large deformation FE
	Qiu *et al*. (2010)	Sand and clay	Large deformation FE
Spudcan operation (under combined or cyclic loadings)	James and Tanaka (1984)	Sand	Centrifuge
	Santa and Maria (1988)	Sand	Centrifuge and plasticity solution
	Dean *et al*. (1995, 1997a, 1997b, 1998)	Sand and clay	Centrifuge, FE and plasticity solution
	Tan (1990)	Sand	Centrifuge and plasticity solution
	Byrne and Houlsby (2001)	Sand	1g model and plasticity solution
	Ng (1999); Ng *et al*. (1994, 1996, 1998, 2002)	Sand	Centrifuge and FE
	Martin (1994); Martin and Houlsby (2000, 2001)	Clay	1g model, FE and plasticity solution

Research area	Researcher	Soil type	Modeling technique
Spudcan operation (under combined or cyclic loadings)	Zhang *et al*. (2010)	NC clay	FE
2D jack-up soil wave interaction	Martin and Houlsby (1999)	Clay	Plasticity solution
	Cassidy (1999)	Sand and clay	Plasticity solution
3D jack-up soil wave interaction	Vlahos *et al.* (2005)	Clay	1g model, FE and plasticity solution
	Bienen (2009); Bienen and Cassidy (2005, 2009a, 2009b)	Sand and clay	Plasticity solution
Spudcan footprint interaction	Stewart and Finnie (1991)	Clay	Centrifuge
	Jardine *et al.* (2001)	Clay	FE
	Gaudin *et al.* (2007)	Clay	Centrifuge
	Cassidy *et al.* (2009)	Clay	Centrifuge
	Gan (2010); Gan *et al.* (2007, 2008)	Clay	Centrifuge
Spudcan pile interaction and lateral load transfer	Siciliano *et al.* (1990)	Clay	Centrifuge
	Craig (1998)	Clay	Centrifuge
	Springman and Schofield (1998)	Clay	Centrifuge
	Stewart (2005)	Clay	Centrifuge
	Xie (2009); Xie *et al.* (2006); Xie *et al.*(2010)	Clay	Centrifuge and PIV
	Leung *et al.* (2006, 2008)	Clay	Centrifuge and PIV

Table 2.1 Summary of spudcan researches to date

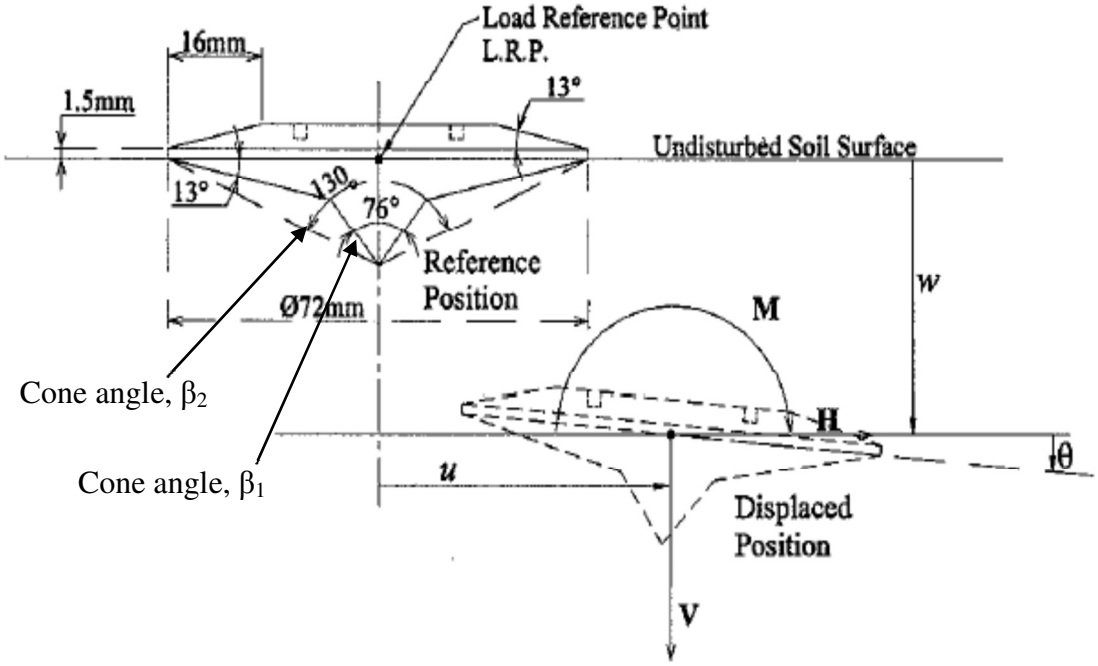

Figure 2.1 Spudcan cone angles (after Vlahos *et al.*, 2005)

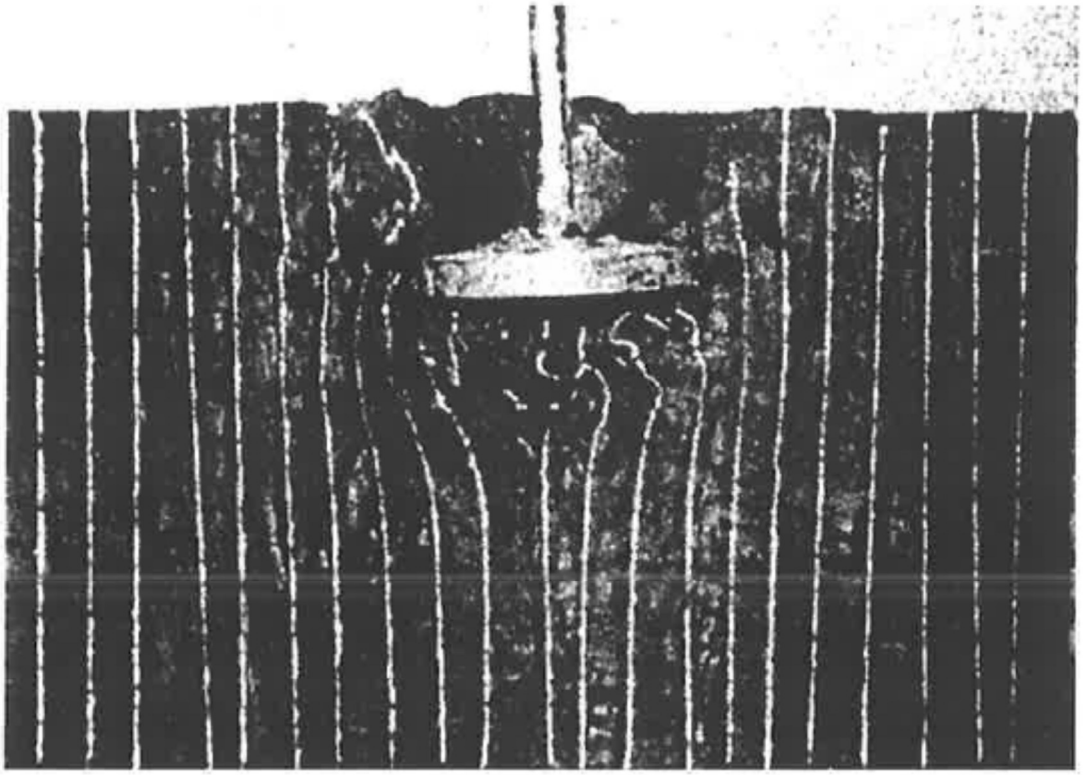

Figure 2.2a Section through the model uniform clay at 0.75D (after Craig and Chua, 1990b)

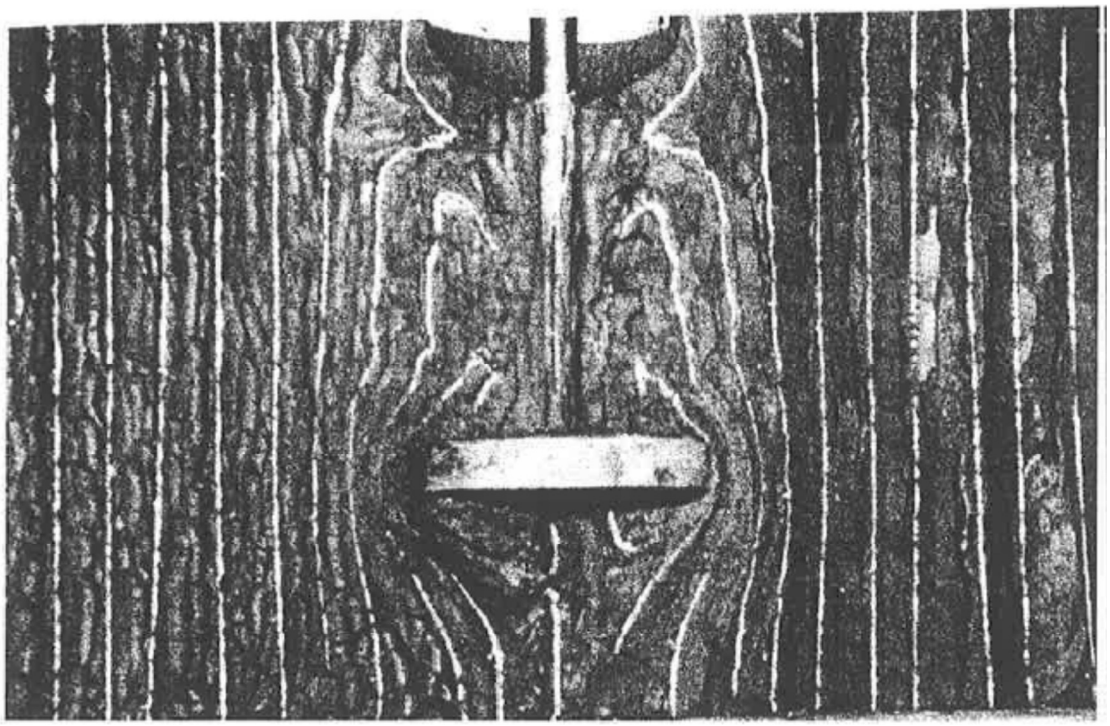

Figure 2.2b Section through the model uniform clay at 1.6D (after Craig and Chua, 1990b)

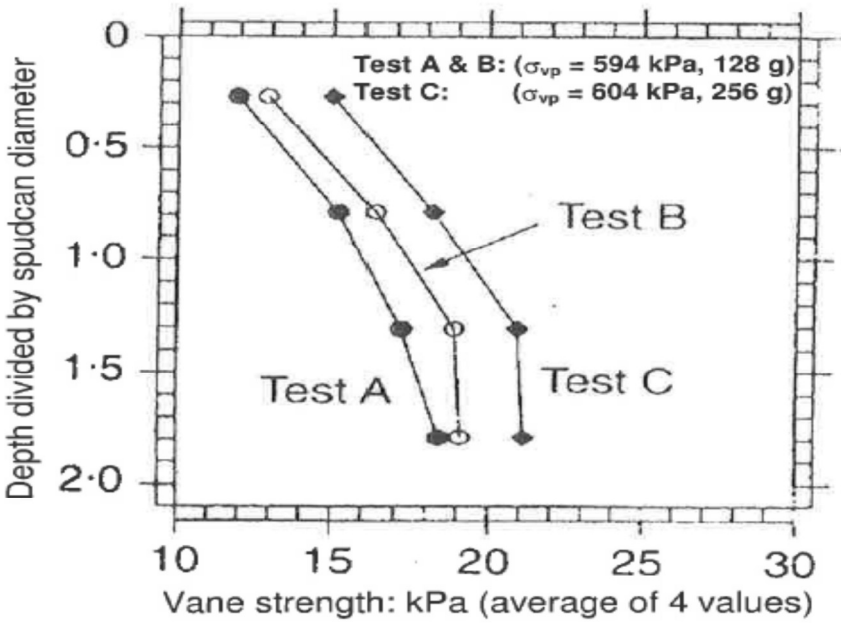

Figure 2.3 Post-test 1g vane strength (after Dean *et al.*, 1998)

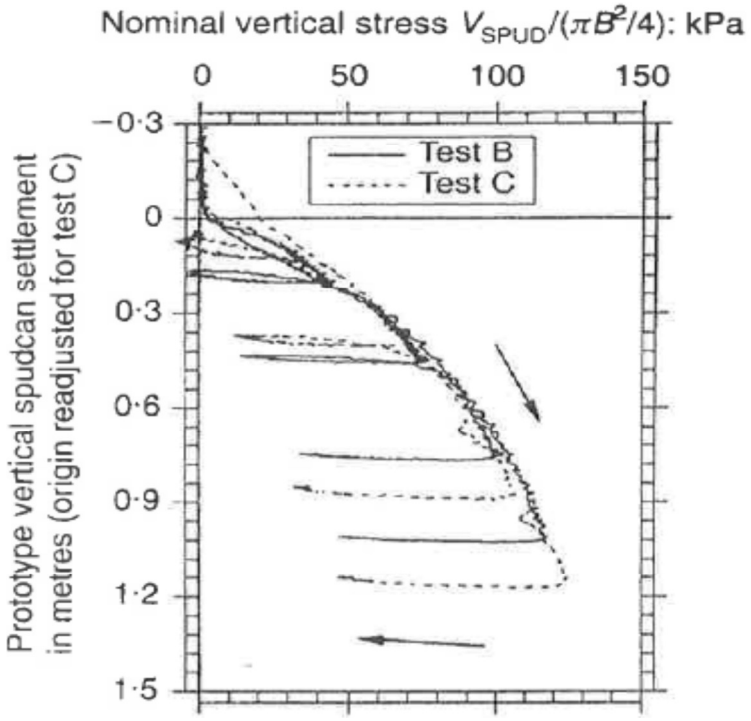

Figure 2.4 Effects of footing diameter on load penetration response (after Dean *et al.*, 1998)

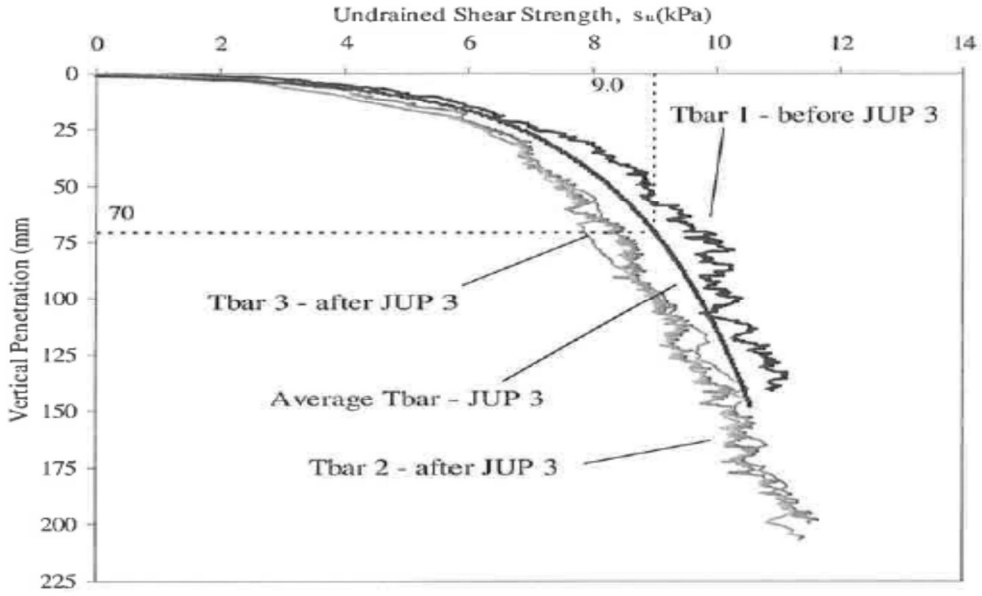

Figure 2.5 Measured undrained shear strength from T bar tests (after Vlahos *et al.*, 2005)

CHAPTER 3 EXPERIMENTAL SETUP AND CLAY SPECIMENS

3.1 GENERAL DESCRIPTION

Firstly, this chapter outlines the design, construction and operation of testing apparatus. The arrangements for load and displacement instrumentation, data acquisition and computerized control of the apparatus are summarized. Secondly, this chapter also describes the testing soil used in centrifuge modeling, sample preparation and evaluation on its basic properties, particularly undrained shear strength and key pressure sensors. Eventually, test strategies and test procedures in this study are presented, together with a focus on tests design with a water layer on top of the soil specimen in the beam centrifuge.

3.2 CENTRIFUGE SCALING CONCEPTS

The centrifuge scaling concepts between small scaled models and full scaled prototype can be derived in two ways such as dimensional analysis and consideration of the governing equations. A list of commonly adopted scaling relations was presented by Leung *et al.* (1991) in Table 3.1 and Garnier *et al.* (2007). It can be observed from Table 3.1 that there will be conflicts in the scaling concepts for different time dependent phenomena in centrifuge modeling. For undrained geotechnical problems in clay which are highly dependent on cohesive strength and gravitational forces, no reasonable modeling accuracy can be achieved without centrifuge modeling (Houlsby and Martin 2003; Hossain *et al.*, 2003, 2004a, 2004b, 2005b; Purwana, 2005, 2006) as 1g test could not generate equivalent overburden stress levels as in the field. Therefore, it will consequently impose soil backflow not

to occur or only occur in deeper penetration. Moreover, the spudcan bearing capacity can be significantly unaffected and induced unreliable outcomes as a result due to the negligible of weights of backfilled soil above the spudcan and overburden soil surcharge under 1g simulation (Endley *et al.*, 1981; Le Tirant and Pérol, 1993; Hossain *et al.*, 2003, 2004a, 2004b, 2005b, 2006). External loadings like bearing stress on a surface foundation can be replicated the normally consolidated and over-consolidated in-situ soil stress properly by means of centrifuge modeling (Stewart and Randolph, 1991; Stewart, 1992) to overcome the abovementioned limitations. Besides simulating the in-situ soil stress correctly, another crucial phenomenon requires to be simulated in the present study is the soil consolidation process. Since the undrained loading process is consistent in speed, the consolidation duration shall not be directly related with dynamic or inertial process but rather with a diffusion process (Tan and Scott, 1985). In this case, the coefficient of consolidation and velocity for both model and prototype scales will be similar. Moreover, the centrifuge modeling principles are well documented (Schofield, 1980; Cooke, 1991; Mitchell, 1991; Taylor, 1995; Muir, 2004; Gaudin *et al.*, 2011) and shall not be described in details. Thus, the function of centrifuge modeling is justifiable and reliable to obtain the accurate results.

3.3 EXPERIMENTAL SETUP

3.3.1 NUS GEOTECHNICAL CENTRIFUGE

All experiments were performed on the National University of Singapore (NUS) geotechnical centrifuge shown in Figure 3.1. The centrifuge comprises mainly of a rotor shaft, a rotating arm and two swing platforms, each has a working area of 750mm by 700mm. The platform, on which the model is to be placed, has a head-room of approximately 1290mm. When the platforms are completely swung up during its operation phase, the radial distance from the center of rotation to the base of the model container is about 2022mm.

The centrifuge is designed to have a payload capacity of 40g-tonnes and a maximum acceleration of 200g. A total of 100 signal rings are equipped on the top of the rotor shaft for signal and power transmission purposes. A twin passage Deublin© hydraulic union is placed above the slip rings supplying a maximum operating pressure of 70 bars (1000 psi). In addition to the standard onboard setup, some additional components can also be mounted onboard for specific tests. More information on the NUS geotechnical centrifuge can be found in Lee *et al.* (1991) and Lee (1992).

3.3.2 FULL SPUDCAN TEST

Figure 3.2 and 3.3 present photographs of the NUS geotechnical centrifuge with a full setup and a closer view of the model setup used in the present study respectively. The key components of the model setup for full spudcan tests consist of a specimen container, two loading actuators, a model full spudcan and a set of sensors to measure the pore pressure and soil responses during the tests. Furthermore, two servo-valve systems to control movements of two loading actuators and a strainmeter were installed on the centrifuge arm, as can be referred from Figure 3.3. Details of each component are elaborated in the following sections.

3.3.2.1 MODEL CONTAINER AND LOADING SYSTEMS

The model container was a cylindrical stainless steel tub of 600mm internal diameter and 400mm high as shown in Figures 3.4a and b. Two double acting actuators with attached potentiometer were fixed on a stainless steel loading frame mounted on top of the container. The first hydraulic cylinder served as the main loading actuator

having a stroke length of approximately 300mm with a piston bore of 60mm diameter and a piston rod of about 20mm diameter. Under a maximum working pressure of 70 bars (1000 psi) available in the NUS geotechnical centrifuge, the hydraulic cylinder could deliver maximum compression and tension forces of 18 and 16 kN respectively. The second cylinder with a stroke length of 300mm, 40mm diameter bore and 15mm diameter piston was used to perform in-flight T-bar tests for measurement of in-situ undrained shear strength. Each cylinder was coupled with a potentiometer to monitor the piston rod movement and was controlled by a separate servo valve system mounted on the centrifuge arm. Since only one hydraulic pressure supply was available onboard of the centrifuge, a hydraulic converter was deployed to split the flow to the two control lines. A schematic diagram of the loading frame is illustrated in Figure 3.5.

Besides the loading frame, three pore pressure transducers were also placed inside the model clay bed to measure the pore pressure response approximate 60mm away from the spudcan's edge. All the pore pressure transducers were placed along the center of the container base or aligned with the y-axis of the centrifuge platform. This was targeted to ensure that all water pressure measurements were made with respect to the lowest point of the curved water surface and soil surface arising from radius centrifugal field.

A valve was also installed adjacent to the base of the container to facilitate water drainage during pre-consolidation at 1g and in-flight consolidation at high acceleration of 100g. Prior to spudcan penetration, the drainage valve was closed mechanically using downward motion of hydraulic piston to facilitate a one way drainage path. This enables a proper modeling of normally consolidated and over-consolidated clays where the bottom drainage layer should be far beneath the spudcan.

3.3.2.2 MODEL FULL SPUDCAN WITH LATTICE LEGS

The circular model spudcan adopted in the present study has a diameter of 120mm comprising of two detachable sections between the spudcan and cylindrical rod as schematically illustrated in Figure 3.6. The bottom section is made up of aluminum alloy with 9° under-base slopes and 80° truncated conical tip at its center. The top portion of the model full spudcan is a 25° conical shaped mild steel welded to a 250mm long cylindrical shaft. In this study, all centrifuge tests were performed in an acceleration field of 100g and hence the model spudcan with or without lattice leg corresponds to a prototype diameter of 12m. After 8 hours reconsolidation, the spudcan was moved down until the tip just touched the soil surface. Displacement controlled mode was used to position the model to the so called "zero penetration level" prior to the simulation. The shape of spudcan is adapted from a typical prototype spudcan fabricated by KeppelFELS through the modeled diameter, corresponds to 12m in 100g, which is also slightly smaller than the typical prototype of 46 – 48 ft (Purwana, 2005, 2006). Similar type of spudcans, with small variations in either diameter or shape, were used by a number of researchers from National University of Singapore (Ng, 1998; Teh, 2008; Xie, 2008 and Gan, 2010; Xue, 2010), University of Western Australia (Vlahos *et al*., 2001; Byrne and Cassidy, 2002; Hossain *et al*., 2003, 2004, 2005, 2006; Hossain and Hu, 2004, 2005 and Hossain and Randolph, 2008, 2009, 2010), Cambridge University (Dean *et al*., 1998), Oxford University (Santa Maria 1998; Houlsby and Martin, 1992; Martin, 1994 and Martin and Houlsby, 2000, 2001) and Noble Denton and Associates (1987). The model full spudcan with lattice legs is specifically designed such that it could be temporarily resisted the backflow soil, as also presented in Figure 3.6.

Circular lattice legs or truss-work with opening ratio, A_r of 0.3, 0.6 and 0, which can be defined as the ratio between opening and surface areas of the sleeve, will be

introduced throughout the entire centrifuge tests for both normally consolidated and over-consolidated clays. Each segment of circular lattice legs is formed by two 3mm thick aluminum alloy plates, which is bent into the respective semi-circular profile (refer to Figure 3.7).

3.3.2.3 SENSORS

a. Potentiometer

   Midori© displacement transducers, with identical stroke length of 300mm and precision up to ± 0.1%, were used to measure displacements of two loading actuators.

b. Pore pressure transducer (PPT)

   Druck© PDCR-81 miniature pore pressure transducers were functioned to measure the total pore pressures in the surrounding soils, as shown in Figure 3.8. All pore pressure transducers (PPT) are of 3 and 7 bars (equivalent to 300 kPa and 700 kPa respectively) with approximate -1 bar capacity in suction. In Appendix A, a detailed calibration chart for pore pressure transducer is presented.

c. Load cell

   A Honeywell© miniature load cell with approximate 8.918 kN in both compression and tension, mounted in between the hydraulic piston and spudcan shaft was used to measure the applied vertical load on the model spudcan (refer to Figure 3.6 and 3.8).

3.3.2.4 SOIL SPECIMEN

The normally consolidated and over-consolidated clay specimens were reconstituted

from Malaysian kaolin clay powder. Several studies conducted by Goh (2003) and Thanadol (2003) on the properties of the kaolin, which is functioned in the present study, will be summarized in Table 3.2. In order to verify the consistency of kaolin clay, the author also investigated its properties, which will also be summarized in Table 3.2.

The clay powder was first mixed with water to produce clay slurry with a moisture content of 120%, which is roughly 1.5 times the liquid limit of the kaolin clay. The mixing process was implemented inside a vacuum mixer for 4 hours, subjected to a continuous vacuum suction of 85 kPa (see Figure 3.9).

Prior to pouring the clay slurry into the container, a layer of grease was applied to the internal wall to reduce the friction between the soil and wall (Wagget, 1989; Khoo *et al.*, 1994). A 30mm thick sand layer was then placed at the bottom of the container to act as a drainage layer during consolidation, followed by a layer of water. Clay slurry was then transferred to the container in batches, interspaced by embedment of de-aired PPTs. At all times, the clay slurry and pore pressure transducers were kept submerged so as to maintain full saturation. Since the desired height of slurry exceeded the container height, an extension sleeve was mounted on top of the container and fastened down the joint sealant. More slurry was then poured into the container till it reached the required level. The container was then covered by an air-tight circular perspex cover and vacuum suction pressure was applied inside the container to remove any air that may remain the model.

Preliminary consolidation of the clay slurry was then conducted at 1g to take up most of the settlement before self-weight consolidation in high g. During 1g consolidation, the clay bed was loaded in stages by pneumatic jack up to a maximum surcharge pressure of 20 kPa for normally consolidated clay (Purwana, 2005, 2006) and 150 kPa for over-consolidated clay (Juneja *et al*., 2010; Yeo *et al.*, 2010) (see Figure 3.10a and

Figure 3.10b). The time taken for the whole process is 1 week and 2 weeks for normally consolidated clay and over-consolidated clay respectively. This surcharge would create a slightly stiffer soil on the upper layer to allow more accurate data collection of T bar penetrometer or else the correction on the T bar penetrometer data at shallow embedment and in very soft soils shall be implemented (White *et al*., 2010).

After the specimen had been fully pre-consolidated under 1g, the surcharge was removed and the specimen was transferred to the centrifuge platform and subjected to 100g self-weight consolidation for 8 hours to reach approximately 95% degree of consolidation (Purwana, 2005, 2006; Juneja *et al*., 2010; Yeo *et al.*, 2010). Readings from the pore pressure transducers installed within the specimen was used to monitor and completion of consolidation.

After in-flight consolidation, the centrifuge was then swung down to permit the installation of the model spudcan, lattice legs in some tests and loading equipment. Upon completion of the model setup, the specimen was reconsolidated to recover any release of effective stress during setting up at 1g. During consolidation, the drainage valve at the bottom of the container was kept open to facilitate two-ways drainage. The final thickness of the specimen after reconsolidation was typically about 270 – 280mm.

3.3.3 DATA ACQUISITION AND CONTROL SYSTEMS

3.3.3.1 DATA ACQUISITION

Analogue signals from load cells, potentiometers and pore pressure transducers were routed to the control room via the electrical slip rings described in Section 3.2. In the control room, all signals from pore pressure transducers and load cell were amplified 100 times and filtered with the built-in low pass filter set at 10 Hz cut-off

frequency. The signals were then digitized by the DAP 3000 a/11 analog to digital (A/D) converter operated by the Dasylab© software. Throughout the test, the sample block was set to 100 Hz and averaged for every 100 samples resulting in a recording speed of 1 data per second.

Signals from T-bar penetrometer were captured by the strainmeter mounted on the centrifuge arm. The strainmeter was remotely controlled by a personal computer in the control room via hard wire connection through the slip rings. The capturing rate was set to 1 data point/sec to be compatible to the recording rate of other sensors in the Dasylab© software. With connection through strainmeter directly, the sensors were not subjected to a continuous excitation but rather signal pick-up at regular interval. This helps to minimize potential temperature drift suffered by the sensors without the temperature compensation.

3.3.3.2 SERVO-CONTROLLED LOADING SYSTEM

The loading system can be operated in either displacement or load controlled mode as presented in Figure 3.11. Digital command signals from the command personal computer were sent to digital/analog (D/A) converter and fed to a servo amplifier in voltage form. Then the servo amplifier generated signals to move a spool in the servo valve which regulated the hydraulic pressure into the hydraulic actuators. The servo system could be switched between displacement and load control modes. Displacement controlled mode was employed during spudcan penetration and extraction. The displacement or load registered by the corresponding transducer was fed back to the servo amplifier, which minimized the difference between the command and feedback.

3.3.4 UNDRAINED SHEAR STRENGTH MEASUREMENT

In the current study, two types of in-flight shear strength measurement devices like cone and T-bar penetrometers can be used as illustrated in Figure 3.12. In the early stage of the study especially in the 90s, in-flight cone penetration tests were conducted on the specimen prior to spudcan penetration and extraction at a large distance away from the spudcan (Tani and Craig, 1995; Purwana, 2005, 2006). However, the cone penetrometer was subsequently replaced by T-bar penetrometer (Stewart and Randolph, 1991) for the present study.

3.4 POST CONSOLIDATED STATE OF CLAY BED

As Figure 3.13a and 3.13c show the moisture content reduced from 71% near the ground surface to 60% at a depth of 25m (in prototype terms). As shown in Figure 3.13b and d, this corresponds to an increase in effective unit weight from 5.4 kN/m^3 to 6.2 kN/m^3, which is reasonable for soft clay and agreed very well with the results of Purwana (2006).

As the soil specimen extractions were conducted at 1g environment for both normally consolidated and over-consolidated clays, they are believed that the actual moisture content during in-flight simulation is slightly smaller associated with larger stress levels. During the geotechnical centrifuge spin down, the intact soil specimen also tends to swell and absorbs some water particularly those near the surface and at the bottom part above the drainage sand layer. This also implies that the associated unit weight is perhaps at the upper end of the above range. Therefore, it is reasonable and logical to assume that the average effective unit weight throughout the specimen height can be approximately 6 kN/m^3.

As shown in Figure 3.14, the undrained shear strength from the T-bar is reasonable with that from the cone penetrometer. The latter appear to underestimate the

undrained shear strength slightly at smaller depths and overestimate the undrained shear strength slightly at larger depths. Some irregularities are evident in the undrained shear strength profile near the ground surface, this can be attributed to the effect of 1g consolidation which created a thin layer of over-consolidated soil near the ground surface.

The measured undrained shear strength, the shear strength derived from prediction based on Modified Cam-clay (Roscoe and Burland, 1968; Phillips, 1988) model was also plotted. This was evaluated using the relationship

$$\frac{s_u}{\sigma'_v} = \frac{M}{2}(OCR)^{\Lambda}2^{-\Lambda} \text{ and } \Lambda = \frac{\lambda-\kappa}{\lambda} \quad (3.1)$$

Where s_u is the undrained shear strength; σ'_v is the effective overburden pressure; M, λ and κ are Modified Cam-clay parameters and OCR is the over-consolidation ratio. Adopting the soil parameters listed in Table 3.2, the $\frac{s_u}{\sigma'_v}$ ratio can be obtained as follow:

$$\frac{s_u}{\sigma'_v} = 0.26(OCR)^{0.79} \quad (3.2)$$

The T-bar result matches the tri-axial prediction remarkably well although there is some over-estimation at large depths of 17m onwards as illustrated in Figure 3.14 by Purwana (2006). This is induced by soil plug in front of the cross bar being dragged down during penetration. As pointed out by Stewart and Randolph (1991), this soil plug may alter the actual geometry of bearing area. Finally, results of vane shear tests conducted at 1g after centrifuge testing appear to underestimate the T-bar and cone results. This is not surprising since a certain amount swelling would have taken place during the vane shear tests.

3.5 EXPERIMENTAL PROCEDURES

The centrifuge model test consists of two phases, namely penetration and extraction. As described in Chapter 1, the installation of jack-up legs in the field was implemented by means of ballast to allow penetration of the spudcans into the seabed until the load is equilibrated by the soil bearing resistance. The maximum preload is then maintained for a minimum duration of 2 to 4 hours (Young *et al.*, 1984) until no further significant settlement is observed. Under normal circumstances, this process is typically finished within 24 to 36 hours (KeppelFELS, 2003). In view of the low permeability of typical marine clay, the entire process of spudcan installation can be considered essentially as a motion controlled penetration under undrained condition.

The penetration phase was conducted under a displacement controlled mode. Finnie (1993) (see Figure 3.15) proposed that undrained penetration is achieved as long as

$$\frac{vD}{c_V} > 30 \tag{3.3}$$

$$\frac{1\text{mm/s} \times 120\text{mm}}{40\,\text{m}^2/\text{yr}} = 94.64 > 30 \tag{3.4}$$

Where v is the velocity; D is the spudcan diameter; and c_v is the coefficient of consolidation. This criterion was met by the selected loading rate of 1mm/sec (model scale), resulting in dimensionless velocity group factor of approximate 95. Hossain and Hu (2004, 2005), Hossain and Randolph (2008, 2009, 2010) and Hossain *et al*. (2003, 2004, 2005, 2006) have also adopted spudcan penetration rate of 0.2mm/sec to maintain the undrained condition throughout a series of drum centrifuge testing involving spudcan diameters of 30mm and 60mm and g-level ranging from 38g to 200g.

To position the spudcan close to the target penetration depth, the installation was carried out in two stages with about 30 to 60 seconds (model time) interval between these two stages. This slight delay will permit the command and feedback to be fully sychronized. For all the model tests, the maximum penetration depth was set at approximately 1.5 times the spudcan diameter or about 200mm below the soil surface.

When the spudcan was about to reach the targeted depth, the corresponding command was maintained and thus led to a constant load acting on the spudcan. This can be translated to deceleration of penetrating spudcan which eventually stopped around the desired depth. The corresponding maximum load is termed as maximum installation load hereafter. After completion of spudcan penetration, the command and feedback were re-synchronized before the spudcan was extracted. This typically took approximate 60 seconds (model time).

The extraction process was then simulated by first reducing the bearing load on the spudcan to zero. The displacement controlled mode was then employed to extract the spudcan at a constant velocity.

Rattley *et al*. (2005) studied the effect of uplift rate of plate anchor in clay in which the experimental results were verified with numerical simulations. Figure 3.16 shows that the uplift resistance increases with pullout velocity. The smaller resistance at a low uplift rate is attributed to the dissipation of suction developed at the anchor base. As can be seen, the extraction force approaches an asymptotic upper bound when the dimensionless velocity exceeds about 10. This implies that using an extraction rate of 1mm/sec in the experiments would allow the upper bound of the extraction force to be manifested.

Hence, the uplift was also set at 1mm/sec.

Parameter	**Prototype**	**Centrifuge model at Ng**
Linear dimension	1	$\frac{1}{N}$
Area	1	$\frac{1}{N^2}$
Volume	1	$\frac{1}{N^3}$
Density	1	1
Mass	1	$\frac{1}{N^3}$
Acceleration	1	N
Velocity	1	1
Displacement	1	$\frac{1}{N}$
Strain	1	1
Energy strain	1	1
Energy	1	$\frac{1}{N^3}$
Stress	1	1
Force	1	$\frac{1}{N^2}$
Time (diffusion)	1	$\frac{1}{N^2}$
Time (dynamic)	1	$\frac{1}{N}$
Time (creep)	1	1

Table 3.1 Centrifuge scaling relations (after Leung *et al.*, 1991)

Parameter	**Unit**	**Value (Goh, 2003 and Thanadol, 2003)**	**Value**
Liquid limit, LL	%	80	80
Plastic limit, PL	%	35	36
Specific gravity, G_s	-	2.60	2.60
Coefficient of consolidation (at 100 kPa), c_v	m^2/yr	40	40
Coefficient of permeability (at 100 kPa), k	m/s	2×10^{-8}	2×10^{-8}
Angle of internal friction, ϕ'	°	23	23
Particle size **	μm	3.0 – 5.5	3.0 – 5.5
Modified Cam clay parameters			
M	-	0.9	0.9
λ	-	0.244	0.244
κ	-	0.053	0.053
N	-	3.35	3.35

** denotes manufacturer data

Table 3.2 Properties of Malaysian kaolin clay (after Goh, 2003 and Thanadol, 2003)

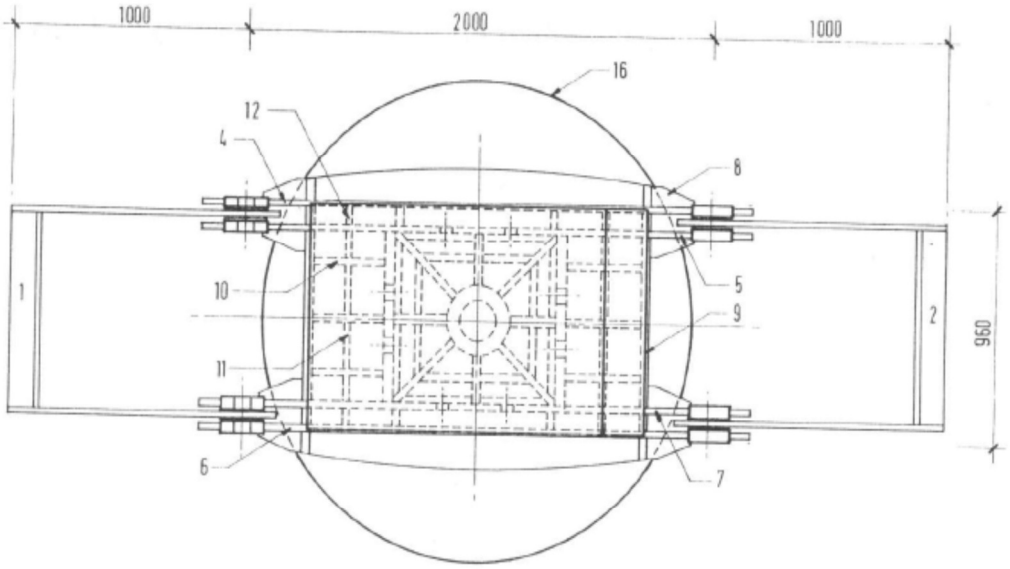

(a) Plan view

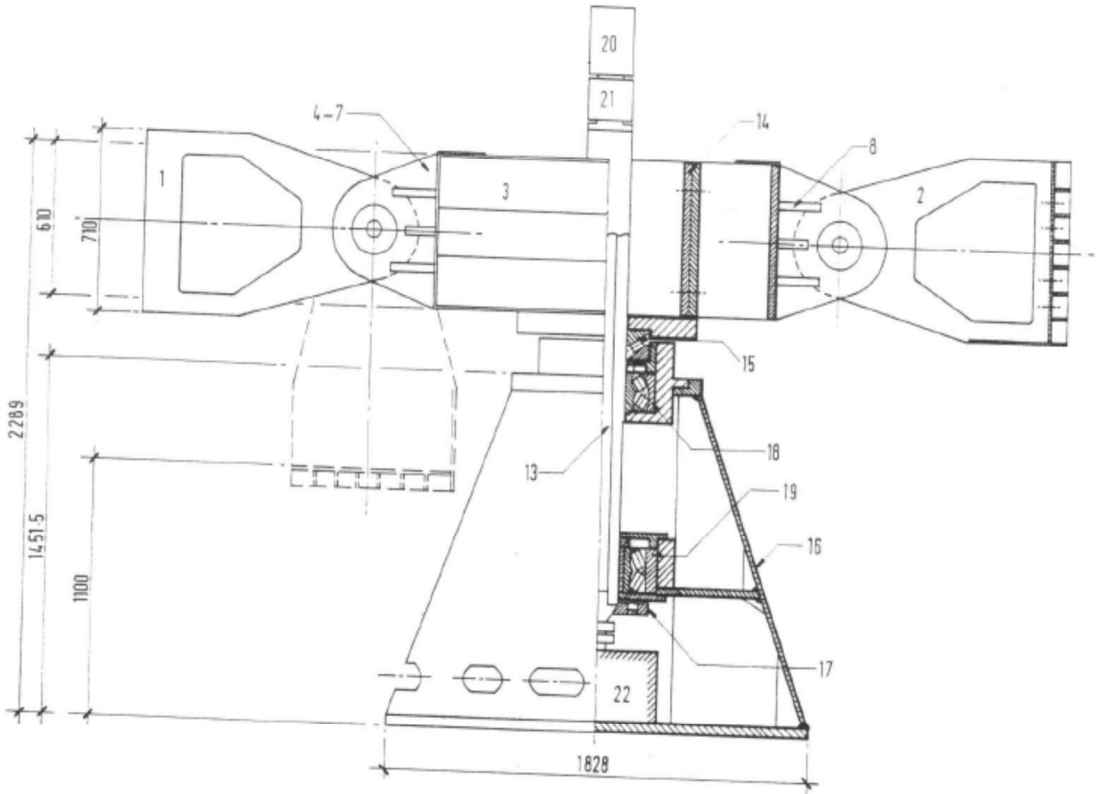

(b) Elevation view

Figure 3.1 NUS Geotechnical Centrifuge (after Lee *et al.*, 1991)

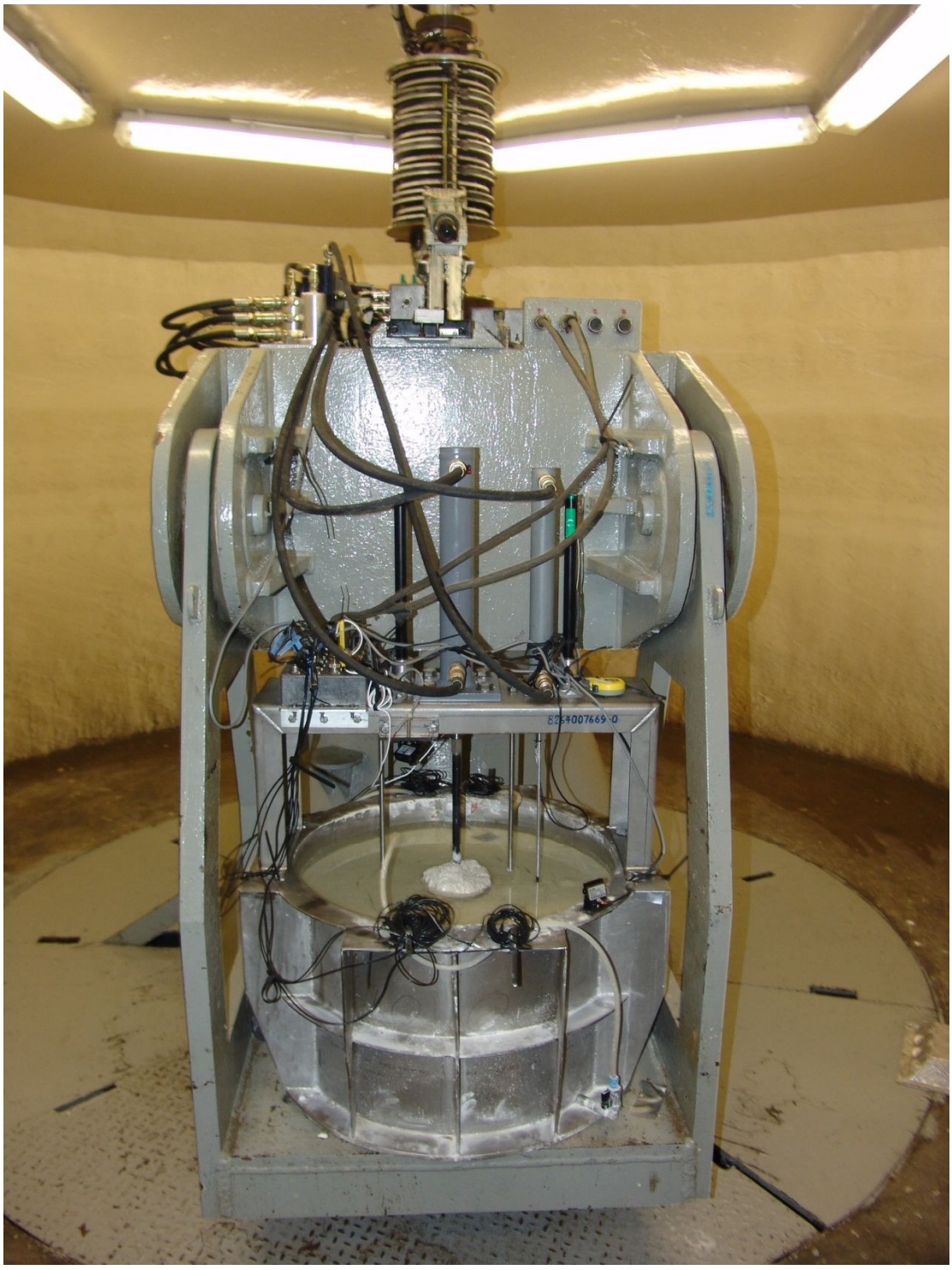

Figure 3.2 Centrifuge model setup for full model spudcan test

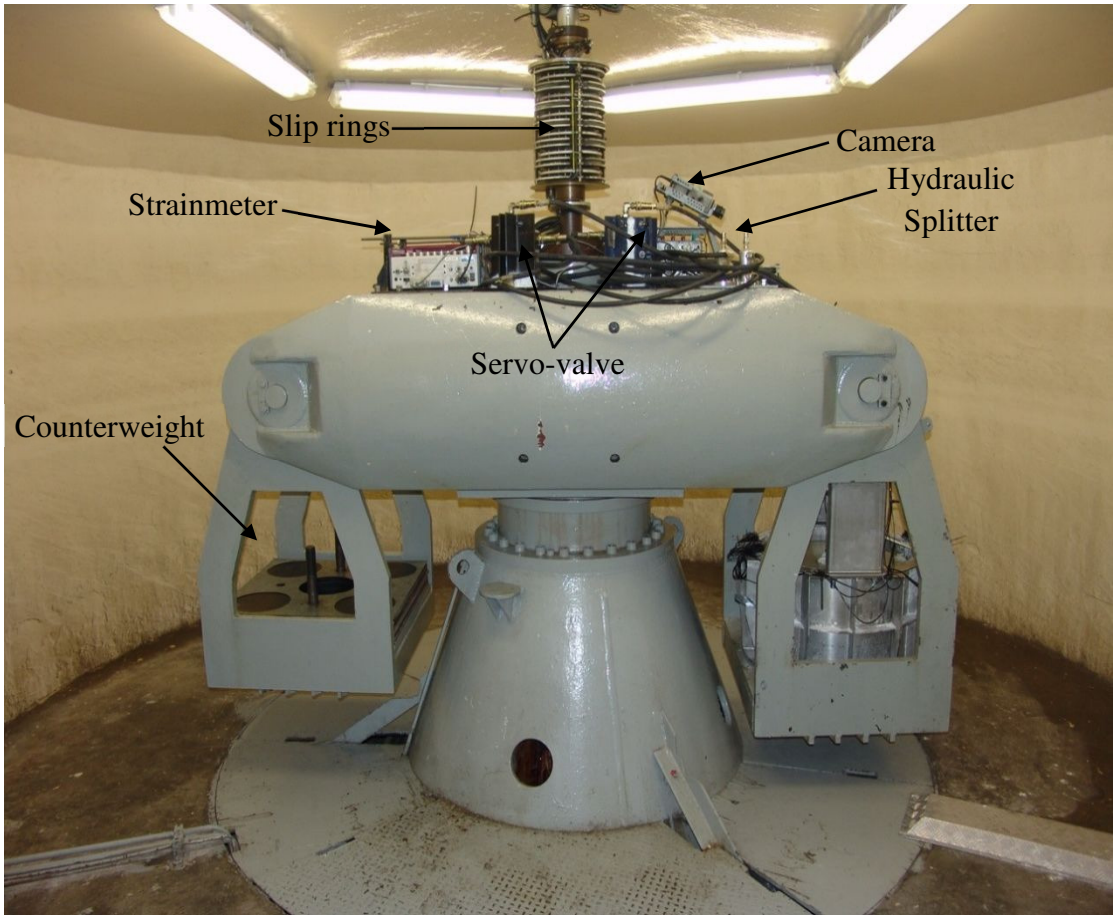

Figure 3.3 NUS geotechnical centrifuge and complete model setup for spudcan test

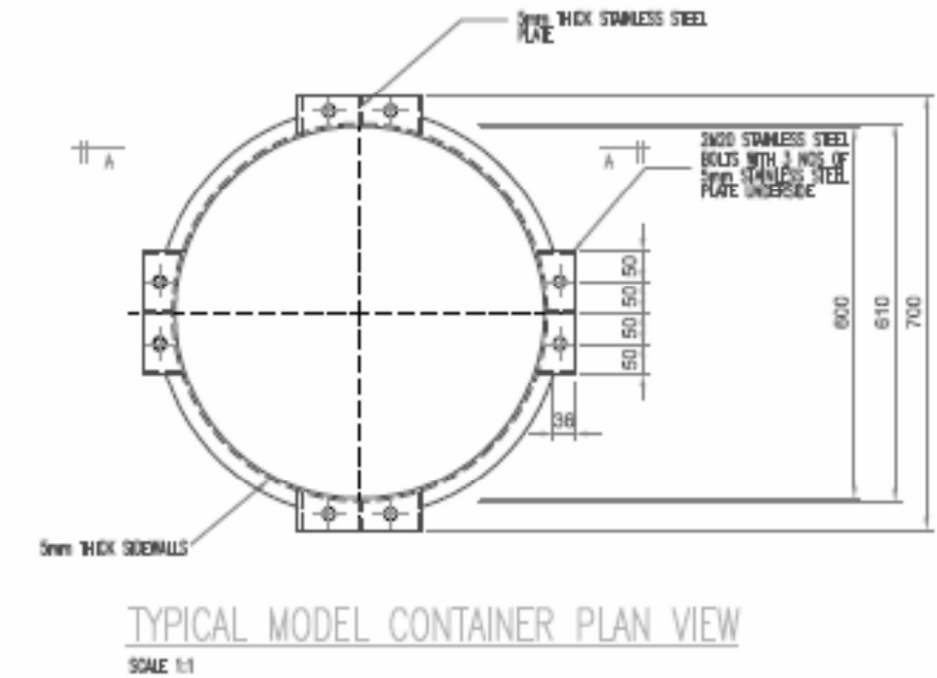

Figure 3.4a Plan of circular container

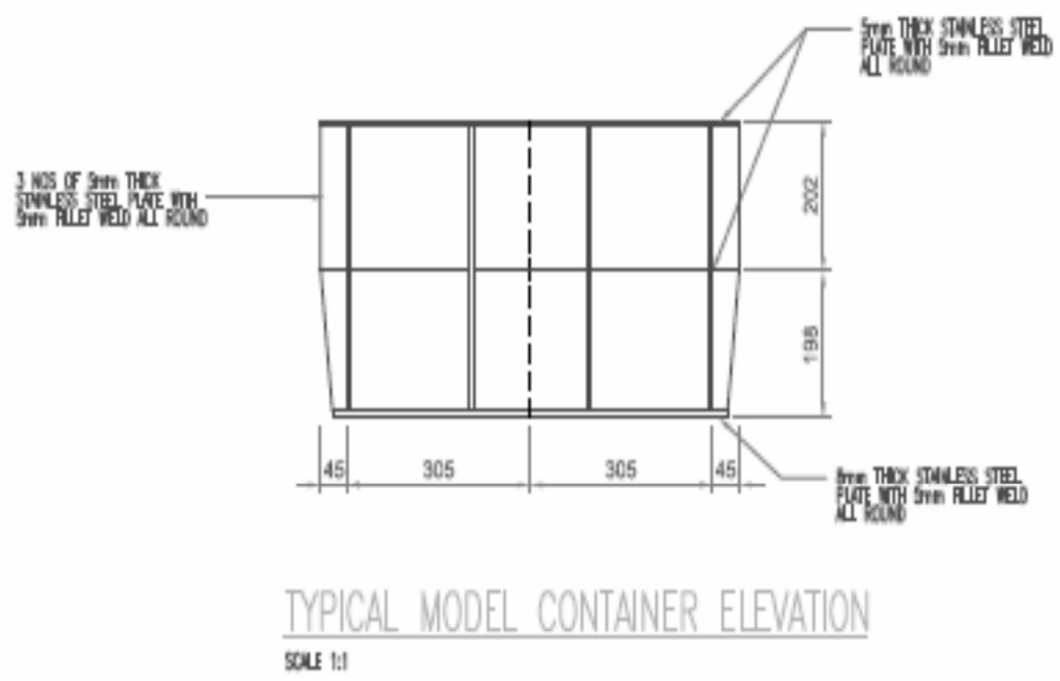

Figure 3.4b Elevation of circular container

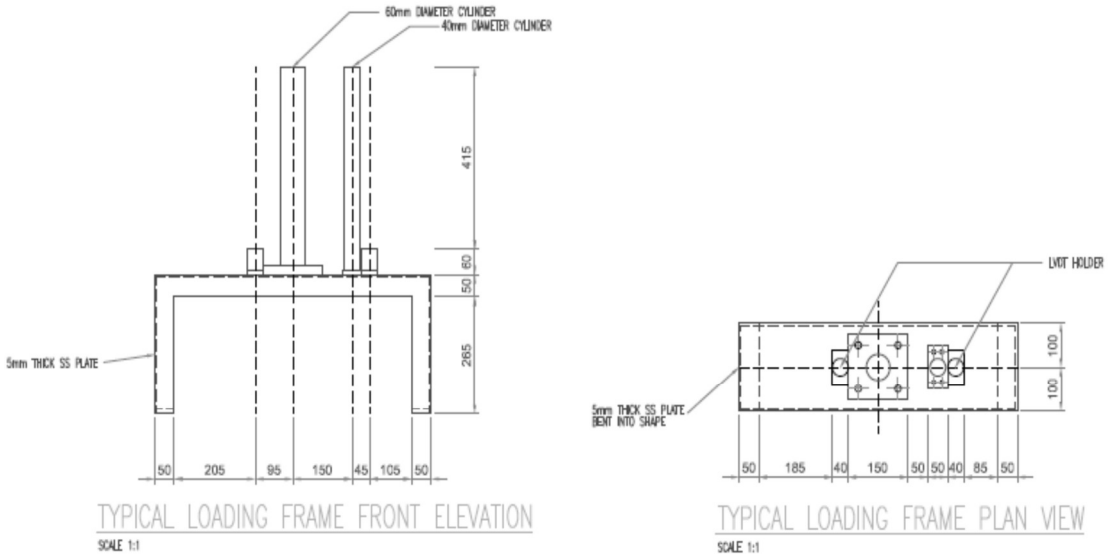

(a) (b)

Figure 3.5 Schematic layout of loading frame with actuators

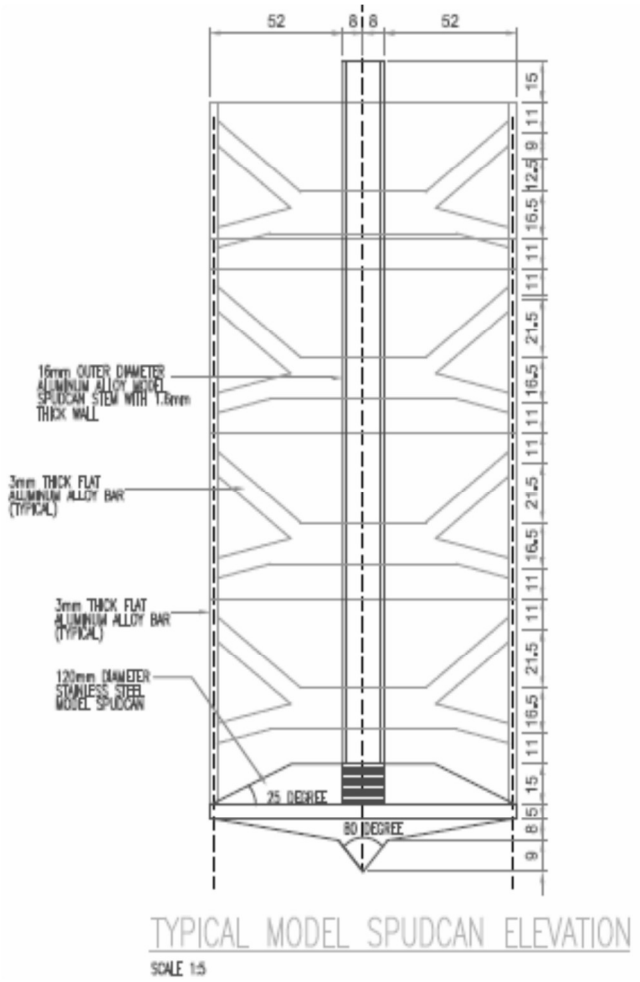

(a)

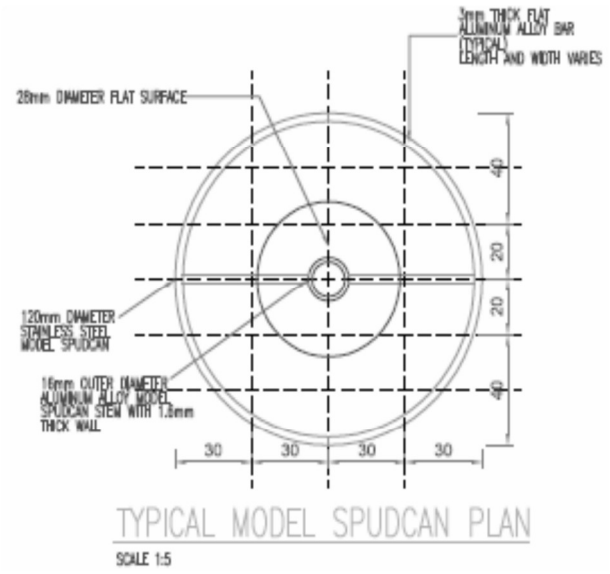

(b)

Figure 3.6 Dimensions or geometries of model spudcan with lattice legs

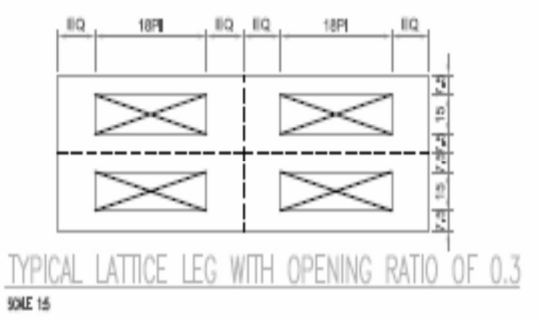

(a)

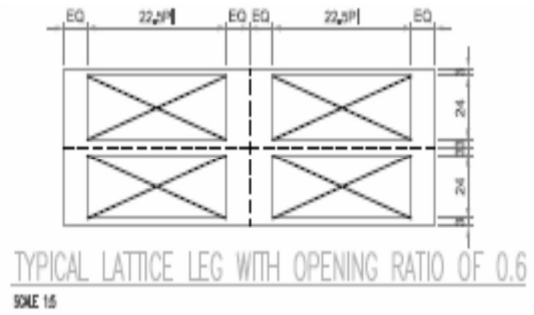

(b)

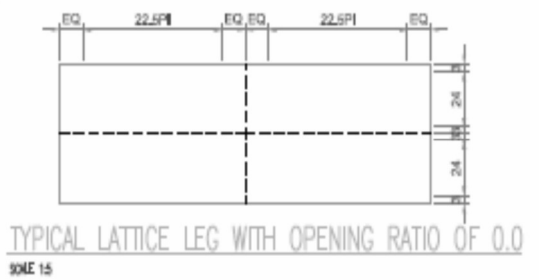

(c)

Figure 3.7 Lattice leg with opening ratio of 0, 0.3 and 0.6

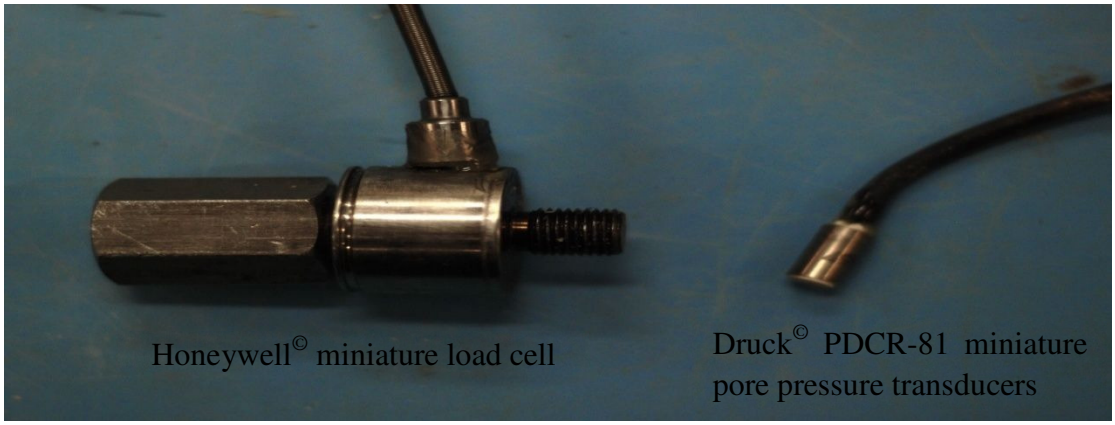

Figure 3.8 Load and pore pressure sensors

Figure 3.9 Sample preparations: clay mixing

Figure 3.10a Sample preparation: pre-consolidation at 20 kPa using pneumatic jack

Figure 3.10b Sample preparation: pre-consolidation at 150 kPa using pneumatic jack

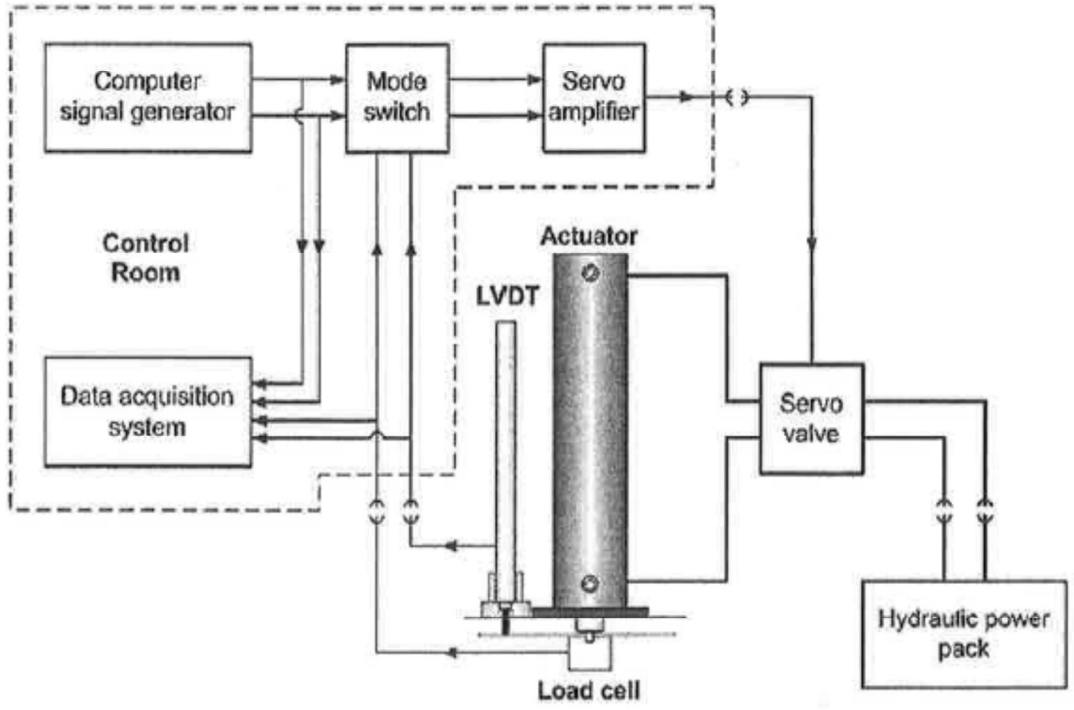

Figure 3.11 Schematic diagram of servo-controlled loading system

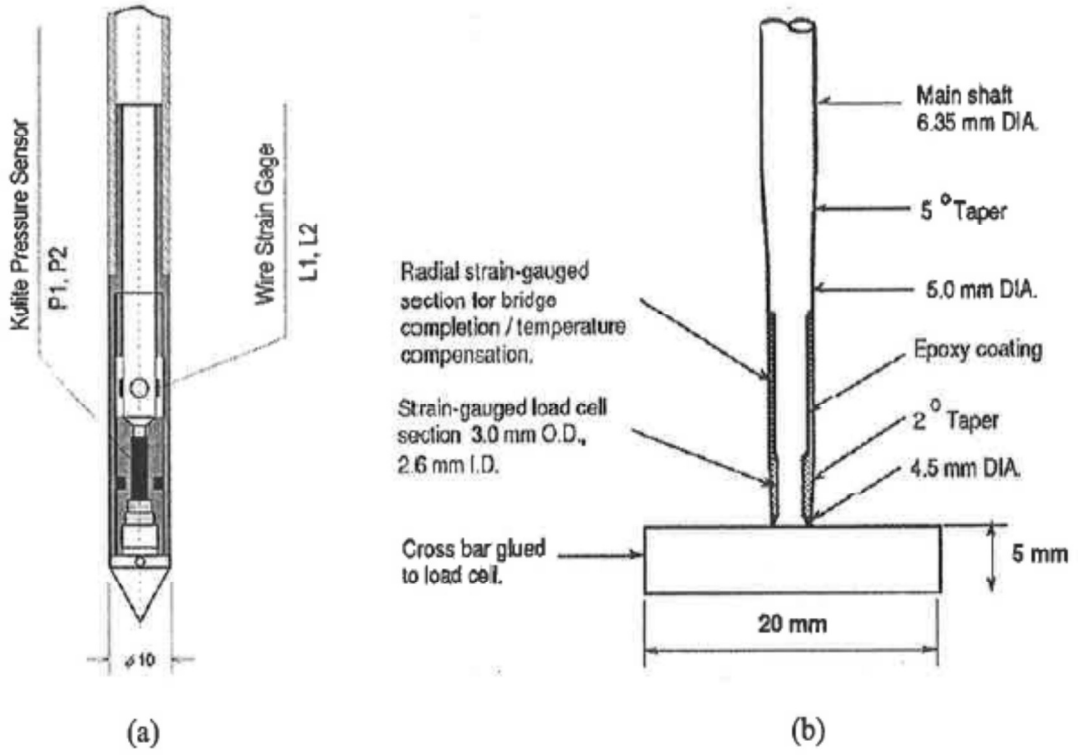

Figure 3.12 Schematic diagram of cone penetrometer and T bar penetrometer

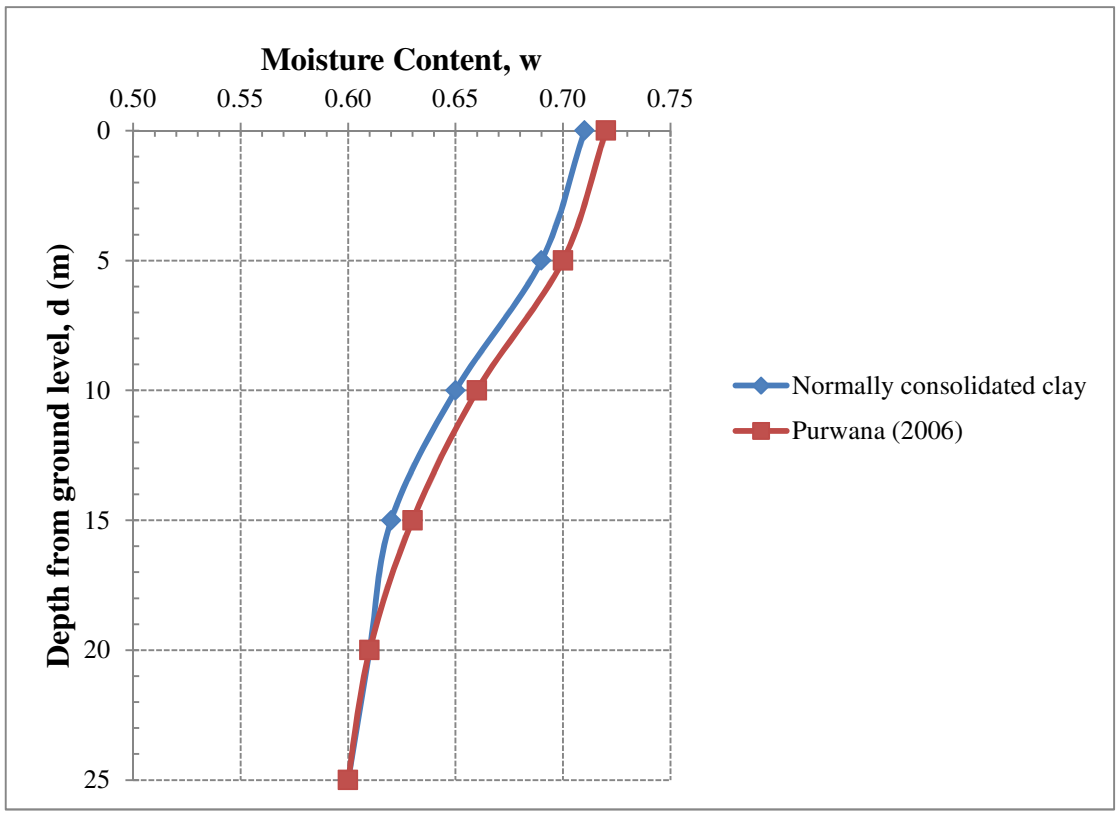

Figure 3.13a Profile of moisture content of normally consolidated clay

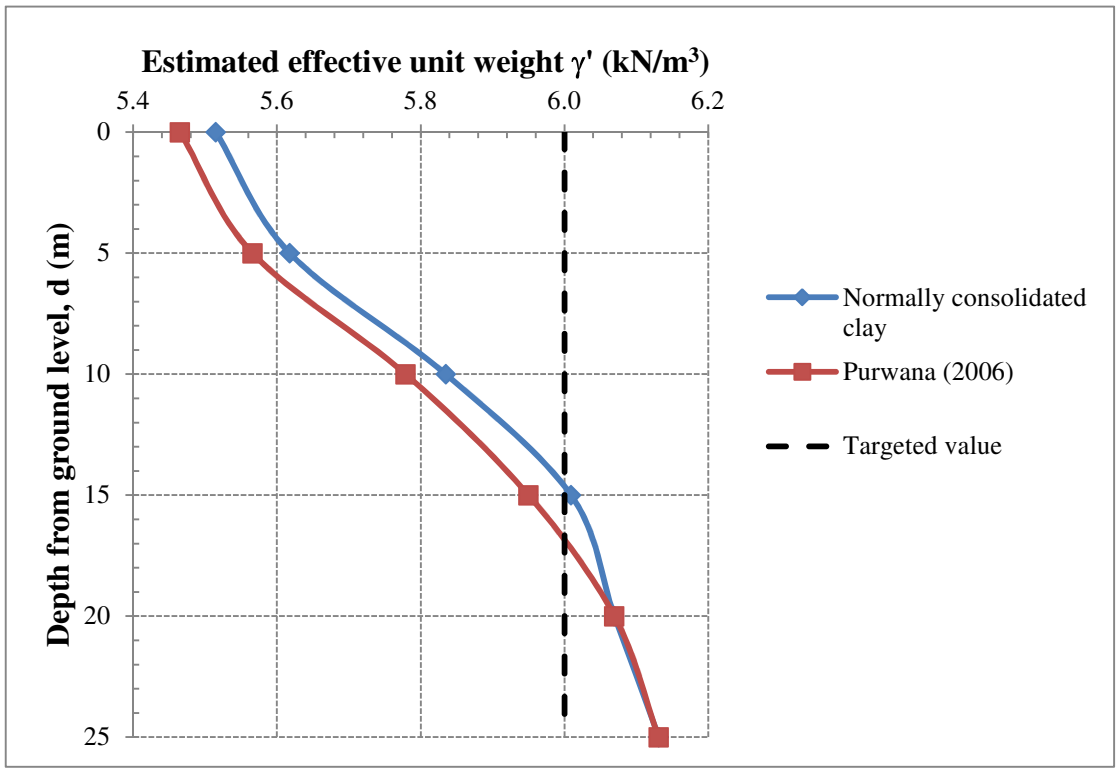

Figure 3.13b Profile of estimated effective unit weight of normally consolidated clay

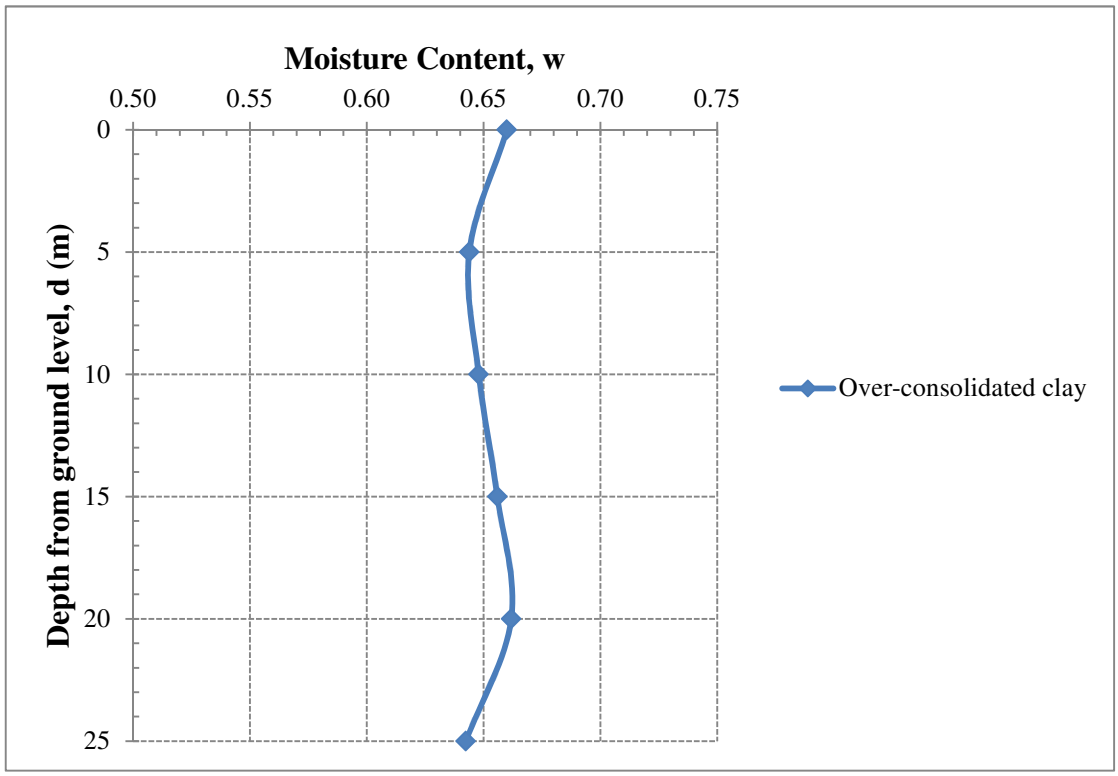

Figure 3.13c Profile of moisture content of over-consolidated clay

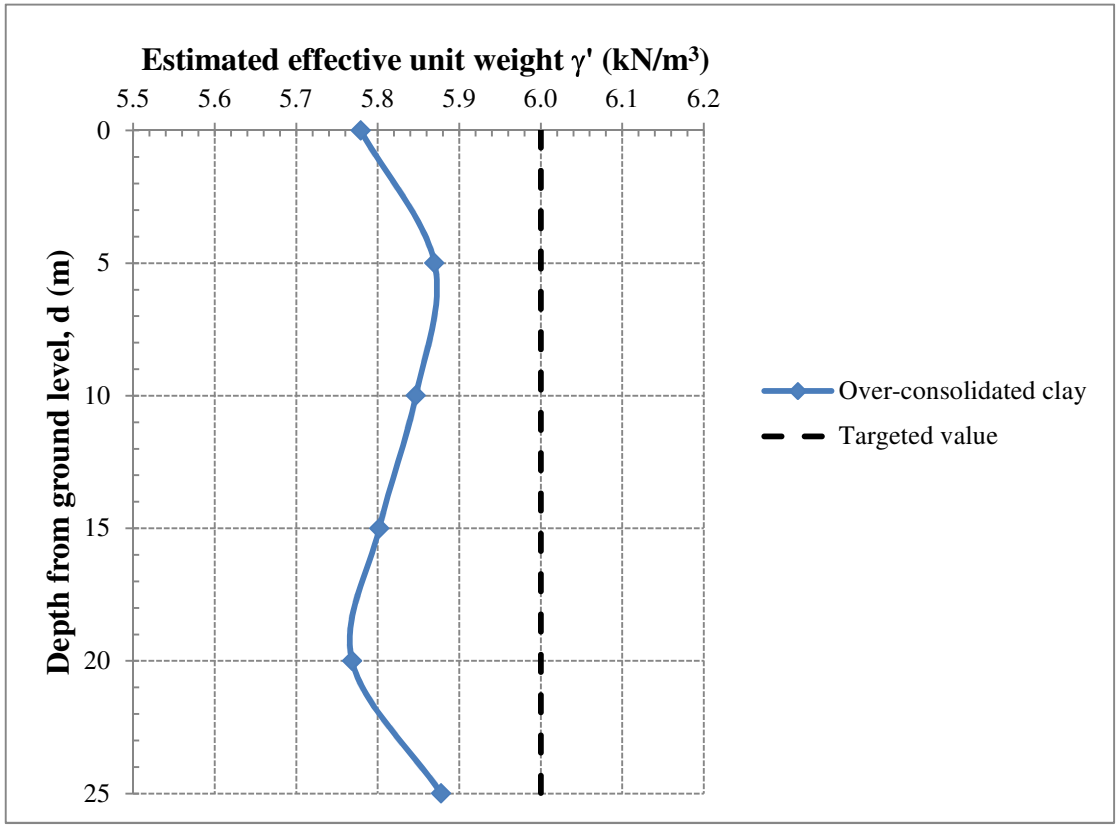

Figure 3.13d Profile of estimated effective unit weight of over-consolidated clay

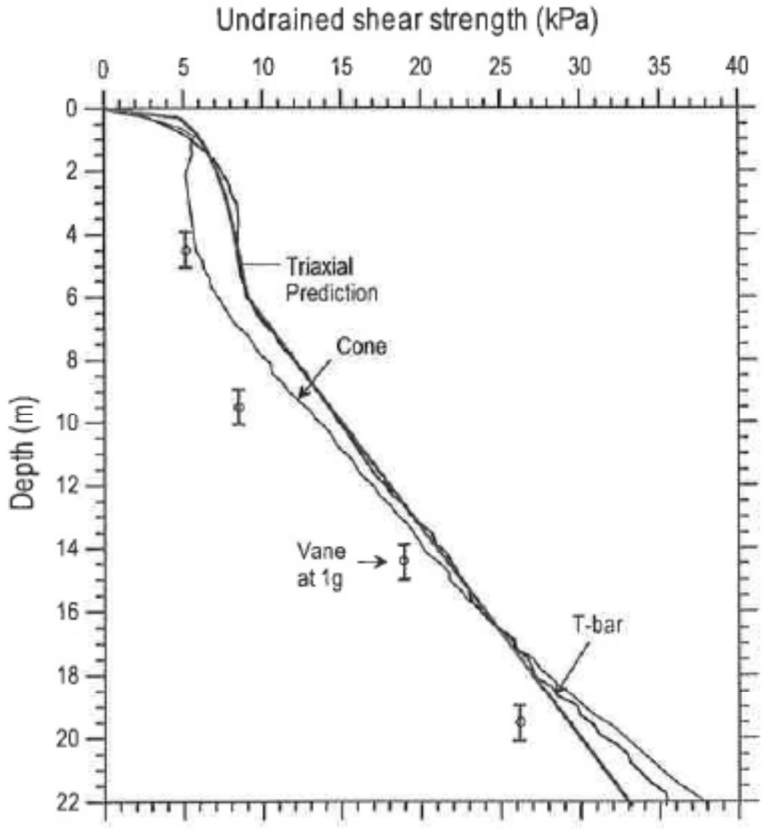

Figure 3.14 Comparison of undrained shear strength profile of soil sample from various methods (after Purwana, 2006)

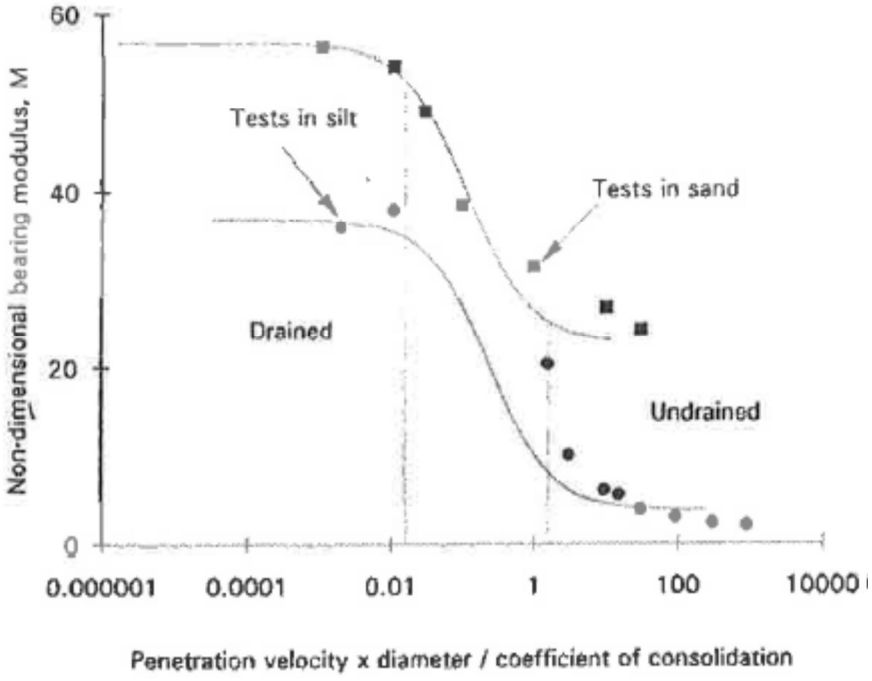

Figure 3.15 Effect of loading rate on bearing response in sand and silt (after Finnie, 1993)

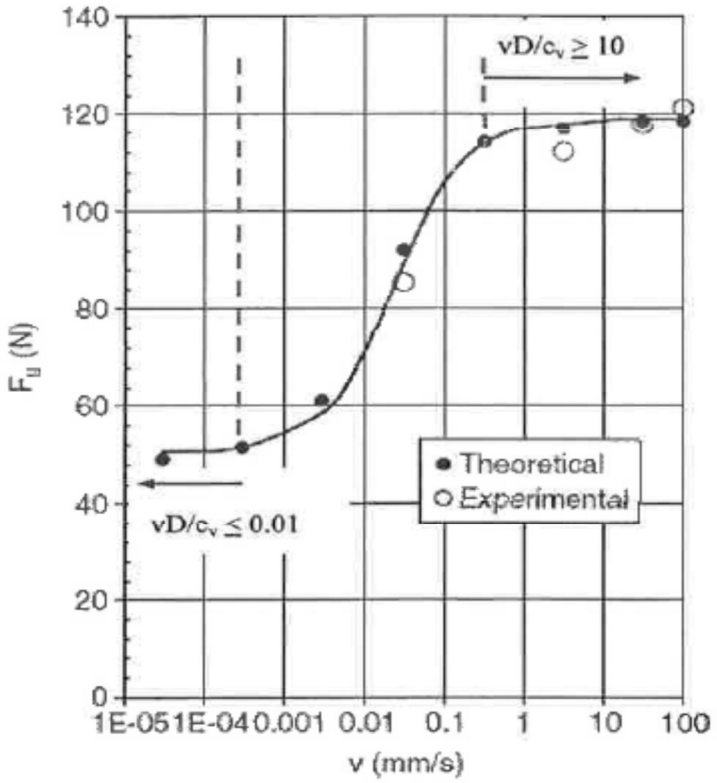

Figure 3.16 Effects of uplift rate on uplift resistance of plate anchors in clay (after Rattley *et al.*, 2005)

CHAPTER 4 RESULTS AND DISCUSSION: EXPERIMENTAL ANALYSIS

4.1 GENERAL

The aim of the experimental programme was to quantify the bearing responses of spudcans with and without lattice legs and factors influencing bearing capacity coefficients of spudcans embedded 1.5 times diameter deep in both normally consolidated and over-consolidated clays. Hence, four series of centrifuge tests each for both normally consolidated and over-consolidated clays were specially designed to examine the effects of lattice legs with different opening ratios on load response behavior and resistance to soil backflow mechanism.

4.2 UNDRAINED SHEAR STRENGTH

4.2.1 SOIL STRENGTH DETERMINATION

The undrained shear strengths for both normally consolidated and over-consolidated clays were measured using a miniature T-bar penetrometer of diameter 5mm and length 25mm (Stewart and Randolph, 1991). These tests were conducted at 3mm/sec, which was sufficiently fast to ensure undrained behavior in kaolin in all centrifuge tests (Finnie, 1993; Randolph and Hope, 2004; Purwana, 2005, 2006). In-flight undrained shear strength assessments were implemented immediately prior to spudcan penetration. For both normally consolidated and over-consolidated clay specimens with free water on top, typical soil profile for each specimen assuming $N_{T\text{-}bar}$ = 10.5 (Stewart and Randolph, 1991) is presented in Figures 4.1 and 4.2

respectively. Representative non-homogeneous soil strengths (Roscoe and Burland, 1968; Ladd and Foott, 1974) were selected from the measured profiles, which are also indicated in Figures 4.1 and 4.2, for use in subsequent analyses on normally consolidated and over-consolidated clays through several reported case histories (Gemeinhardt and Focht, 1970; Gemeinhardt and Yan, 1978; Lunne *et al.*, 1981; Rapoport and Young, 1988; Poulos, 1988; Ahrendsen *et al.*, 1989; Cassidy *et al.*, 2002; Quiros and Little, 2003; Randolph, 2004).

4.2.2 STRENGTH PROFILES

Following the approaches of Roscoe and Burland (1968) and Ladd and Foott (1974), the soil strength, s_u, was fitted by the relations:

$$s_u = 2.2\ \text{kPa} + 1.56z \tag{4.1}$$

and $$s_u = 20\ \text{kPa} + 1.05z \tag{4.2}$$

for normally consolidated and over-consolidated clays, respectively, in which z is the depth below mud line in meters and k is the rate of increase in undrained shear strength. Eqs. 4.1 and 4.2 imply a mud line strength of 2.2kPa and 20kPa for normally consolidated and over-consolidated clays. It should be noted that the normally consolidated clay beds have a thin layer (~3.5cm in model terms or 3.5m in prototype terms) of over-consolidated clay at the top due to the application of the 1-g surcharge pressure of 20kPa. This explains the non-zero undrained shear strength at the mud line and the change of profile at about 3m depth Figure 4.1. The chosen parameters for this study are summarized in Table 4.1, encompassing two types of clays: normally consolidated and over-consolidated.

4.3 SINGLE SPUDCAN PENETRATION RESPONSE ON NON-HOMOGENEOUS CLAYS

The results from centrifuge modeling of single spudcan penetration responses on non-homogeneous clays are expressed in terms of vertical penetration load, V_o, and a function of penetration depth, z .

4.3.1 NORMALLY CONSOLIDATED CLAY

Figure 4.3 illustrates a typical profile of load displacement response, V_o, for a single spudcan, which is also termed as spudcan penetration response, in normally consolidated clay throughout the installation process. It should be noted that the vertical penetration resistance is the net vertical load after deduction of backfilled soil weight. The installation process is denoted by points A and B where a compression with magnitude of 24.6 MN was mobilized on the spudcan to penetrate to the targeted penetration depth of 18m. This spudcan penetration response curve for normally consolidated clays agrees quite well with the load displacement curves obtained from the following bearing capacity equations proposed by Hossain and Randolph (2009b) for both smooth and rough spudcan:

$$q_u = N_{co}s_{uo} + \gamma' z + \frac{\gamma' V_b}{A} \qquad \text{when } z < H \tag{4.3}$$

$$q_u = N_{co}s_{uo} + \frac{\gamma' V}{A} \qquad \text{when } z > H \tag{4.4}$$

$$H = D\left(S^{0.55} - \frac{S}{4}\right) \text{ where } S = \left(\frac{s_{um}}{\gamma' D}\right)^{\left(1-\frac{k}{\gamma'}\right)} \tag{4.5}$$

$$N_{co} = 5.45\left[1 + \frac{0.161\left(\frac{kD}{s_{uo}}\right)^{0.8}}{\left(1+\frac{z}{D}\right)^{2}}\right] \quad \text{for smooth footing} \qquad (4.6)$$

$$N_{co} = 6.05\left[1 + \frac{0.191\left(\frac{kD}{s_{uo}}\right)^{0.8}}{\left(1+\frac{z}{D}\right)^{1.5}}\right] \quad \text{for rough footing} \qquad (4.7)$$

where N_{co} is the bearing capacity factor at depth of penetration, z, relative to its widest cross sectional area, s_{uo} is the undrained shear strength at depth of penetration, z, V_b is the embedded volume of spudcan below maximum diameter, A is largest cross sectional area of the spudcan, V is the volume of embedded spudcan inclusive of shaft, D is the spudcan diameter, H is the backflow depth, γ' is the effective unit weight, k is the gradient of increase in undrained shear strength and s_{um} is the undrained shear strength at mud-line.

4.3.2 OVER-CONSOLIDATED CLAY

Figure 4.4 presents a typical profile of load displacement response, V_o, for a single spudcan in over-consolidated clay during the penetration process. The preloading process is also indicated by points C and D where a compressive force with magnitude of 34.76 MN was utilized to penetrate to the desired depth of 18m. Similarly, the spudcan penetration response curve for over-consolidated clays also matched fairly well with the load displacement curves calculated from the bearing capacity equations suggested by Hossain and Randolph (2009b).

4.4 SLEEVED SPUDCAN PENETRATION RESPONSE OF SPUDCANS WITH LATTICE LEGS AND SLEEVES

The results from centrifuge modeling of sleeved spudcan penetration responses on non-homogeneous clays are also elaborated in terms of vertical penetration load, V_o, and a function of penetration depth, z.

4.4.1 NORMALLY CONSOLIDATED CLAY

Figure 4.5 shows the load penetration response, V_o, for sleeved spudcans with different opening area ratios, Ar, of 0, 0.3 and 0.6, which is also defined as the ratio between the opening and surface areas of the sleeve, in normally consolidated clays. The installation process for these respective sleeved spudcans is denoted by points E and F where penetration resistance of 50 MN, 30.5 MN and 27.2 MN were encountered by the sleeved spudcans with area ratio of 0, 0.3 and 0.6 respectively at penetration depth of about 18m. As Figure 4.5 shows, the sleeved spudcan with the lowest opening area ratio gives the greatest penetration resistance in normally consolidated clays. This kind of behavior, which can be due to its resistance to soil backflow mechanism (Menzies and Roper, 2008) and shaft resistance enhancement (Randolph and Houlsby, 1984), will be discussed later.

4.4.2 OVER-CONSOLIDATED CLAY

Figure 4.6 presents the corresponding load penetration response, V_o, for sleeved spudcans with different opening area ratios, Ar, of 0, 0.3 and 0.6, which is also defined as the ratio between the opening and surface areas of the sleeve, in over-consolidated clays during the preloading process. The preloading process for these respective sleeved spudcans is also indicated by points G and H where compressive forces with magnitudes of 59.16 MN, 53.18 MN and 42.45 MN were utilized on the latticed spudcans with different opening area ratio of 0, 0.3 and 0.6 respectively to penetrate to the desired depth of about 18m. As Figure 4.6 shows, the sleeved spudcan with no opening exhibits the highest penetration resistance in

over-consolidated clays. This behavior is same as that for normally consolidated clays and will be further discussed later.

4.5 EFFECTS OF LATTICE LEGS ON SPUDCAN

Figures 4.3 and 4.4 prove that the single spudcan bearing responses in both normally consolidated and over-consolidated clays agreed well with the results of Hossain and Randolph (2009b) in regardless of smooth and rough footings. Similarly, figures 4.5 and 4.6 also show that there will be a direct proportional increase in lattice spudcan bearing responses in both normally consolidated and over-consolidated clays with equivalent reduction in opening area ratios. The increases in penetration resistance may be attributed to the following factors:

1. Lattice side friction and soil backflow resistance
2. Bearing capacity coefficient, N_c

Thus, it is extremely necessary to investigate or examine the extent of contributing factors individually.

4.5.1 LEG FRICTION AND SOIL BACKFLOW RESISTANCE

The results from centrifuge modeling of all sleeved spudcan penetration responses on non-homogeneous clays are also elaborated in terms of vertical penetration load, V_o, a combination of bearing capacity, Q_p, side friction, Q_s and negating effects of backflow soil, $A\gamma' H_f$, and a function of penetration depth, z .

4.5.1.1 NORMALLY CONSOLIDATED CLAY

Figure 4.7 shows the penetration resistance of the fully enclosed sleeved spudcan in normally consolidated clays. As can be seen, the vertical penetration resistance can be summed up by the bearing capacity equation by Hossain and Randolph (2009b) and side friction of the lattice legs. This is not surprising since a sleeved spudcan may be viewed as circular pile (Randolph and Houlsby, 1984). Therefore, the vertical penetration load for this sleeved spudcan can be expressed as:

$$V_o = Q_p + Q_s = A\left(N_{co}s_{uo} + \gamma' z + \frac{\gamma' V_b}{A}\right) + Q_s \quad (4.8)$$

$$Q_s = V_o - Q_p = V_o - A\left(N_{co}s_{uo} + \gamma' z + \frac{\gamma' V_b}{A}\right) \quad (4.9)$$

The shaft friction, Q_s, can be determined by adopting the measured vertical penetration force, V_o, subtracted away the mean value of Hossain and Randolph's (2009b) theoretical prediction of both rough and smooth footings for vertical bearing force, Q_p, since the sleeved spudcan can be assumed as a circular pile (Randolph and Houlsby, 1984).

The side friction of fully enclosed sleeved spudcan definitely continued to increase gradually till 18m deep as presented in Figure 4.7. For the sleeved spudcan with opening area ratio of 0.3 and 0.6, slightly different trends in comparison with the zero opening area ratio sleeved spudcan are illustrated in Figures 4.8 and 4.9. Both vertical penetration loads for both sleeved spudcan with opening area ratio, Ar, of 0.3 and 0.6 gradually increase till limiting cavity depth, H, at about 2.67m, which can be determined by the critical cavity height equation by Hossain *et al.*, (2005c, 2006) and also substantiated by the on board camera footage during centrifuge testing. Beyond the limiting cavity depth, H, the vertical penetration load for both sleeved spudcan with opening area ratio of 0.3 and 0.6, tend to increase slower than at shallower depths. This is led by the negative contribution of backfilling soil due to onset of

soil backflow (Hossain *et al.*, 2005c, 2006). Moreover, the significant difference between centrifuge results for sleeved spudcan with both opening area ratio, Ar, of 0.3 and 0.6 and the mean theoretical prediction of vertical penetration load by equations (4.6) and (4.7) is due to the weight of backfilled soil. This also suggested that the bearing capacity equation, which is proposed by Hossain and Randolph (2009b) considering backflow mechanism, can underestimate the vertical penetration load at deeper penetrations. Therefore, the vertical penetration load for these two sleeved spudcans can be simply termed as:

$$V_o = Q_p + (1 - Ar)Q_s - A\gamma' H_f \qquad (4.10)$$

Where (1-Ar)Q_s is the proportional inferred quantity of shaft friction attained from the results of fully enclosed sleeved spudcan multiply with the factor of (1-Ar) and $A\gamma' H_f$ is the calculated backfilled soil weight from equation (4.10).

Before moving on to the effect of lattice on the shaft frictions for two sleeved and one fully enclosed sleeved spudcans as presented in Figure 4.10, the shaft friction for each sleeved case can be achieved by using the shaft friction of the fully enclosed sleeved spudcan, Q_s, multiply with the factor (1-Ar).

Intuitively, one would expect the sleeved spudcan with opening area ratio, Ar, of 0.3 to provide more resistance to soil backflow mechanism resulting in smaller amount of backfilled soil on top of the spudcan. However, test observations showed that soil will ingress even though the smaller openings for sleeved spudcan with opening area ratio of 0.3 in normally consolidated clay especially at larger depths of penetration. Even though the sleeved spudcan with opening area ratio, Ar, of 0.3 contributed higher side friction than one with opening area ratio, Ar, of 0.6, as illustrated in Figure 4.10, this is astonishingly true that the sleeved spudcan with opening area ratio, Ar, of 0.6 experiences the smaller amount of backfilled soil at deeper penetrations than one

with opening area ratio, Ar, of 0.3 because of its larger opening size to permit the backfilling soil from flowing in and out of the lattice legs more freely and easily.

4.5.1.2 OVER-CONSOLIDATED CLAY

Figure 4.11 presents the penetration resistance of fully enclosed sleeved spudcan in over-consolidated clays. As can be seen, the vertical penetration resistance agrees well with the bearing capacity equation by Hossain and Randolph (2009b) and side friction of the lattice legs since this sleeved spudcan can be possibly viewed as circular pile (Randolph and Houlsby, 1984). Therefore, the vertical penetration load for this sleeved spudcan can be identically expressed as:

$$V_o = Q_p + Q_s = A\left(N_{co}s_{uo} + \gamma' z + \frac{\gamma' V_b}{A}\right) + Q_s \tag{4.11}$$

$$Q_s = V_o - Q_p = V_o - A\left(N_{co}s_{uo} + \gamma' z + \frac{\gamma' V_b}{A}\right) \tag{4.12}$$

As can be seen, the leg friction for the fully enclosed sleeved spudcan continued to increase with penetration depth.

As Figures 4.12 and 4.13 are shown, vertical penetration loads for both sleeved spudcan with opening area ratio, Ar, of 0.3 and 0.6 gradually increase. Beyond the limiting cavity depth, H of 5m, the vertical penetration load for both sleeved spudcan with opening area ratio, Ar, of 0.3 and 0.6, tend to increase slower than at shallower depths. This is led by the negative contribution of backfilling soil due to soil backflow mechanism (Hossain *et al.*, 2005c, 2006). Moreover, the minor difference between centrifuge results for sleeved spudcan with both opening area ratio, Ar, of 0.3 and 0.6 and the theoretical prediction of vertical penetration load by equations (4.8) and (4.9) is due to the weight of backfilled soil. This also suggested that the bearing

capacity equation, which is proposed by Hossain and Randolph (2009b) considering backflow mechanism, can also underestimate the vertical penetration load at deeper penetrations. Therefore, the vertical penetration load for these two sleeved spudcans can also be simply and similarly termed as:

$$V_o = Q_p + (1 - Ar)Q_s - A\gamma' H_f \quad (4.13)$$

Where (1-Ar)Q_s is the proportional inferred quantity of shaft friction attained from the results of fully enclosed sleeved spudcan multiply with the factor of (1-Ar) and $A\gamma' H_f$ is the calculated backfilled soil weight from equation (4.13).

Identically, before touching on the effect of lattice on the shaft frictions for two sleeved and one fully enclosed sleeved spudcans as presented in Figure 4.14, the shaft friction for each sleeved case can also be determined by using the shaft friction of the fully enclosed sleeved spudcan, Q_s, multiply with the factor (1-Ar).

For opening area ratio of 0.3 and 0.6, observation shows that the amount of backfilled soil at deeper penetration is roughly similar. In both cases, the amount of backflow soil is much less than the tests involving normally consolidated soil. This implies that the larger strength of the soil prevented it from ingress through the openings in the sleeves.

4.5.2 BEARING CAPACITY COEFFICIENT

In this section, the results from centrifuge tests are elaborated in terms of bearing capacity coefficient and normalized penetration depth, $\frac{z}{D}$ and opening area ratio, Ar.

4.5.2.1 NORMALLY CONSOLIDATED CLAY

Figure 4.15 shows the bearing capacity coefficient of un-sleeved and sleeved spudcan with different opening area ratios in normally consolidated clays. The bearing capacity coefficient, N_c for the sleeved spudcan with different opening ratios, Ar of 1, 0.6 and 0.3 tended to reach consistent values of 7.17, 7.90 and 8.80 from normalized embedment, $\frac{z}{D} = 1.25$ to $\frac{z}{D} = 1.50$. These values, which were obtained from centrifuge modeling, agreed fairly well with the bearing capacity coefficient for weightless soil of about 8 to 9 proposed by Hossain and Randolph (2009b). The difference between experimental bearing capacity coefficient and Hossain and Randolph (2009b) limiting values is due to the presence of softer material around and beneath the spudcan in normally consolidated clays (Lu *et al.*, 2001; Erbrich, 2005; Hossain and Randolph, 2009b). As for zero opening area ratio sleeved spudcan, the bearing capacity coefficient did not reach a constant value from normalized penetration depth, $\frac{z}{D} = 1.25$ to $\frac{z}{D} = 1.50$ because this latticed spudcan was able to prevent backflow.

Figure 4.16 illustrates on the effect of opening area ratio, Ar, on bearing capacity coefficient in normally consolidated clays. For the un-sleeved spudcan (i.e. opening area ratio of 1.0), the bearing capacity coefficient decreases gradually with depth. On the other hand, for the sleeved spudcan with zero opening ratios, the bearing capacity coefficient increases with depth from the normalized embedment, $\frac{z}{D} = 0$ to $\frac{z}{D} = 0.15$ before decreasing gradually with depth. This is because the fully enclosed sleeved spudcan does not allow backflow to occur at the shallower depths.

4.5.2.2 OVER-CONSOLIDATED CLAY

Figure 4.17 shows bearing capacity coefficient of un-sleeved and sleeved spudcan in over-consolidated clays. The bearing capacity coefficient for the sleeved spudcan

with different opening ratios of 1, 0.6, 0.3 and 0 tended to increase steadily to 7.87, 9.65, 12.11 and 13.87 at normalized embedment, $\frac{z}{D} = 1.50$. These values, which were obtained from centrifuge modeling, are higher than the bearing capacity coefficient of about 6, obtained by Hossain and Randolph (2009b) for weightless soil. The actual difference between experimental bearing capacity coefficient and Hossain and Randolph (2009b) limiting values is due to the assumption of presence of softer material around and beneath the spudcan in normally consolidated clays (Lu *et al.*, 2001; Erbrich, 2005; Hossain and Randolph, 2009b). However, soft remolded clay may not remain around the leg and beneath the spudcan in over-consolidated clays as the stiff clay tended to move away from the penetrating spudcan in regardless of spudcan roughness and opening area ratio. As for all opening area ratio sleeved spudcan, the bearing capacity coefficient did not reach a constant value from normalized penetration depth, $\frac{z}{D} = 1.25$ to $\frac{z}{D} = 1.50$.

Figure 4.18 illustrates on the effect of opening area ratio, Ar, on bearing capacity coefficient in over-consolidated clays. It was obvious that the bearing capacity coefficient, N_c, for the sleeved spudcan with opening area ratio, Ar, of 1 would increase gradually with depth rather than those in normally consolidated clays decrease steadily with depth. As for the sleeved spudcan with zero opening area ratios, the bearing capacity exhibited the similar trend with the one with unity opening area ratio even though the increase in bearing capacity coefficient for sleeved spudcan is greater than.

Description	**D (m)**	**s_{um} (kPa)**	**k (kPa/m)**	**γ' (kN/m^3)**	**$\frac{s_{um}}{\gamma' D}$**	**$\frac{kD}{s_{um}}$**
Normally consolidated clays	12	2.2	1.56	6	0.031	8.51
Over-consolidated clays	12	20	1.05	6	0.277	0.63

Table 4.1 Summary of soil properties on nonhomogeneous clay performed by centrifuge testing ($\frac{kD}{s_{um}} > 0$)

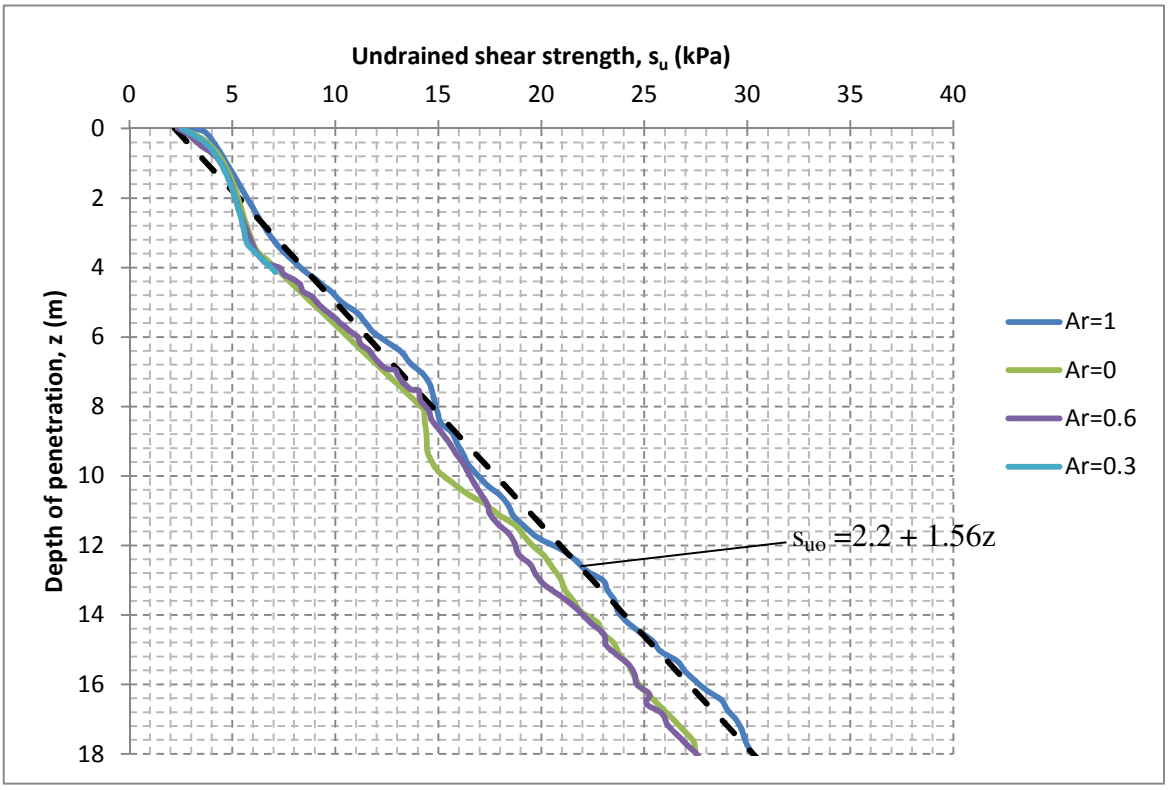

Figure 4.1 Shear strength profiles for normally consolidated clays

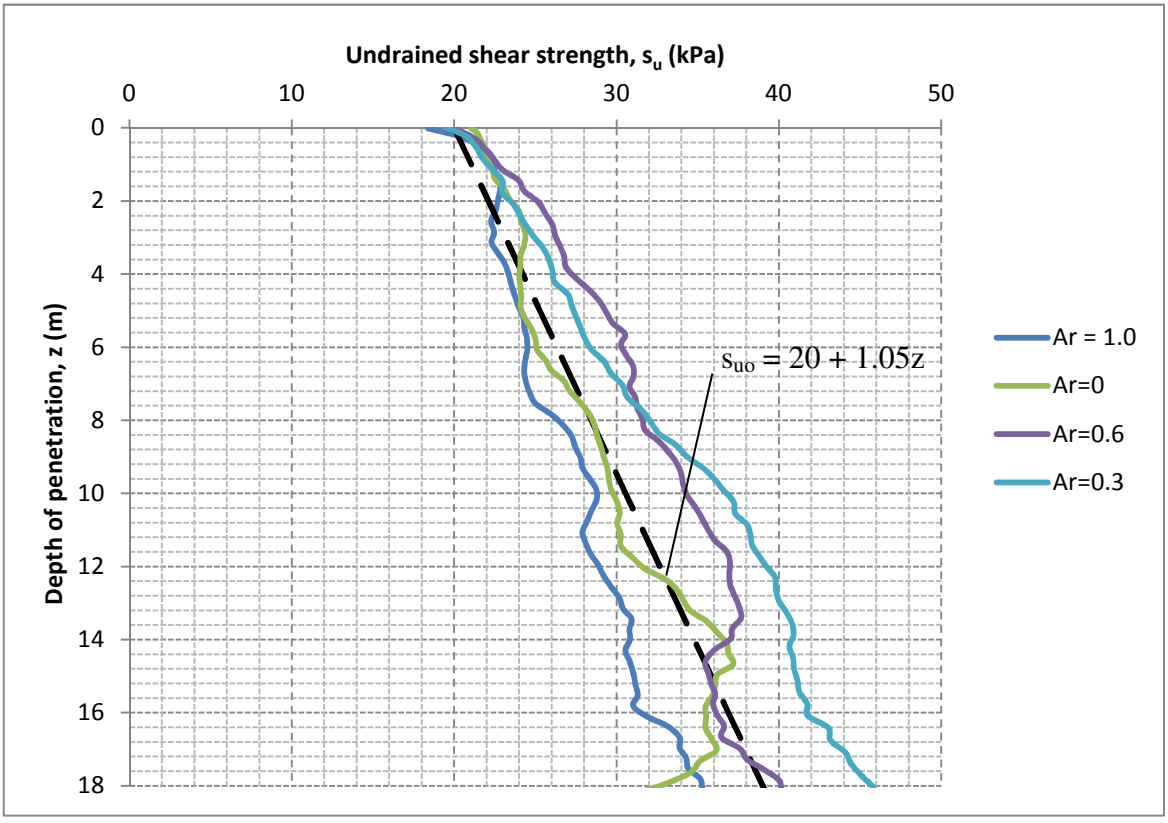

Figure 4.2 Shear strength profiles for over-consolidated clays

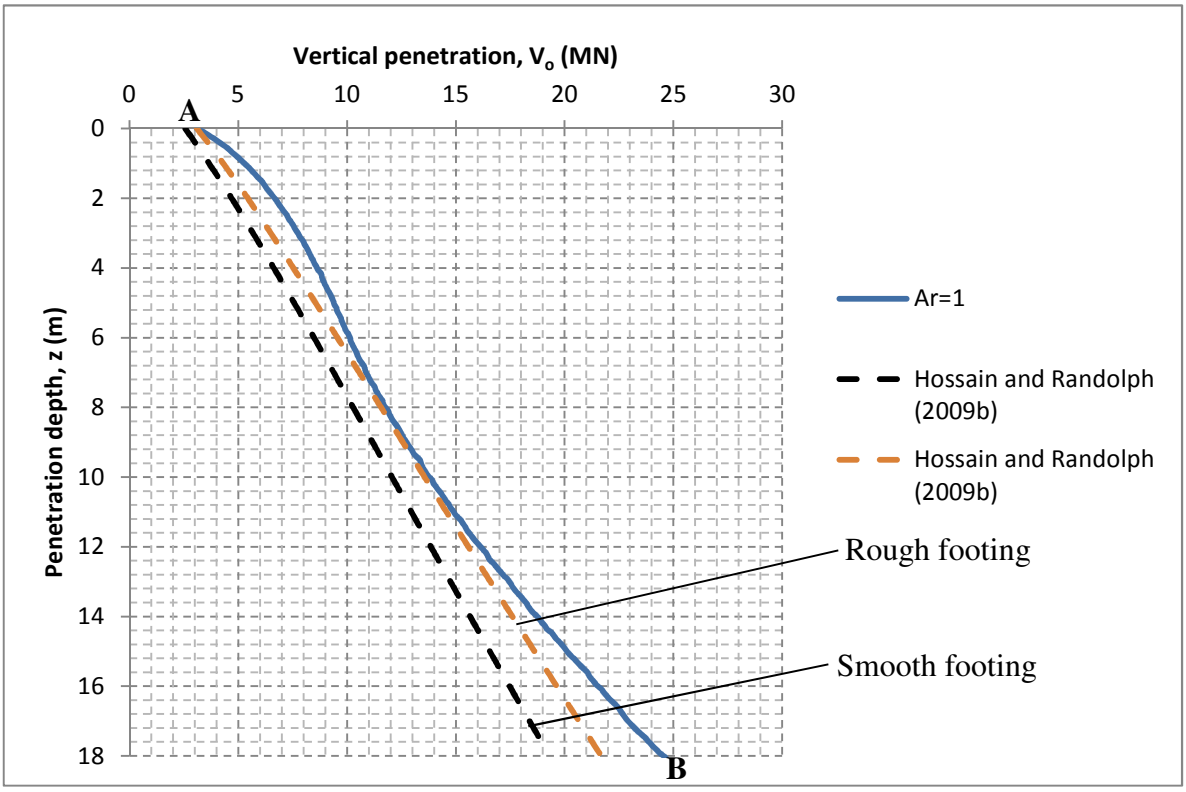

Figure 4.3 Single spudcan penetration responses in normally consolidated clays

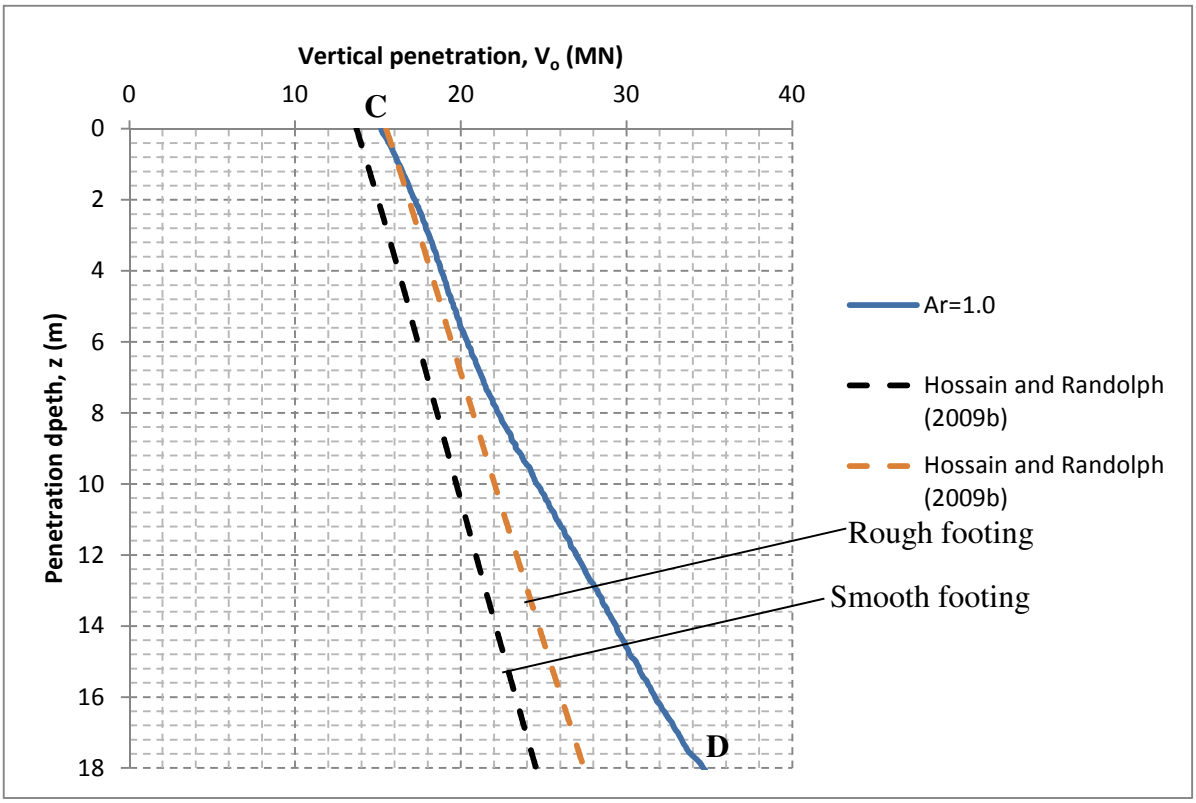

Figure 4.4 Single spudcan penetration responses in over-consolidated clays

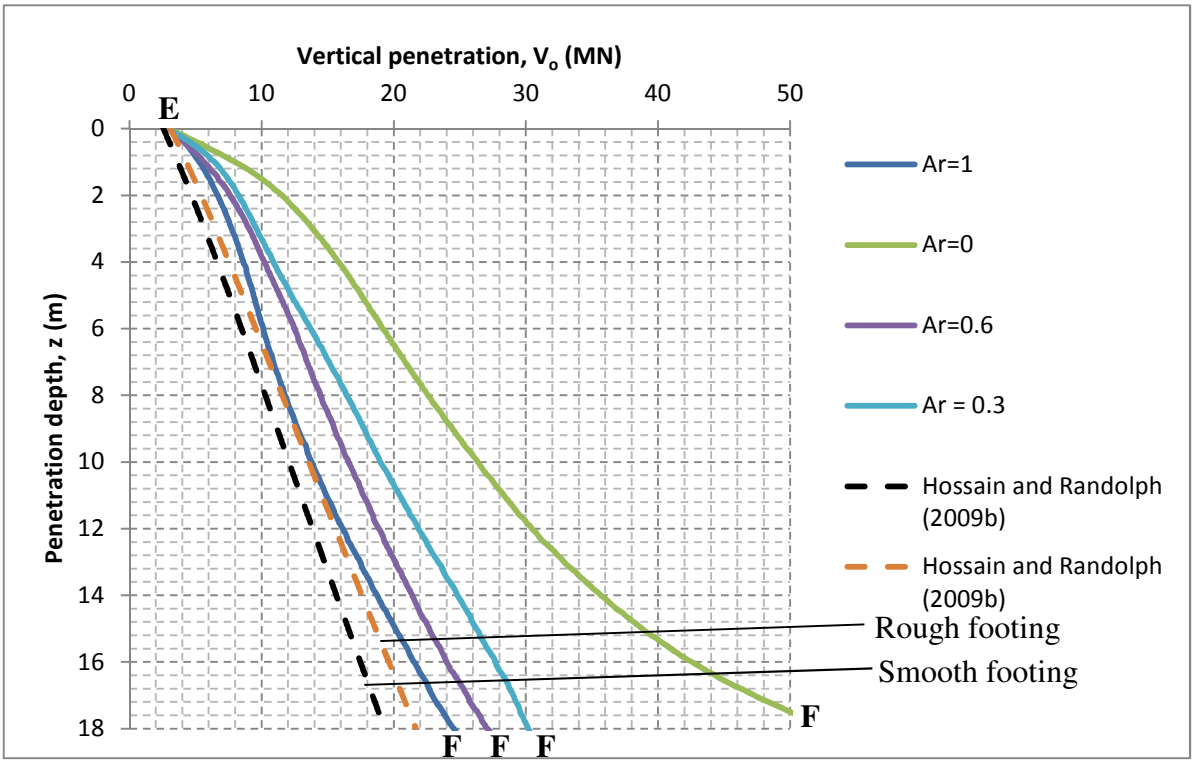

Figure 4.5 Single and sleeved spudcan penetration responses in normally consolidated clays

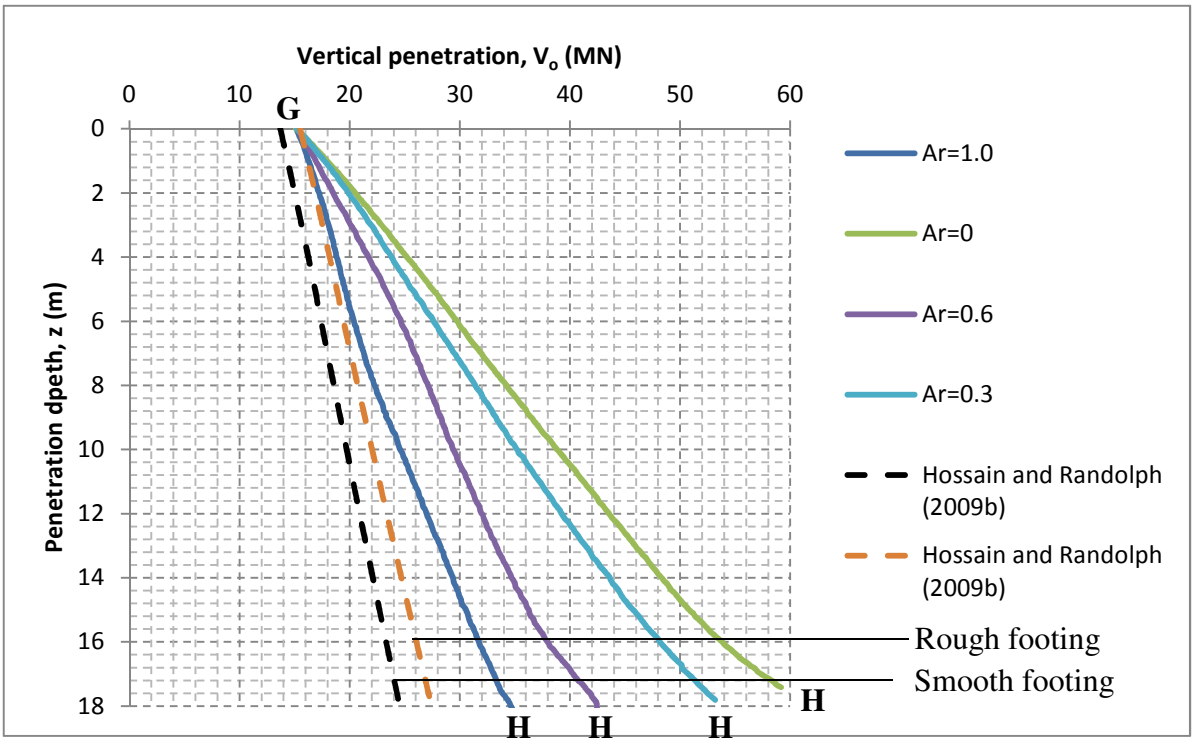

Figure 4.6 Single and sleeved spudcan penetration responses in over-consolidated clays

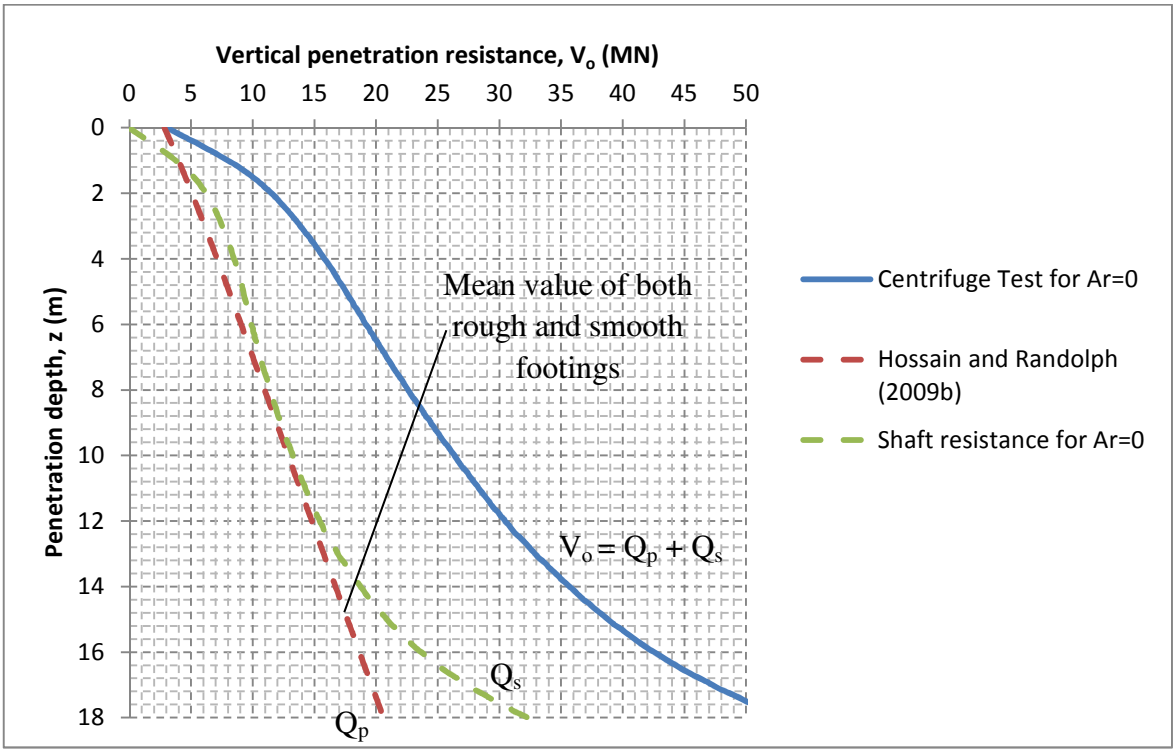

Figure 4.7 Sleeved spudcan with opening area ratio, Ar = 0, penetration response in normally consolidated clay

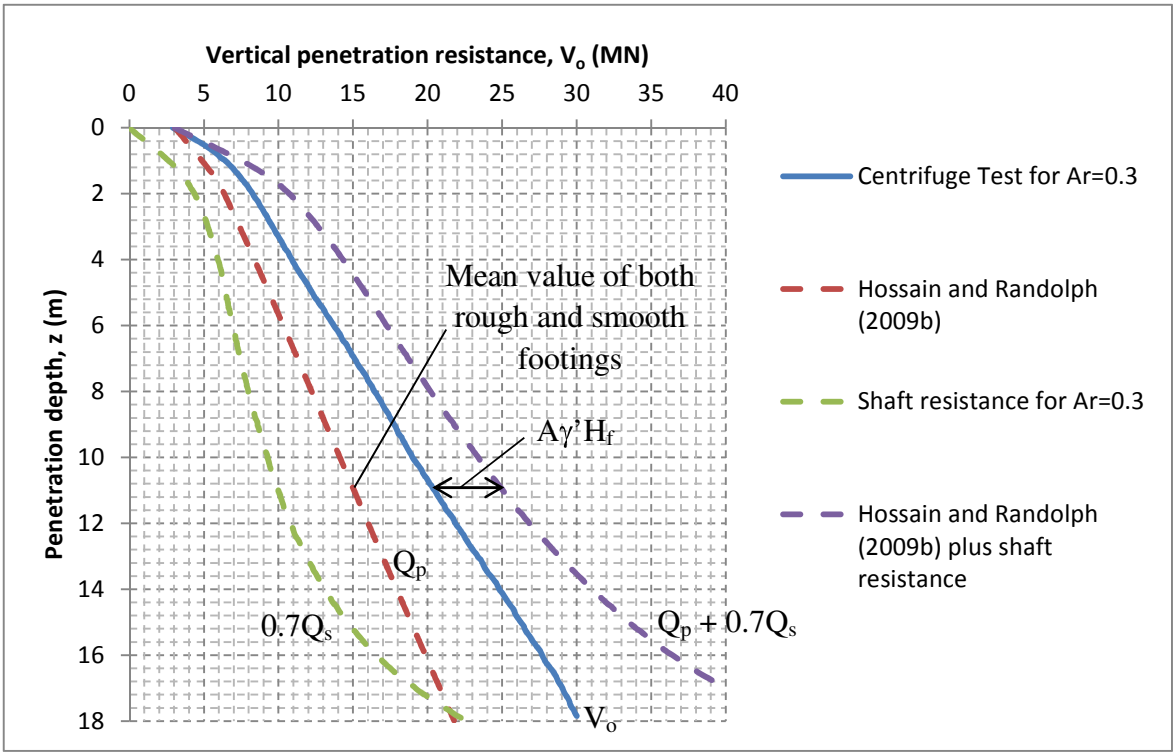

Figure 4.8 Sleeved spudcan with opening area ratio, Ar = 0.3, penetration response in normally consolidated clay

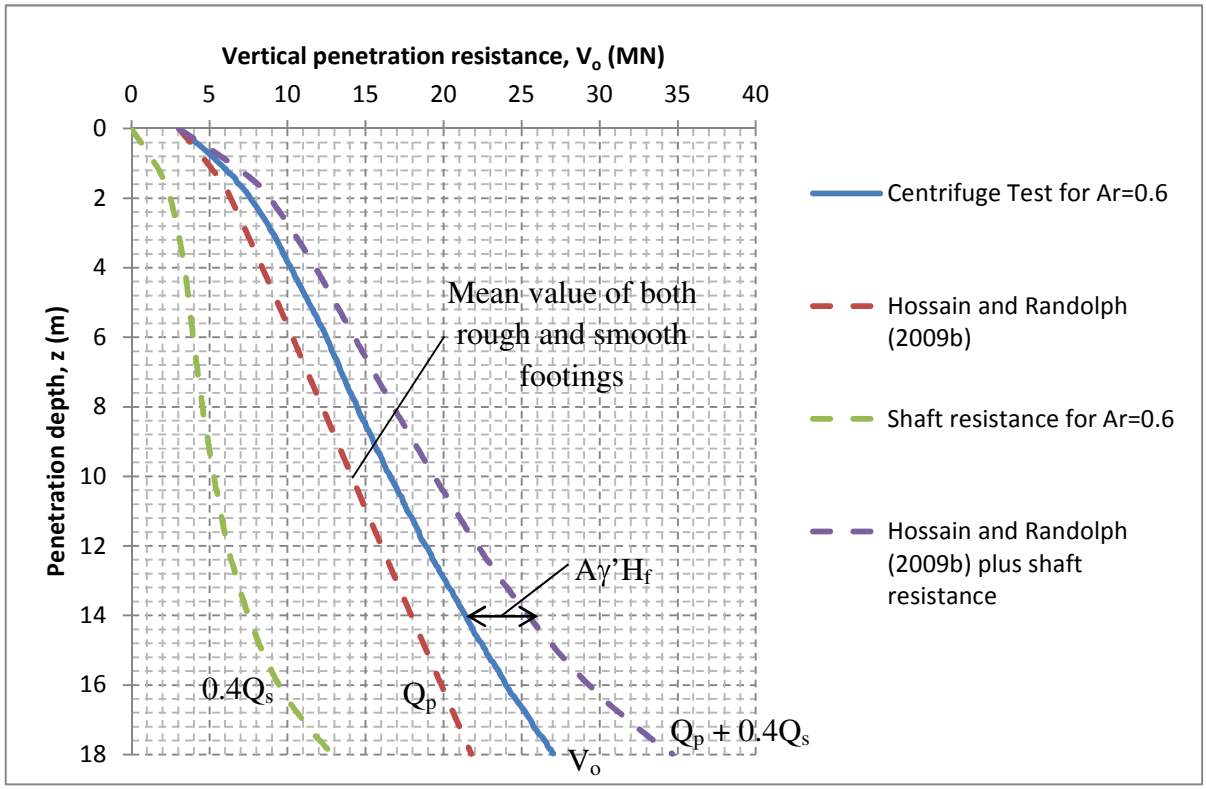

Figure 4.9 Sleeved spudcan with opening area ratio, Ar = 0.6, penetration response in normally consolidated clay

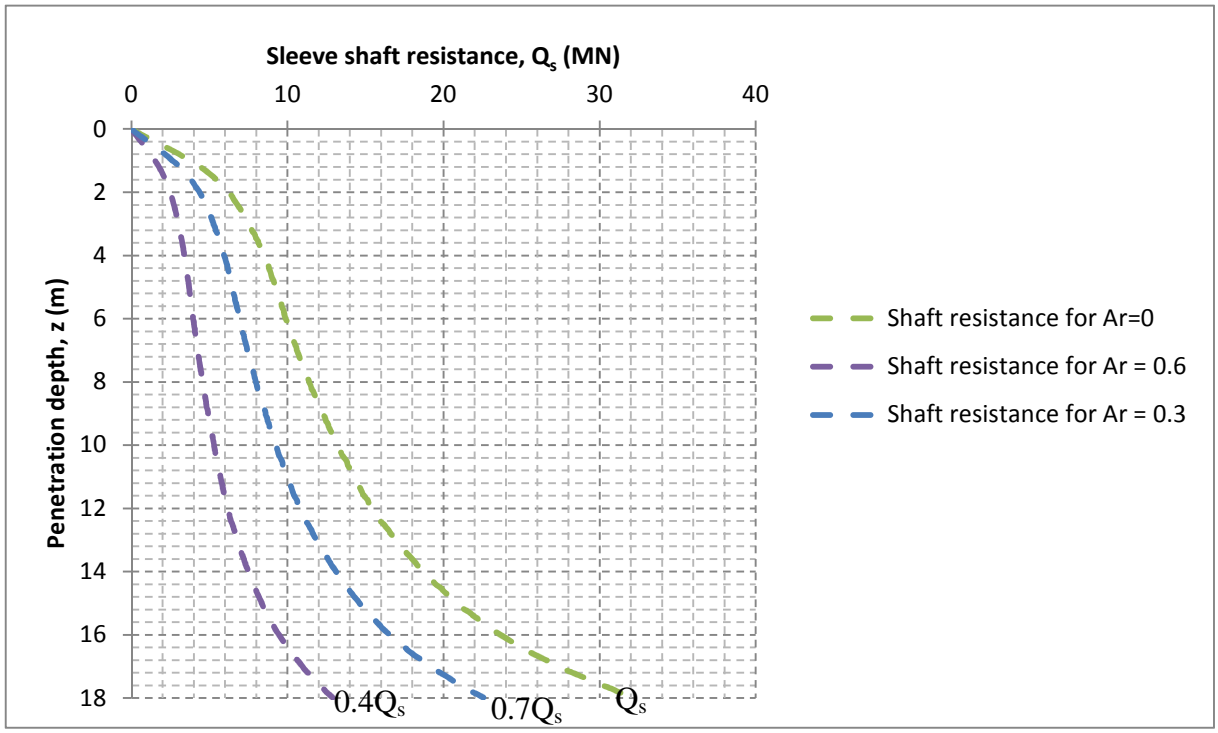

Figure 4.10 Shaft friction of sleeved spudcan with different opening ratios in normally consolidated clays

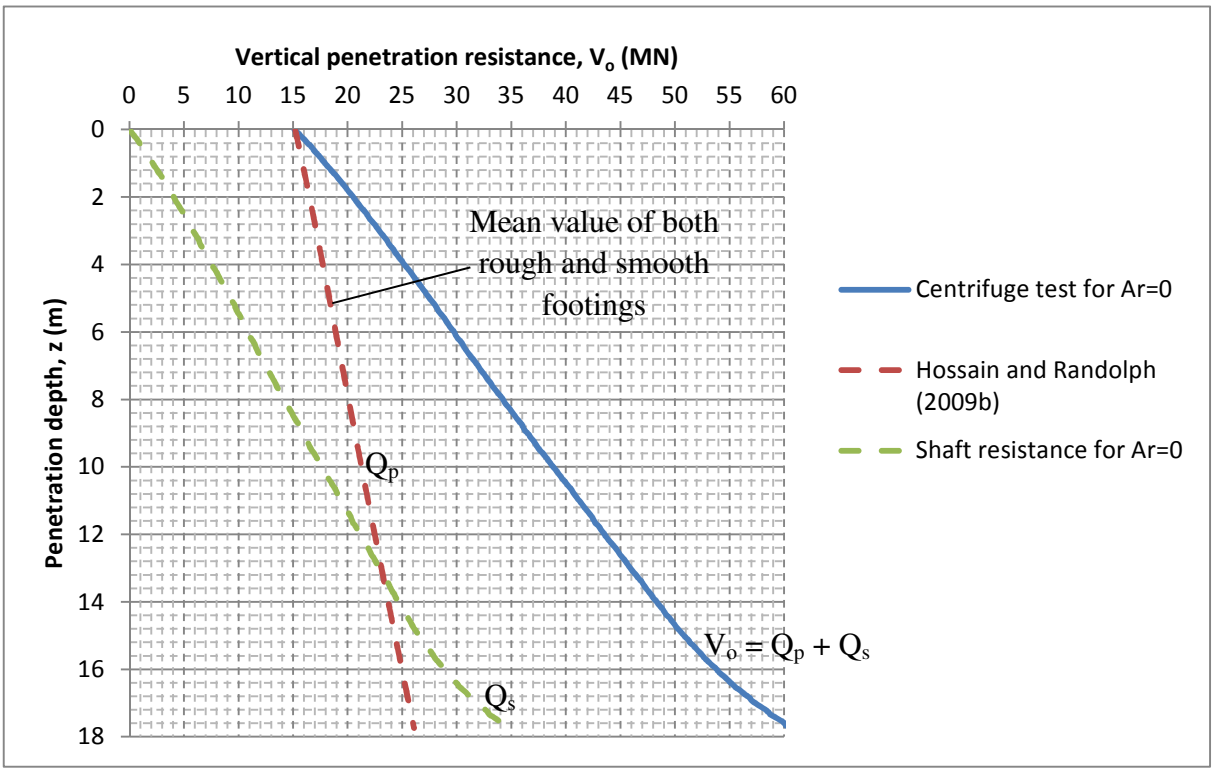

Figure 4.11 Sleeved spudcan with opening area ratio, Ar = 0, penetration response in over-consolidated clay

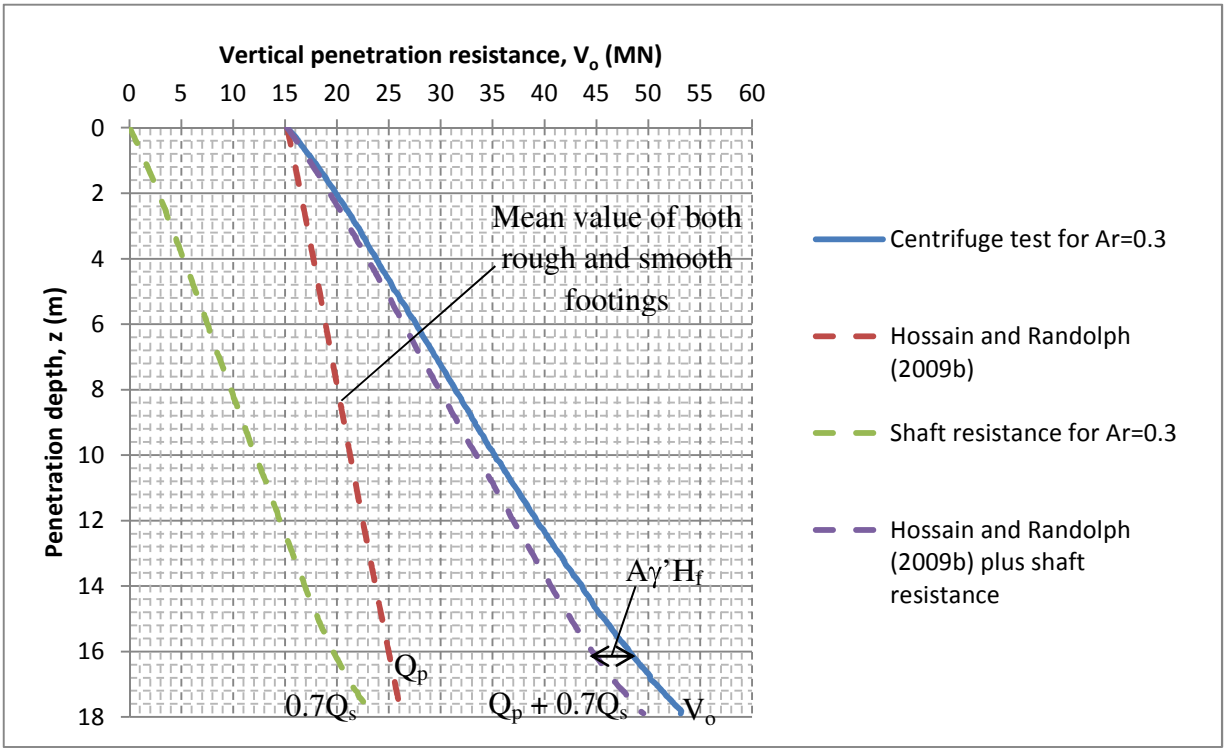

Figure 4.12 Sleeved spudcan with opening area ratio, Ar = 0.3, penetration response in over-consolidated clay

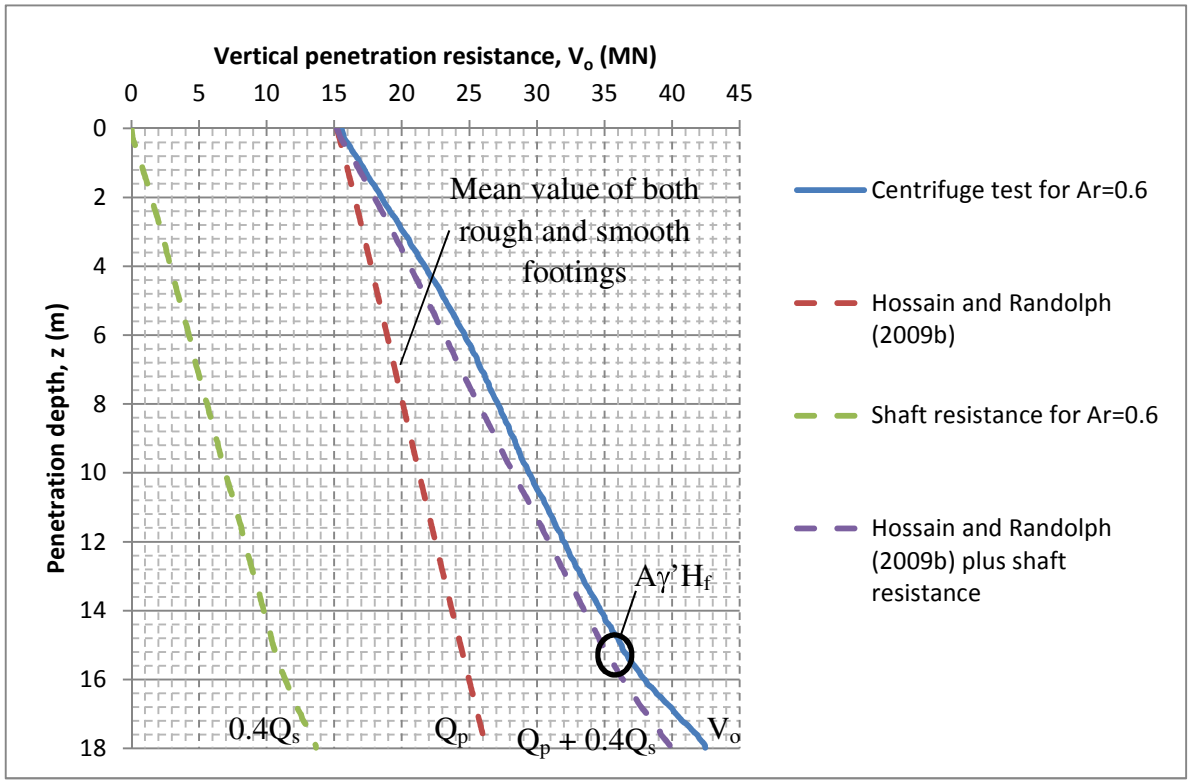

Figure 4.13 Sleeved spudcan with opening area ratio, Ar = 0.6, penetration response in over-consolidated clay

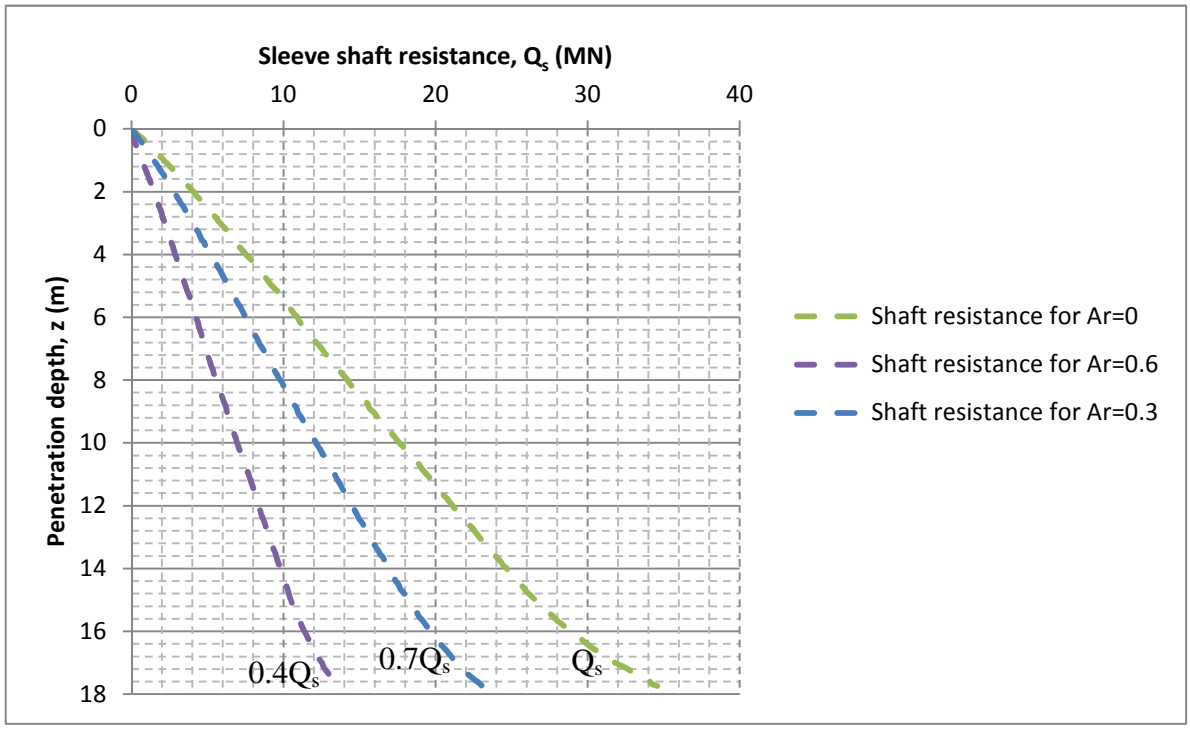

Figure 4.14 Shaft friction of sleeved spudcan with different opening ratios in over-consolidated clays

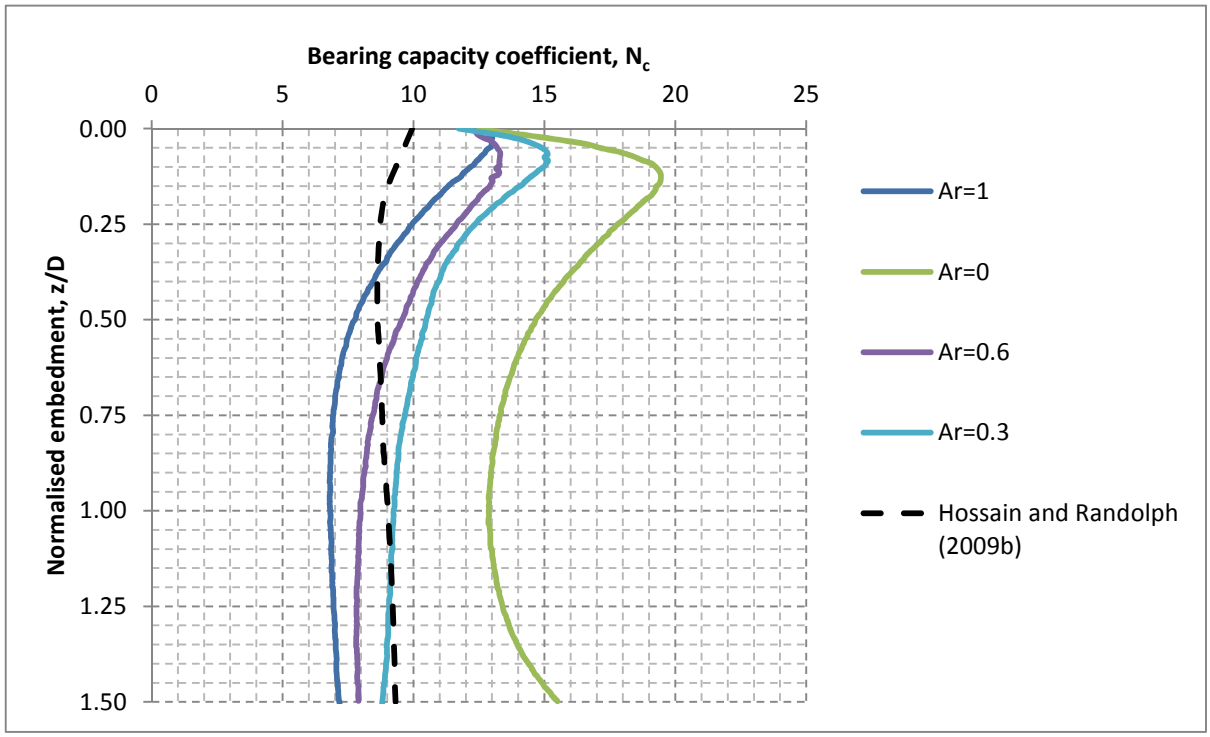

Figure 4.15 Bearing capacity coefficient of single and sleeved spudcan with different opening area ratios in normally consolidated clays

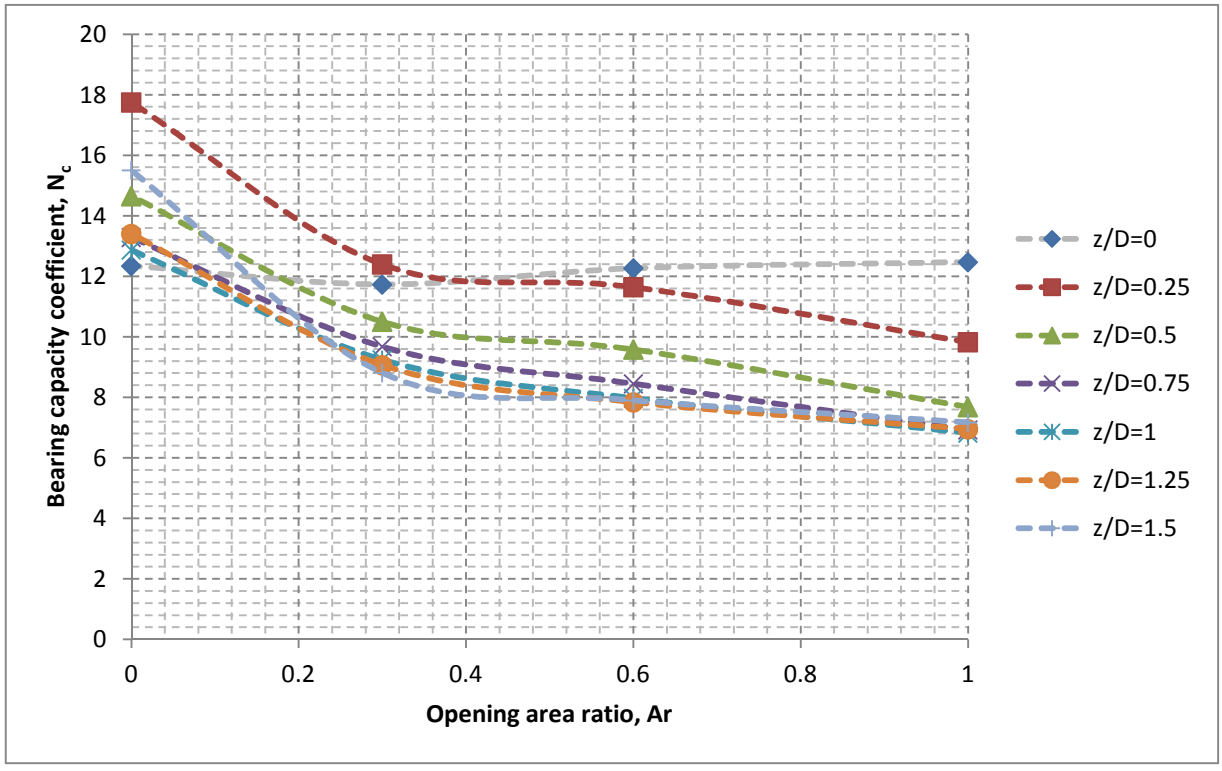

Figure 4.16 Effect of opening area ratio on bearing capacity coefficient of single and sleeved spudcan in normally consolidated clays

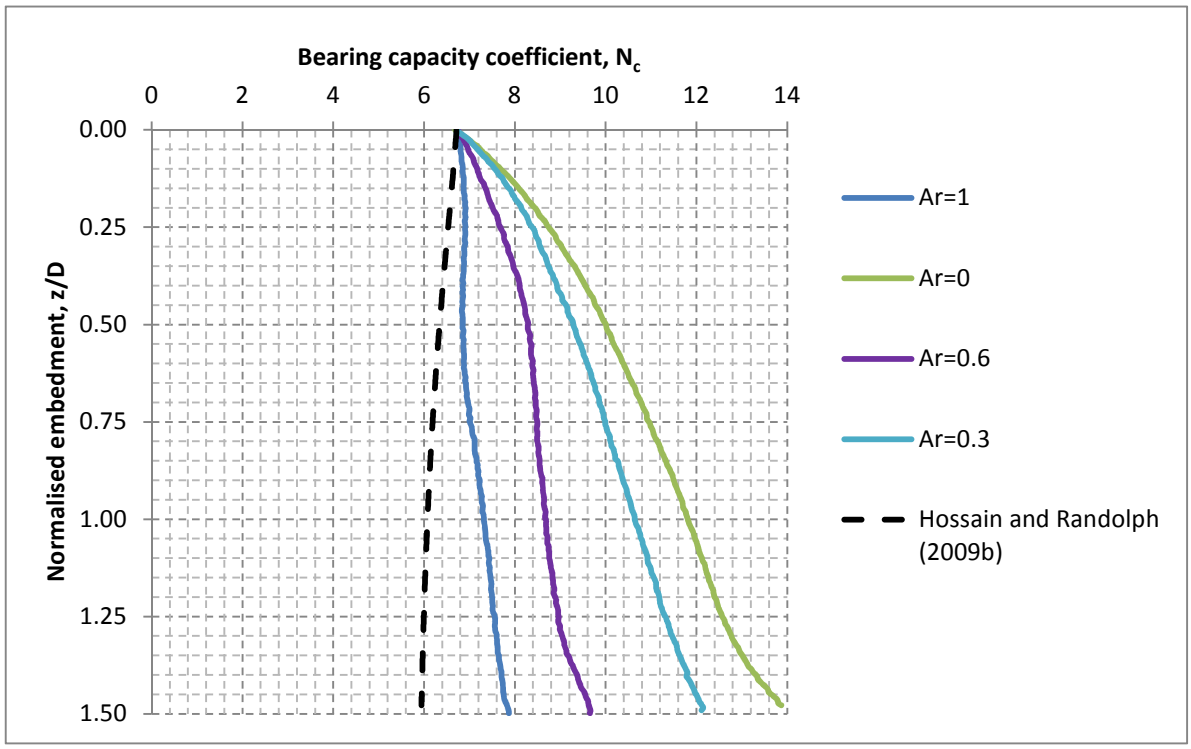

Figure 4.17 Bearing capacity coefficient of single and sleeved spudcan with different opening area ratios in over-consolidated clays

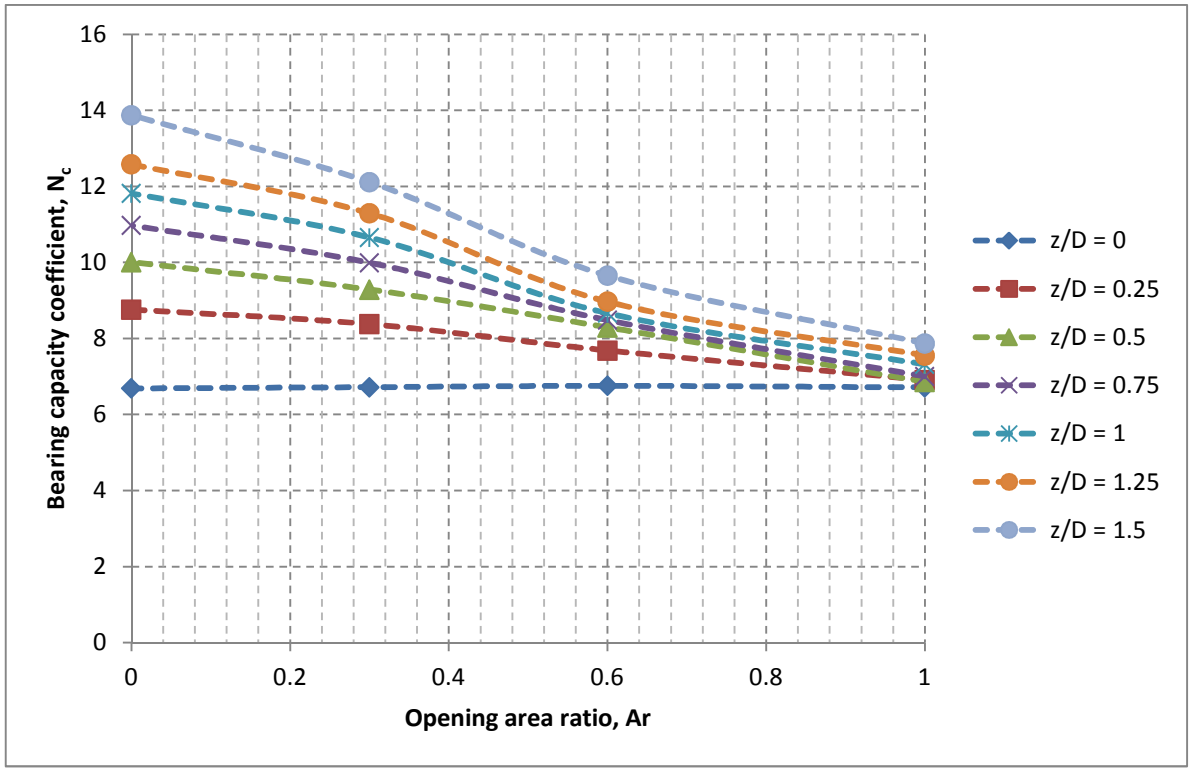

Figure 4.18 Effect of opening area ratio on bearing capacity coefficient of single and sleeved spudcan in over-consolidated clays

CHAPTER 5 CONCLUSIONS

Finally, this chapter will summarize the important conclusions drawn from this study and provide some recommendations or suggestions for future research.

5.1 SUMMARY OF FINDINGS

In this study, the effects of the latticed legs on spudcan penetration behavior were examined using centrifuge models of sleeved spudcans with different opening area ratio on both normally consolidated and over-consolidated clays. The findings of this centrifuge model study are summarized below:

1) During the preloading process, the vertical penetration loads of the sleeved spudcans with different opening area ratio on over-consolidated clays are larger than those on normally consolidated clays. On the other hand, sleeved frictions in over-consolidated clays are lower than those in normally consolidated clays. This is consistent with Tomlinson's (1977) suggestion that the over-consolidated clays tend to move away from the sleeved spudcans during vertical penetration whereas normally consolidated clay has greater tendency to collapse around the spudcan and the sleeve.

2) The ultimate bearing capacity of the sleeved spudcan consists of the tip resistance and side friction during deep penetration. The fully enclosed spudcan can be viewed as a circular pile with backflow being completely prevented. For sleeved spudcans with openings, soil backflow still occurs within over-consolidated and normally consolidated clays. However, the amount of backfilled soil is less for over-consolidated clays compared to normally consolidated clays. Therefore, the amount of backfilled soil on

spudcan top and resistance to soil backflow mechanism are also closely attributed by the amount of opening area ratio of the lattices for both normally consolidated and over-consolidated clays.

3) The bearing capacity coefficients of the sleeved spudcans on both normally consolidated and over-consolidated clays remained stagnant during deep penetrations with the opening area ratio of more than 0.6 and 0.8 respectively.

Based on the results in the previous chapter, some design implications may be suggested and discussed in the next section.

5.2 DESIGN IMPLICATIONS

In the latest Recommended Practice for Site Specific Assessment of Mobile Jack-up Unit published by Society of Naval Architects and Marine Engineers (SNAME, 2008), the vertical bearing capacity of the spudcan footing has been normally determined by the conventional bearing capacity equations (Skempton, 1951) for clays before Hossain and Randolph (2009b) proposed the new bearing capacity equation for spudcan taking into account of soil backflow mechanism. In this approach, the single spudcan is considered as a circular footing penetrating deeply into the seabed with a load penetration curve defined by a function of footing diameter, rate of increase of soil strength and soil strength at mudline. The spudcan is assumed to be unable to resist the soil backflow mechanism during deep penetration.

As presented in the previous chapter, soil backflow can occur in un-sleeved and sleeved spudcans with openings. In addition, the sleeve, and presumably the lattice leg also contributes to side friction in both normally-consolidated and over-consolidated clays. Hence, the bearing capacity equation by Hossain and Randolph, (2009b) may be under-estimated the penetration resistance of deep

penetrated spudcans with lattice legs. The concentration of this research is the spudcan performance with different opening area ratio and the mechanism giving rise to it. Further work is needed to develop more suitable equation for practical uses. Some recommendations in line with the above objectives will be illustrated and discussed in the upcoming section.

5.3 RECOMMENDATIONS FOR FUTURE STUDY

The recommendations for future study are listed below:

1) In this study, most of the proposed mechanisms are based on Hossain and Randolph's (2009b) findings and observation during centrifuge testing. However, soil deformation beneath and under single or sleeved spudcan footing was not monitored. Thus, particle image velocimetry (PIV) (White *et al.*, 2003) coupled with pore pressure and total stress transducers on the spudcan top shall be adopted to investigate the soil deformation below and around single and sleeved spudcans.

2) In oil and gas industry practice, the spudcan may be founded on clayey or sandy soils and most likely on non-homogeneous stratified soils. In such soil conditions, the spudcan bearing response is most probably different as sands may not have ability to stay vertical or exhibit the soil backflow mechanism as that observed in clays. Therefore, the vertical penetration resistance of the sleeved spudcan on homogeneous and layered soils especially sands is worth investigating.

3) In present study, only circular shaped lattices were tested. The difference in shape of lattices may change the failure and deformation mechanisms. However, the design of sleeved spudcan remains as one of the least studied

topics. The interaction between the lattice shapes and its static and cyclic behaviors may be examined to propose the optimum design guidelines for sleeved spudcans.

REFERNCES

Ackland, D.F. (1949). Moving heaven and earth, R.G. Le Tourneau. Marshall Morgan and Scott, London.

Adrian, R.J. (1991). Particle imaging techniques for experimental fluid mechanics. Annual Review of Fluid Mechanics, Vol. 23, pp. 261 – 304.

Ahmad, A. and J.H. Chandler. (1999). Photogrammetric capabilities of the Kodak DC40, DCS420 and DCS460 digital cameras. Photogrammetric Record, Vol. 16(94), pp. 601 – 615.

Ahrendsen, B.K., R.N. Dutt and W.B. Ingram. (1989). Jackup footing performance: an integrated approach to geotechnical assessment. Proc. Offshore Technology Conf., Texas, USA, OTC 6027.

Allersma, H.G.B., B. Hospers and J.G. den Braber. (1997). Centrifuge tests on the sliding behaviour of spudcans. Canadian Geotechnical Journal, Vol. 34, pp. 658 – 663.

API. (1993). Recommended practice for planning, designing and constructing fixed offshore platforms load and resistance factor design. RP 2A LRFD, First edition, Washington DC: American Petroleum Institute.

Asaoka, A. (1978). Observational procedure of settlement prediction. Soils and Foundations, Vol. 18(4), pp. 87 – 101.

Baerheim, M., D. Manschot and T. Nortvedt. (1997). Use of jack-up as a permanent

installation for the marginal Siri field. Proc. 6th Int. Conf., the jackup platform, design, construction and operation, City University, London.

Bassett, W.T., M.C.R. Davis, M.J. Gunn and R.H.G Parry. (1981). Centrifuge models to evaluate numerical models. Proc. 10th Int. Conf. on Soil Mechanics & Geotechnical Engineering, Stockholm.

Baglioni, V.P., G.S. Chow and S.N. Endley. (1982). Jackup foundation stability in stratified soil profiles. Proc. Offshore Technology Conf., Texas, USA, OTC 4409.

Barbosa-Cruz, E.R. and M.F. Randolph. (2005). Bearing capacity and large penetration of a cylindrical object at shallow embedments. Proc. Int. Symp. Frontiers in Offshore Geotechnics, Perth, Australia, pp. 615 – 621.

Bennett and Associate and KeppelFELS OTD. (2005). Jackup units: a technical primer for the offshore industry professional. KeppelFels.

Bennett, W.T. and B.P.M Sharples. (1987). Jackup legs to stand on? Mobile Offshore Structures, Elsevier, London, pp. 1 – 32.

Bienen, B. (2009). Predicting the load displacement response of a mobile jackup drilling rig on sand. Australian Geomechanics, Vol. 44(4), pp. 1 – 12.

Bienen, B., B. Byrne, G.T. Houlsby and M.J. Cassidy. (2006). Investigating six degree of freedom loading of shallow foundations on sand. Géotechnique, Vol. 56(6), pp. 367 – 379.

Bienen, B., C. Gaudin and M.J. Cassidy. (2007). Centrifuge tests of shallow footing behavior on sand under combined vertical torsional loading. Int. Journal of Physical

Modelling in Geotechnics. Vol. 7(2), pp. 1 – 21.

Bienen, B., C. Gaudin and M.J. Cassidy. (2009). The influence of pullout load on the efficiency of water jetting during spudcan extraction. Applied Ocean Research. Vol. 31(3), pp. 202 – 211.

Bienen, B. and M.J. Cassidy. (2005). Simulation of the soil-structure-fluid interaction of jack-up structures. Proc. 11th Int. Conf. International Association of Computer Methods and Advances in Geomechanics IACMAG, Italy, Vol. 3, pp. 603 – 610.

Bienen, B. and M.J. Cassidy. (2009). Physical modeling of the push-over capacity of a jackup structure on sand in a geotechnical centrifuge. Canadian Geotechnical Journal, Vol. 46(2), pp. 190 – 207.

Bienen, B. and M.J. Cassidy. (2009). Three dimensional numerical analysis of centrifuge experiments on a model jackup drilling rig on sand. Canadian Geotechnical Journal, Vol. 46(2), pp. 208 – 224.

Brekke, J.N., J.D. Murff, R.B. Campbell and W.C. Lamb. (1989). Calibration of jackup leg foundation model using full scale structural measurements. Proc. Offshore Technology Conf., Texas, USA, OTC 6127.

Brekke, J.N., R.B. Campbell, W.C. Lamb and J.D. Murff. (1990). Calibration of a jackup structural analysis procedure using field measurement from a North Sea jackup. Proc. Offshore Technology Conf., Texas, USA, OTC 6465.

Britto, A.M. and O. Kusakabe. (1983). Stability of axisymmetric excavations in clay. Journal of Geotechnical Engineering, ASCE, Vol. 105(9), pp. 666 – 681.

Butterfield, R., G.T. Houlsby and G. Gottardi. (1997). Standardized sign convention and notation for generally loaded foundation. Géotechnique, Vol. 47(5), pp. 1051 – 1054.

Byrne, B.W. and G.T. Houlsby. (2001). Observations of footing behaviour on loose carbonate sands. Géotechnique, Vol. 51(5), pp. 463 – 466.

Byrne, B.W. and M.J. Cassidy. (2002). Investigating the response of offshore foundations in soft clay soils. Proc. OMAE'02, 21st Int. Conf. Offshore Mechanics and Arctic Engineering, Oslo.

Carlsen, C.A., H. Kjeoy and K. Eriksson. (1986). Structural behaviour of harsh environment jack-ups. The jackup drilling platform design and operation, London, Collins, pp. 90 – 136.

Cassidy, M.J. (1999). Non-linear analyses of jack-up structures subjected to random waves. D.Phil Thesis, University of Oxford.

Cassidy, M.J. (2007). Experimental observations of the combined loading behavior of circular footings on loose silica sand. Géotechnique, Vol. 57(4), pp. 397 – 401.

Cassidy, M.J., B.W. Byrne and G.T. Houlsby. (2002). Modeling the behavior of circular footings under combined loading on loose carbonate sand. Géotechnique, Vol. 52(10), pp. 705 – 712.

Cassidy, M.J., B.W. Byrne and M.F. Randolph. (2004). A comparison of combined load behavior of spudcan and caisson foundations on normally consolidated clay. Geotechnique, Vol. 54(2), pp. 91 – 106.

Cassidy, M.J., C.M. Martin and G.T. Houlsby. (2004). Development and application of force resultant models describing jackup foundation behavior. Marine Structures, Vol. 17, pp. 165 – 193.

Cassidy, M.J., G.T. Houlsby, G.T. Hoyle and M. Marcom. (2002). Determining appropriate stiffness levels for spudcan foundations using jackup case records. Proc. OMAE'02, 21st Int. Conf. Offshore Mechanics and Arctic Engineering, Oslo.

Cassidy, M.J., C.K. Quah and K.S. Foo (2009). Experimental investigation of the reinstallation of spudcan footings close to existing footprints. Journal of Geotechnical and Geoenvironmental Engineering, ASCE, Vol. 135(4), pp. 474 – 486.

Chiba, S., T. Onuki and K. Sao. (1986). Static and dynamic measurement of bottom fixity. The jackup drilling platform: design and construction, London, pp. 307 – 327.

Chung, S.F. and M.F. Randolph. (2004). Penetration resistance in soft clay for different shaped penetrometers. Proc. 2nd Int. Conf. on Site Characterization, Porto, Portugal, Vol. 1, pp. 671 – 678.

Cooke, B (1991). Selection of operative centrifuge radius to minimize stress error in calculations. Canadian Geotechnical Journal, Vol. 28, pp. 160 – 161.

Craig, W.H. (1984). Proceedings of the international symposium application of centrifuge modeling to geotechnical design, Manchester, United Kingdom.

Craig, W.H. (1998). Spudcan foundations: installation with deep penetration and subsequent removal. Proc. Institution Civil Engineers and Geotechnical Engineering, Vol. 131, pp. 146 – 151.

Craig, W.H. and K. Chua. (1990a). Deep penetration of spudcan foundations on sand and clay. Géotechnique, Vol. 40(4), pp. 541 – 556.

Craig, W.H. and K. Chua. (1990b). Extraction forces for offshore foundations under undrained loading. Journal of Geotechnical Engineering, ASCE, Vol. 116(5), pp. 868 – 884.

Craig, W.H. and K. Chua. (1991). Large displacement performance of jackup spudcans. Proc. Centrifuge '91, Balkema, Rotterdam, pp. 139 – 144.

Craig, W.H. and M.D. Higham. (1985). The application of centrifugal modeling to the design of jackup rig foundations. Proc. Conf. Offshore Site Investigation, Society for Underwater Technology, pp. 293 – 305.

Craig, W.H. and N.K.S Al-Saoudi (1981). The behavior of some model offshore structures. Proc. 10th Int. Conf. on Soil Mechanics and Foundation Engineering, Stockholm, Sweden, pp. 541 – 556.

Davis, E.H. and J.R. Booker. (1973). The effect of increasing stress with depth on the bearing capacity of clays. Géotechnique, Vol. 23(4), pp. 551 – 563.

Davis, E.H. and J.T. Christian. (1971). Bearing capacity of anisotropic cohesive soils. Journal of Soil Mechanics and Foundation Engineering Division, ASCE, Vol. 97(5), pp. 753 – 769.

Dean, E.T.R. (2007). Consistent preload calculations for jackup spudcan penetration in clays. Canadian Geotechnical Journal, Vol. 45, pp. 705 – 714.

Dean, E.T.R., R.G. James, A.N. Schofield, F.S.C. Tan and Y. Tsukamoto. (1993). The bearing capacity of conical footings on sand in relation to the behavior of spudcan footings of jackups. Predicitive Soil Mechanics, Thomas Telford, London, pp. 230 – 253.

Dean, E.T.R., R.G. James, A.N. Schofield, P.C. Wong and J.D. Murff. (1995). Centrifuge modeling of 3 leg jackups with skirted and non-skirted spuds on partially drained sand. Proc. Offshore Technology Conf., Texas, USA, OTC 7839.

Dean, E.T.R., R.G. James, A.N. Schofield and Y. Tsukamoto. (1998). Drum centrifuge study of three leg jackup models on clay. Geotechnique, Vol. 48(6), pp. 761 – 785.

Dean, E.T.R and R. Metters. (2009). Cyclic stiffness degradation in nonlinear jackup dynamics. Proc. Offshore Technology Conf., Texas, USA, OTC 19998.

Dier, A., B. Carroll and S. Abolfathi. (2004). Guidelines for jack-up rigs with particular reference to foundation integrity. MSL Engineering Limited, Egham Surrey UK. Research report 289.

Einav, I. and M.F. Randolph. (2005). Combining upper bound and strain path methods for evaluating penetration resistance. Int. Journal of Numerical Methods in Engineering. Vol. 63(14), pp. 1991 – 2016.

Endley, S.N., V. Rapoport, P.J. Thompson and V.P. Baglioni. (1981). Prediction of jackup rig footing penetration. Proc. Offshore Technology Conf., Texas, USA, OTC 4144.

Erbich, C.T. (2005). Australian frontiers – spudcans on the edge. Int. Symp.

Frontiers in Offshore Geotechnics, Perth, Australia.

Ethrog, U. (1994). Strain measurement by digital image processing. Proc. 10th Conf. Recent Advances in Experimental Mechanics, Balkema, Rotterdam, pp. 411 – 415.

Finnie, I.W.S. (1993). Performance of shallow foundations in calcareous soils. Ph.D Thesis, University of Western Australia, Perth.

Finnie, I.M.S. and M.F. Randolph. (1994a). Bearing response of shallow foundations in uncemented calcareous sand. Proc. Centrifuge'94, Balkema, Rotterdam.

Finnie, I.W.S. and M.F. Randolph. (1994b). Punch through and liquefaction induced failure of shallow foundations on calcareous sediments. Proc. Int. Conf. Behaviour of Offshore Structures BOSS, pp. 217 – 230.

Gan, C.T. (2010). Centrifuge model study on spudcan footprint interaction. Ph.D Thesis, National University of Singapore.

Gan, C.T., C.F. Leung and Y.K. Chow. (2007). A study on spudcan footprint interaction. Proc. 16th Southeast Asia Geotechnical Conf., Kuala Lumpur, Malaysia, pp. 735 – 740.

Gan, C.T., C.F. Leung and Y.K. Chow (2008). A study on spudcan footprint interaction. Proc. 2nd BGA Int. Conf. on Foundations, Dundee, Scotland, pp. 861 – 872.

Garnier, J., C. Gaudin, S.M. Springman, P.J. Culligan, D. Goodings, D. König, B.

Kutter, R. Phillips, M.F. Randolph and L. Thorel. (2007). Catalogue of scaling laws and similitude questions in centrifuge modeling. Int. Journal of Physical Modelling in Geotechnics, Vol. 7(3), pp. 1 – 24.

Gaudin, C., B. Bienen and M.J. Cassidy. (2010). Investigation of the potential of bottom water jetting to ease spudcan extraction in soft clay. Géotechnique, accepted.

Gaudin, C., E.C. Cluckey, J. Garnier and R. Phillips. (2010). New frontiers for centrifuge modeling in offshore geotechnics. Int. Symp. Frontiers in Offshore Geotechnics, Perth, Australia.

Gaudin, C., M.J. Cassidy and T. Donovan. (2007). Spudcan reinstallation near existing footprints. Proc. 6th Int. Conf. Offshore Site Investigation and Geotechnics, 11 – 13 September, London, pp. 285 – 292.

Gaudin, C., M.J. Cassidy, B. Bienen and M.S. Hossain. (2011). Recent contributions of geotechnical centrifuge modeling to the understanding of jackup spudcan behaviour. Ocean Engineering, in press.

Gemeinhardt, J.P. and J.A. Focht. (1970). Theoretical and observed performance of mobile rig footings on clay. Proc. Offshore Technology Conf., Texas, USA, OTC 1201.

Goh, T.L. (2003). Stabilization of an excavation by an embedded improved soil layer. Ph.D Thesis, National University of Singapore.

Hambly, E.C., G.R. Imm and B. Stahl. (1990). Jackup performance and foundation fixity under developing storm conditions. Proc. Offshore Technology Conf., Texas, USA, OTC 6466.

Hambly, E.C. and B.A. Nicholson. (1991). Jackup Dynamic Stability Under Extreme Storm Conditions. Proc. Offshore Technology Conf., Texas, USA, OTC 6590.

Heikkila, J. and Silven, O. (1998). A four step camera calibration procedure with implicit image correction. IEEE Computer Society Conf. on Computer Vision and Pattern Recognition, San Juan, Puerto Rico.

Hossain, M.S. (2004). Investigation of soil failure mechanisms during spudcan foundation installation. Master Thesis, Curtin University of Technology.

Hossain, M.S. (2008). New mechanism-based design approaches for spudcan foundations on clays. Ph. D. Thesis, University of Western Australia.

Hossain, M.S. and M.F. Randolph. (2008a). Overview of spudcan performance on clays: current research and SNAME. Proc. 2nd Jack-up Asia Conf. and Exhibition, Singapore.

Hossain, M.S. and M.F. Randolph. (2009a). Effect of strain rate and strain softening on the penetration resistance of spudcan foundations on clay. Int. J. Geomechanics, ASCE, Vol. 9, No. 3.

Hossain, M.S. and M.F. Randolph (2009b). New mechanism-based design approach for spudcan foundations on single layer clay. Journal of Geotechnical and Geoenvironmental Engineering, ASCE, Vol. 135(9), pp. 1264 – 1274.

Hossain, M.S. and M.F. Randolph. (2009c). New mechanism based design approach for spudcan foundations on stiff over soft clay. Proc. Offshore Technology Conf., Texas, USA, OTC 19907.

Hossain, M.S. and M.F. Randolph. (2009d). Bearing behaviour of shallow foundations on clays - offshore and onshore, research and practice. Proc. 17th Int. Conf. on Soil Mechanics & Geotechnical Engineering, Alexandria.

Hossain, M.S. and M.F. Randolph. (2010a). Deep penetrating spudcan foundations on layered clays: centrifuge tests. Géotechnique, Vol. 60(3), pp. 157 – 170.

Hossain, M.S. and M.F. Randolph. (2010b). Deep penetrating spudcan foundations on layered clays: numerical analysis. Géotechnique, Vol. 60(3), pp. 171 – 184.

Hossain, M.S. and Y. Hu. (2004a). Investigation of the response of spudcan foundations in uniform clay. Proc. 9th Australia New Zealand Conf. on Geomechanics, pp. 102 – 108.

Hossain, M.S. and Y. Hu. (2005a). Soil failure mechanisms associated with spudcan foundations on clay. Australian Geomechanics 40(3), pp. 103 – 110.

Hossain, M. S., M.J. Cassidy. and D. Daley. (2008b). Experimental investigation of Swiss cheese drilling in stiff-over-soft clay. Proc. 2nd Jack-up Asia Conf. and Exhibition, Singapore.

Hossain, M.S., Y. Hu and M.F. Randolph. (2003). Spudcan foundation penetration into uniform clay. Proc. 13th Int. Offshore and Polar Engineering Conf., pp. 647 – 652.

Hossain, M.S., Y. Hu and M.F. Randolph. (2004b). Bearing behaviour of spudcan foundation on uniform clay during deep penetration. Proc. 23rd Int. Conf. on

Offshore Mechanics and Arctic Engineering, Vancouver, OMAE2004-51153.

Hossain, M.S., Y. Hu., M.F. Randolph and D. J. White. (2005b). Punch-through of spudcan foundations in two-layer clay. Proc. 1st Int. Symp. on Frontiers in Offshore Geotechnics, Perth, pp. 535 – 541.

Hossain, M.S., Y. Hu, M.F. Randolph and D.J. White. (2005c). Limiting cavity depth for spudcan foundations penetrating clay. Géotechnique, Vol. 55(9), pp. 679 – 690.

Hossain, M.S., Y. Hu, M.F. Randolph and D.J. White. (2006). Cavity stability and bearing capacity of spudcan foundations on clay. Proc. Offshore Technology Conf., Texas, USA, OTC 17770.

Hossain, M.S., Z. Mehryar, Y. Hu. and M.F. Randolph. (2004c). Deep penetration of spudcan foundation into NC clay. Proc. 23rd Int. Conf. on Offshore Mechanics and Arctic Engineering, Vancouver, OMAE2004-51154.

Houlsby, G.T. (2003). Modeling of shallow foundations for offshore structures. Proc. 1st BGA Int. Conf. on Foundations, Dundee, Scotland, pp. 11 – 26.

Houlsby, G.T. and C.M. Martin. (1993). Modelling of the behavior of foundations of jackup units on clay. Predicitive Soil Mechanics, Thomas Telford, London, pp. 339 – 358.

Houlsby, G.T. and C.M. Martin. (2003). Undrained bearing capacity factors for conical footings on clay. Géotechnique, Vol. 53(5), pp. 513 – 520.

Houlsby, G.T. and M.J. Cassidy. (2002). A plasticity model for the behavior of

footings on sand under combined loading. Géotechnique, Vol. 52(2), pp. 117 – 129.

House, A.R., J.R.M.S. Oliveira and M.F. Randolph. (2001). Evaluating the coefficient of consolidation using penetration tests. Int. Journal of Physical Modelling in Geotechnics, Vol. 3, pp. 17 – 26.

Jack, R.L., Hoyle, M.J.R., Hunt, R.J. and Smith, N.P. (2007). Jackup accident statistics: lots to learn. Proc. 11th Int. Conf., the jackup platform, design, construction and operation, City University, London.

James, R.G. (1965). Stress and strain fields in sand. Ph.D Thesis, Cambridge University.

James, R.G. and H. Tanaka. (1984). An investigation of the bearing capacity of footings under eccentric and inclined loading on sand in a geotechnical centrifuge. Proc. Symp. Recent Advance in Geotechnical Centrifuge Modelling, University of California, Davis, pp. 88 – 115.

Jardine, R.J., N.M.J.R. Kovecevic, H.K. Hoyle, Sidhu and A. Letty. (2001). A study of eccentric jack-up penetration into infilled footprint craters. Proc. 8th Int. Conf., the jackup platform, design, construction and operation, City University, London.

Juneja, A., A. Hedge, F.H. Lee and C.H. Yeo. (2010). Centrifuge modeling of tunnel face reinforcement using forepoling. Tunnelling and Underground Space Technology, Vol. 25, pp. 377 – 381.

Kee, R. and B.W. Ims. (1984). Geotechnical hazards associated with leg penetration of jackup rigs. Seabed Mechanics, pp. 169 – 174.

Khoo, E., T. Okmura and F.H. Lee. (1994). Side friction effects in plane strain models. Proc. Int. Conf. Centrifuge 94, Singapore, pp. 115-120.

König, D., H.L. Jessberger, M. Bolton, R. Phillips, G. Bagge, R. Renzi and J. Garnier (1994). Pore pressure measurement during centrifuge model tests: Experience of five laboratories. Proc. Int. Conf. Centrifuge 94, Singapore, pp. 101–108.

Kraft, L.M. (1982). Effective stress capacity model for piles in clay. ASCE Journal of Geotechnical Engineering Division, 108 (GT11), pp. 1387 – 1404.

Ladd, C.C. and R. Foott. (1974). New design procedures for stability of soft clays. ASCE Journal of Geotechnical Engineering Division, 100 (GT7), pp. 786 – 793.

Lee, F.H. (1992). The National University of Singapore Geotechnical Centrifuge Users Manual. Research Report No. CE001.

Lee, F.H. (2001). The philosophy of modeling versus testing. Proc. Int. Symp, on Constitutive and Centrifuge Modelling: Two Extremes, Monte Verita, Switzerland, pp. 113 – 131.

Lee, F.H., T.S. Tan, C.F. Leung, K.Y. Yong, G.P. Karunarate and S.L. Lee. (1991). Development of Geotechnical Centrifuge Facility at National University of Singapore. Proc. Centrifuge '91, Balkema, Rotterdam.

Lee, F. H., A. Juneja, C. Wen, G.R. Dasari and T.S. Tan (2002). Performance of total stress cells in model experiments in soft clays. Proc. Int. Conf. on physical modelling in geotechnics, St John's, Canada, pp.101–106.

Lee, K.K. (2009). Investigation of potential punch through failure on sands

overlying clay soils. Ph.D Thesis, University of Western Australia.

Lee, K.K., M.F. Randolph and M.J. Cassidy. (2009). New simplified conceptual model for spudcan foundations on sand overlying clay soils. Proc. Offshore Technology Conf., Texas, USA, OTC 20012.

Le Tirant, P. (1979). Seabed reconnaissance and offshore soil mechanics for the installation of petroleum structures. Technip, Paris.

Le Tirant, P. and C. Pérol. (1993). Stability and operation of jack-ups, Technip, Paris.

Leung, C.F., C.T. Gan and Y.K. Chow. (2007). Shear strength changes within jackup spudcan footprint. Proc. Int. Offshore and Polar Engineering Conf., pp. 1504 – 1509.

Leung, C.F., F.H. Lee and T.S. Tan. (1991). Principles and application of geotechnical model testing. Journal of Institute of Engineers, Singapore, Vol. 31(4), pp. 39 – 45.

Leung, C.F., Y. Xie and Y.K. Chow. (2006). Centrifuge model study of spudcan pile interaction. Proc. Int. Offshore and Polar Engineering Conf., pp. 530 – 535.

Leung, C.F., Y. Xie and Y.K. Chow. (2008). Use of PIV to investigate spudcan pile interaction. Proc. Int. Offshore and Polar Engineering Conf., pp. 721 – 726.

Lu, Q., Y. Hu and M.F. Randolph. (2001). Deep penetration in soft clay with strength increasing with depth. Proc. Int. Offshore and Polar Engineering Conf., pp. 453 – 458.

Martin, C.M. (1994). Physical and numerical modeling of offshore foundations under combined loads. D.Phil Thesis, University of Oxford.

Martin, C.M. (2001). Impact of centrifuge modeling on offshore foundation design. Proc. Int. Symp. on Constitutive and Centrifuge Modelling: Two Extremes, Monte Verita, Switzerland, pp. 135 – 154.

Martin, C.M. and G.T. Houlsby. (1999). Jackup units on clay: structural analysis with realistic modeling of spudcan behavior. Proc. Offshore Technology Conf., Texas, USA, OTC 10996.

Martin, C.M. and G.T. Houlsby. (2000). Combined loading of spudcan foundations on clay: laboratory test. Géotechnique, Vol. 50(4), pp. 325 – 338.

Martin, C.M. and G.T. Houlsby. (2001). Combined loading of spudcan foundations on clay: numerical modelling. Géotechnique, Vol. 51(8), pp. 687 – 700.

Martin, C.M. and M.F. Randolph. (2001). Applications of the lower and upper bound theorems of plasticity to collapse of circular foundations. Proc. 10th IACMAG Conf., Tucson, USA, Vol. 2, pp. 1417 – 1428.

McCarron, W.O. and M.D. Broussard. (1992). Measured jackup response from spudcan seafloor interaction for an extreme storm event. Proc. Int. Conf. Behaviour of Offshore Structures BOSS, pp. 349 – 361.

McClelland, B., A.G. Young and B.D. Remmes. (1981). Avoiding jackup rig foundation failures. Proc. Int. Symp. Geotechnical Aspects of Coastal and Offshore Structures, Bangkok.

Menzies, D. and R. Ropers. (2008). Comparison of jackup rig spudcan penetration methods in clay. Proc. Offshore Technology Conf., Texas, USA, OTC 19545.

Muir Wood, D.M. (2004). Geotechnical modeling. Spon Press, Taylor and Francis.

Murff, J.D. (1996). The geotechnical centrifuge in offshore engineering. Proc. Offshore Technology Conf., Texas, USA, OTC 8265.

Murff, J.D., J.M. Hamilton, E.T.R Dean, R.G. James, O. Kusakabe and A.N. Schofield. (1991). Centrifuge testing of foundation behavior using full jackup. Proc. Offshore Technology Conf., Texas, USA, OTC 6516.

Murff, J.D., M.D. Prins, E.T.R Dean, R.G. James and A.N. Schofield. (1992). Jackup rig foundation modeling. Proc. Offshore Technology Conf., Texas, USA, OTC 6807.

Nataraja, R., M.J.R. Hoyle, K. Nelson and N.P. Smith. (2004). Calibration of seabed fixity and system damping from GSF Magellan full scale measurements. Marine Structures, Vol. 17, pp. 245 – 260.

Nelson, K., R.W.P. Stonor and T. Versavel. (2001). Measurements of seabed fixity and dynamic behavior of the Santa Fe Magellan jackup. Marine Structures, Vol. 17, pp. 245 – 260.

Ng, T.G., F.H. Lee, C.Y. Liaw and E.S. Chan. (1994). Development of a dynamic loading device for model foundation. Proc. Centrifuge'94, Balkema, Rotterdam.

Ng, T.G., F.H. Lee, C.Y. Liaw and E.S. Chan. (1996). Centrifuge modeling of

jackup foundation under cyclic vertical loading. Proc. 12th Southeast Asian Geotechnical Conference, Kuala Lumpur, pp. 107 – 112.

Ng, T.G. (1999). Cyclic behavior of spudcan footing on sand. Ph.D Thesis, National University of Singapore.

Ng, T.G. and F.H. Lee. (2002). Cyclic settlement behavior of spudcan foundations. Géotechnique, Vol. 52(7), pp. 469 – 480.

Noble Denton and Associates. (1987). Foundation fixity of jackup units: a joint industry study. Noble Denton and Associates.

Okamura, M., J. Takemura and T. Kimura. (1997). Centrifuge model test on bearing capacity and deformation of sand layer overlying clay. Soils and Foundations, Vol. 37(1), pp. 73 – 88.

Osborne, J.J., J.C. Trickey, G.T. Houlsby and R.G. James. (1991). Findings from a joint industry on foundation fixity of jackup units. Proc. Offshore Technology Conf., Texas, USA, OTC 6615.

Osborne, J.J., K.L. Teh, C.F. Leung, M.J. Cassidy, G.T. Houlsby, N. Chan, D. Devoy, P. Handidjaja, P. Wong and K.S. Foo. (2008). An introduction to the InSafe JIP. Proc. 2nd Jackup Asia Conf., Singapore.

Osborne, J.J., G.T. Houlsby, K.L. Teh, B. Bienen, M.J. Cassidy, M.F. Randolph and C.F. Leung. (2009). Improved guidelines for the prediction of geotechnical performance of spudcan foundations during installation and removal of jackup units. Proc. Offshore Technology Conf., Texas, USA, OTC 20291.

Pedersen, R.C., R.E. Olsen and A.F. Rausch. (2003). Shear and interface strength of clay at very low effective stresses. ASTM Geotech. Testing Journal, Vol. 26(1), pp. 71 – 78.

Phillips, R. (1988). Centrifuge lateral pile tests in clay. Lynxvale Ltd report.

Puech, A., M. Orozco-Calderon and P. Foray. (2010). Mini T bar testing at shallow penetration. Proc. 2nd Int. Symp. on Frontiers in Offshore Geotechnics, Perth, pp. 305 – 310.

Purwana, O.A. (2006). Centrifuge model study on spudcan extraction in soft clay. Ph.D Thesis. National University of Singapore.

Purwana, O.A., C.F. Leung, Y.K. Chow and K.S. Foo. (2005). Influence of base suction on extraction of jackup spudcans. Géotechnique, Vol. 55(10), pp. 741 – 753.

Purwana, O.A., C.F. Leung, Y.K. Chow and K.S. Foo. (2006). Breakout failure mechanism of jackup spudcan extraction. Proc. 6th Int. Conf. Physical Modelling in Geotechnics, Hong Kong, pp. 667 – 672.

Purwana, O.A., M. Quah, K.S. Foo, C.F. Leung and Y.K. Chow. (2008). Understanding spudcan extraction problem and mitigation devices. Proc. 2nd Jackup Asia Conf., Singapore.

Purwana, O.A., M. Quah, K.S. Foo, S. Nowak and P. Handidjaja. (2009). Leg extraction/pullout resistance – theoretical and practical perspectives. Proc. 12th Int. Conf., the jackup platform, design, construction and operation, City University, London.

Randolph, M.F. (2004). Characterization of soft sediments for offshore applications.

Keynote lecture. Proc. 2nd Int. Conf. on Site Characterisation, Porto, Portugal, Vol. 1, pp. 209 – 231.

Randolph, M.F. and C.P. Wroth. (1981). Application of the failure state in undrained simple shear to shaft capacity of driven piles. Géotechnique, Vol. 31(1), pp. 143 – 157.

Randolph, M.F. and S. Hope. (2003). Effect of cone velocity on cone resistance and excess pore pressures. Proc. Int. Symp. Engineering Practice and Performance of Soft Deposits, Osaka, Japan, pp. 147 – 152.

Randolph, M.F., J.P. Carter and C.P. Wroth. (1979). Driven piles in clay – the effects of installation and subsequent consolidation. Géotechnique, Vol. 29(4), pp. 361 – 393.

Randolph, M.F., M.J. Cassidy, S.M. Gourvenec and C. Erbich. (2005). Challenges of offshore geotechnical engineering. Proc. 16th Int. Conf. on Soil Mechanics and Geotechnical Engineering, Osaka, Japan, pp. 123 – 176.

Randolph, M.F., C. Gaudin, S.M. Gourvenec, D.J. White, N. Boylan and M.J. Cassidy. (2010). Recent advances in offshore geotechnics for deep water oil and gas developments. Ocean Engineering, in press.

Randolph, M. F., Wang, D., Zhou, H., Hossain, M. S. & Hu, Y. (2008). Large deformation finite element analysis for offshore applications. Keynote Lecture, Proc. 12th Int. Conf. of Int. Association for Computer Methods and Advances in Geomechanics, Goa, pp. 3307-3318.

Rapoport, V. and J. Alford. (1989). Preloading of independent leg units at locations

with difficult seabed conditions. Marine Structures, Vol. 2, pp. 451 – 462.

Reardon, M.J. (1986). Review of the geotechnical aspects of jackup units operations. Ground engineering, Vol. 19(7), pp. 21 – 26.

Rowe, P.W. and W.H. Craig. (1981). Applications of models to the prediction of offshore gravity platform foundation performance. Proc. Int. Conf. on Offshore Site Investigation, London, pp. 269 – 281.

Schofield, A.N. (1980). Cambridge geotechnical centrifuge operation. Géotechnique, Vol. 30(3), pp. 227 – 268.

Sciliano, R.J., J.M. Hamilton, J.D. Murff and R. Phillips. (1990). Effect of jackup spudcans on piles. Proc. Offshore Technology Conf., Texas, USA, OTC 6467.

Skempton, A.W. (1951). The bearing capacity of clays. Building Research Congress, London 1, pp. 180 – 189.

Sladen, J.A. (1992). The adhesion factor: applications and limitations. Canadian Geotechnical Journal, Vol. 29, pp. 322 – 326.

SNAME. (1994). Recommended practice for site specific assessment of mobile jackup units. T and R Bulletin 5-5A. First Edition. Society of Naval Architects and Marine Engineers, New Jersey.

SNAME. (1997). Recommended practice for site specific assessment of mobile jackup units. T and R Bulletin 5-5A. First Edition. Revision 1. Society of Naval Architects and Marine Engineers, New Jersey.

SNAME. (2002). Recommended practice for site specific assessment of mobile jackup units. T and R Bulletin 5-5A. First Edition. Revision 2. Society of Naval Architects and Marine Engineers, New Jersey.

SNAME. (2008). Recommended practice for site specific assessment of mobile jackup units. T and R Bulletin 5-5A. First Edition. Revision 3. Society of Naval Architects and Marine Engineers, New Jersey.

Springett, C.N., R.W.P. Stonor and X. Wu. (1996). Results of a jack-up measurement programme in the North Sea and their comparison with the structural analysis. Marine Structures, Vol. 9, pp. 53 – 70.

Springman, S.M. and A.N. Schofield. (1998). Monotonic lateral load transfer from a jackup platform lattice leg to a soft clay deposit. Proc. Centrifuge'98, Balkema, Rotterdam.

Stewart, D.P. (1992). Lateral loading of pile bridge abutments due to embankment constrcution. Ph.D Thesis, University of Western Australia.

Stewart, D.P. (2005). Influence of jackup operation adjacent to a piled structure. Proc. Int. Symp. Frontiers in Offshore Geotechnics, Perth, Australia, pp. 543 – 550.

Stewart, D.P. and M.F. Randolph. (1991). A new site investigation tool for centrifuge. Proc. Centrifuge'91. Balkema, Rotterdam, pp. 531 – 538.

Stewart, D.P. and I.M.S Finnie. (2001). Spudcan footprint interaction during jackup workovers. Proc. Int. Offshore and Polar Engineering Conf., pp. 61 – 65.

Stock, D.J., D.R. Lewis, T.C. Baucke and H.Y. Hsu. (2000). Hurricane Georges

hindcast assessment of LeTourneau 116-C and 82-SD-C jackups. Proc. Offshore Technology Conf., Texas, USA, OTC 12075.

Tan, F.S.C. (1990). Centrifuge and numerical modeling of conical footings on sand. Ph.D Thesis, Cambridge University.

Taylor, R.N. (1995). Centrifuge in modeling: principles and scale effects. Geotechnical Centrifuge Technology. Black Academics and Professional.

Taylor, R.N., R.J. Grant, S. Robson and J. Kuwano. (1998). An image analysis system for determining plane and 3D displacements in soil models. Proc. Centrifuge'98. Balkema, Rotterdam, pp. 73 – 78.

Teh, K.L. (2008). Punch through of spudcan penetration in sand overlying clay. Ph.D Thesis, National University of Singapore.

Teh, K.L., C.F. Leung and Y.K. Chow. (2005). Spudcan penetration in sand overlying clay. Proc. Int. Symp. Frontiers in Offshore Geotechnics, Perth, Australia, pp. 529 – 534.

Teh, K.L., M.J. Cassidy, C.F. Leung, Y.K. Chow, M.F. Randolph and C.K. Quah. (2008). Revealing the bearing failure mechanisms of a penetrating spudcan through sand overlying clay. Geotechnique, Vol. 58(10), pp. 793 – 804.

Teh, K.L., M.J. Cassidy, Y.K. Chow and C.F. Leung. (2006). Effects of scale and progressive failure on spudcan ultimate bearing capacity in sand. Proc. Int. Symp. on Ultimate States of Geotechnical Structures, Marnela-Valee, France, pp. 481 – 489.

Teh, K.L., C.F. Leung, Y.K. Chow and P. Handidjaja. (2009). Prediction of punch

through for spudcan penetration in sand overlying clay. Proc. Offshore Technology Conf., Texas, USA, OTC 20060.

Teh, K.L., C.F. Leung, Y.K. Chow and M.J. Cassidy. (2010). Centrifuge model study of spudcan penetration in sand overlying clay. Géotechnique, Vol. 60(11), pp. 825 – 842.

Temperton, I., R.W.P. Stonor and C.N. Springett. (1999). Measured spudcan fixity: analysis of instrumentation data from three North Sea jackup units and correlation to site assessment procedures. Marine Structures, Vol. 12, pp. 277 – 309.

Templeton III, J.S., D.R. Lewis and Brekke, J.N. (2003). Spudcan fixity in clay: first findings of a 2003 IADC study. Proc. 9th Int. Conf. the jackup platform, design, construction and operation, City University, London.

Templeton III, J.S., D.R. Lewis and Brekke, J.N. (2005). Spudcan fixity in clay: final findings of a 2003 IADC study. Proc. 10th Int. Conf. the jackup platform, design, construction and operation, City University, London.

Templeton III, J.S. (2006). Jackup foundation performance in clay. Proc. Offshore Technology Conf., Texas, USA, OTC 18367.

Thanadol, K. (2003). Behaviour of an embedded improved soil berm in an excavation. Ph.D Thesis, National University of Singapore.

Tomlinson, M.J. (1957). The adhesion of piles driven in clay soils. Proceedings of 4th International Conference on soil mechanics and foundation engineering, London, Vol. 2, pp. 66 – 71.

Tomlinson, M.J. (1977). Pile design and construction practice. Viewpoint Publications, London.

Tsukamoto, Y. (1994). Drum centrifuge tests of three leg jackups on sand. Ph.D Thesis, Cambridge University.

Van Langen, H. and B. Hospers. (1993). Theoretical model for determining rotational behavior of spudcans. Proc. Offshore Technology Conf., Texas, USA, OTC 7302.

Vazquez, J.H., R.P. Michel, J.H. Alford, M. Quah and K.S. Foo. (2005). Jack-up units. A technical primer for the offshore industry professionals.

Vlahos, G., C.M. Martin, M.S. Prior and M.J. Cassidy. (2005). Development of a model jackup unit for the study of soil-structure interaction on clay. Int. Journal of Physical Modelling in Geotechnics, Vol. 2, pp. 31 – 48.

Wagget, P.R. (1989). The effects of lubricants on the interaction between soil and perspex. Cambridge University Part II Project Report.

Watson, P.G., N. Suemasa and M.F. Randolph. (2000). Evaluating undrained shear strength using the vane shear apparatus. Proc. 10th Int. Offshore and Polar Engineering Conf., Seattle, pp. 485 – 493.

White, D.J. (2002). An investigation into the behavior of pressed-in piles. Ph.D Thesis, Cambridge University.

White, D.J., K.L. Teh, C.F. Leung and Y.K. Chow. (2008). A comparison of the bearing capacity of flat and conical circular foundations on sand. Géotechnique, Vol.

58(10), pp. 781 – 792.

White, D.J. and W.A. Take. (2002). GeoPIV: Particle Image Velocimetry (PIV) software for use in geotechnical testing. D-Soils-TR322, Cambridge University Engineering Department Technical Report.

White, D.J., W.A. Take and M.D. Bolton. (2003). Soil deformation measurement using particle image velocimetry (PIV) and photogrammetry. Géotechnique, Vol. 30(1), pp. 49 – 65.

White, D.J., C. Gaudin, N. Boylan and H. Zhou. (2010). Interpretation of T bar penetrometer tests at shallow embedment and in very soft soils. Canadian Geotechnical Journal, Vol. 47, pp. 218 – 229.

Wong, P.C., J.C. Chao, J.D. Murff, E.T.R. Dean, R.G. James, A.N. Schofield and Y. Tsukamoto. (1993). Jackup rig foundation modeling II. Proc. Offshore Technology Conf., Texas, USA, OTC 7303.

Xie, Y. (2009). Centrifuge model study on spudcan pile interaction. Ph.D Thesis, National University of Singapore.

Xie, Y., C.F. Leung and Y.K. Chow. (2006). Effects of spudcan penetration on adjacent piles. Proc. 6th Int. Conf. Physical Modelling in Geotechnics, Hong Kong, pp. 701 – 706.

Xie, Y., C.F. Leung and Y.K. Chow. (2010). Study of soil movements around a penetrating spudcan. Proc. 7th Int. Conf. Physical Modelling in Geotechnics, Zurich, pp. 1075 – 1080.

Xue, J. (2010). Rotational stiffness and bearing capacity variation of spudcan under undrained and partially drained condition in clay. M.Eng Thesis, National University of Singapore.

Yeo, C.H., F.H. Lee, A. Hedge and A. Juneja (2010). Centrifuge modeling of a steel pipe umbrella arch for tunneling in clay. Proc. 7th Int. Conf. Physical Modelling in Geotechnics, Zurich, pp. 611 – 616.

Young, A.G., B.D. Remmes and B.J. Meyer. (1984). Foundation performance of offshore jackup drilling rigs. Journal of Geotechnical Engineering, ASCE, Vol. 110(7), pp. 841 – 859.

APPENDIX A

CALIBRATION OF PORE PRESSURE TRANSDUCERS

A.1 PORE PRESSURE SENSORS

A significant aspect in the centrifuge experiment is the reliability of the pore pressure transducers to monitor pore water pressure changes particularly during spudcan penetration in which a quick change was expected. The Druck© PDCR-81 miniature pore pressure sensors, which were originated for use in centrifuge modeling applications, are commonly known to be reliable for measuring positive pore water pressures. Although the spudcan penetration is designed to be initiated at relatively high water pressures, there are still some possibilities that the total pore pressures exceed their capacity. However, in all centrifuge tests, the total pore pressures were found to be within their capacity.

The calibration was performed using a Druck© DPI-601 digital pressure indicator thereby a prescribed level of air pressure can be effectively applied to the transducers. The calibration curve can be obtained by varying the applied pressure in the positive ranges. Additionally, the transducer was also re-calibrated in high g environment using water for a range of positives pressures. The standard calibration chart is illustrated in Figure A1 in which the relation between the applied pressure and the corresponding output reading appears linear in positive ranges. Moreover, the calibration factor obtained from both methods was found to be similar.

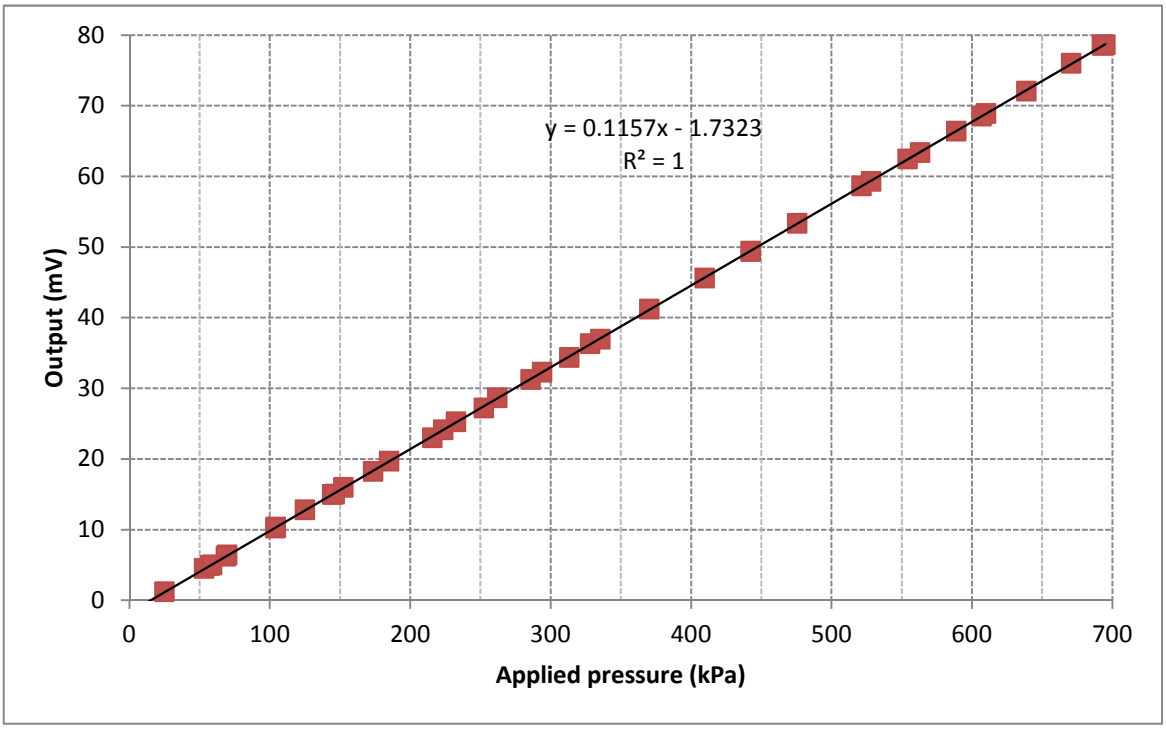

Figure A1 Typical calibration curve for pore pressure sensors adopted in this study